Mechanistic studies on the regulation of Ran-function by post-translational lysine-acetylation

Inaugural-Dissertation

zur

Erlangung des Doktorgrades

der Mathematisch-Naturwissenschaftlichen Fakultät

der Universität zu Köln

vorgelegt von

Susanne de Boor (geb. Haase)

aus Rostock

Köln, 2015

Berichterstatter: Dr. Michael Lammers (Betreuer)

Prof. Dr. Kay Hofmann

Tag der letzten mündlichen Prüfung: 02.06.2015

Zusammenfassung

Das kleine G-Protein Ran ist an elementaren zellulären Prozessen wie dem nukleozytoplasmatischen Transport sowie dem Aufbau der Kernhülle und der mitotischen Spindeln beteiligt. Die zwei nukleotidabhängigen Zustände, GTP- und GDP-gebunden, zeichnen sich durch unterschiedliche Konformationen zweier regulatorischer Schleifen (Switch I und Switch II) aus, welche maßgeblich die Effektor-Bindung beeinflussen. Der Übergang zwischen den zwei Zuständen wird durch regulatorische Proteine unterstützt, welche die Hydrolyse und den Austausch des Nukleotides beschleunigen. Die unterschiedliche zelluläre Lokalisation dieser Proteine führt zur Ausbildung eines Ran·GDP/GTP-Gradienten. Eine umfangreiche massenspektrometrische Studie im Jahr 2009 identifizierte fünf Acetylierungsstellen in humanem Ran, welche mittlerweile auch durch Folgestudien in anderen Organismen bestätigt wurden. Ziel dieser Arbeit war es, die Auswirkungen der Ran-Acetylierung auf die Funktion von Ran zu untersuchen. Des Weiteren sollten Einblicke in die Stöchiometrie und Regulation dieser post-translationalen Modifikation von Ran gewonnen werden um eine Einschätzung der physiologische Relevanz zu ermöglichen.

Im Zuge der Arbeit wurde mittels Erweiterung des genetischen Codes von *E.coli* stellen-spezifisch acetyliertes Ran (an den Lysinen 37, 60, 71, 99 und 159) hergestellt. Die Proteine wurden gereinigt und hinsichtlich ihrer intrinsischen Eigenschaften sowie der Interaktion mit dem Nukleotid-Austauschfaktor RCC1, dem wichtigsten Import-Rezeptor Importin-β und dem Ran-bindenden Protein NTF2 untersucht. Die umfangreiche *in vitro* Charakterisierung zeigt, dass die Acetylierung einzelner Lysine die RCC1-Interaktion und Nukleotid-Austauschrate, sowie die Ran-Lokalisierung und die Bildung von Import-Komplexen beeinflusst. Ran-Acetylierung an den Lysinen 37, 99 oder 159 hat eine höhere Importin-β-Affinität zur Folge. Acetyliertes Lysin 71 hat einen dominant negativen Effekt bezüglich RCC1 welcher mit dem der T24N-Mutante vergleichbar ist: die Bindungsaffinität ist erhöht, während die Nukleotid-Austauschrate herabgesetzt ist. Weiterhin verhindert diese Acetylierung die Interaktion mit NTF2, was wiederum die Ausbildung des Ran-Gradienten bzw. die Lokalisation von Ran beeinträchtigt. Für Lysin 99-acetyliertes Ran war ein

überwiegender Verlust der RCC1-Regulation zu beobachten, basierend auf einer verringerten Affinität und einem drastisch verringerten Nukleotid-Austausch.
Die durchgeführten Untersuchungen zur Regulation der Ran-Acetylierung führten zur Identifikation Ran-spezifischer Acetyltransferasen und Deacetylasen *in vitro* und *in vivo*. Sirt1, -2 und -3 wirken als Deacetylasen auf Acetyl-Lysin 37, wohingegen Acetylierung an Lysin 71 spezifisch von Sirt2 entfernt wird. Immunoblotting und massenspektrometrische Untersuchungen identifizierten Tip60, p300 und CBP als Ran-spezifische Acetyltransferasen und die Lysine 37, 134 und 142 als hauptsächliche Acetyl-Akzeptoren. Zusammengefasst deutet die vorliegende Arbeit auf ein hohes regulatorische Potential für die Acetylierung von Ran in Abhängigkeit vom zellulären Kontext hin.

"Absence of evidence is not evidence of absence."

Carl Edward Sagan, Astronomer

Abstract

The small GTP-binding protein Ran regulates fundamental cellular processes such as nucleocytoplasmic transport, nuclear envelope formation and mitotic spindle assembly. The two nucleotide states of Ran, GTP- and GDP-bound, are characterized by distinct conformations of two regulatory regions (switch I and switch II) which determine effector binding. The interconversion of these two states is facilitated by regulatory proteins (RanGAP, RCC1). The differential localization of these proteins leads to the formation of a Ran∗GDP/GTP gradient. A mass-spectrometrical screen of the acetylome of human cell lines in 2009 identified five acetylation sites in Ran, which were confirmed by subsequent screens in different organisms. The aim of this thesis was to study the impact of Ran-acetylation on Ran-function. Furthermore, the abundance and regulation of this post-translational modification was investigated to judge the physiological relevance of Ran-acetylation.

In this study, recombinant Ran was site-specifically acetylated at lysines 37, 60, 71, 99 and 159 using the genetic-code expansion concept in *E.coli*. The proteins were purified and characterized regarding their intrinsic properties and the interaction with the nucleotide exchange factor RCC1, the major import receptor Importin-β and the Ran-shuttling protein NTF2 (nuclear transport factor 2). The comprehensive *in vitro* characterization revealed that acetylation of single lysines impacts on RCC1-interaction and -catalysis, Ran-localization and import-complex formation. Ran acetylated at lysines 37, 99 or 159 exhibits a higher binding affinity for Importin-β. Acetylation of lysine 71 (in switch II) has a dominant negative effect on RCC1 analogous to the T24N-mutant of Ran. Furthermore, it abolishes NTF2-interaction, which consequently affects Ran-localization and the formation of the Ran-gradient. Moreover, Ran acetylated at lysine 99 resembles a loss-of-function mutant regarding RCC1, lowering affinity and nucleotide exchange rates. Regulatory enzymes for Ran-specific de-/acetylation were identified *in vitro* and *in vivo*. Sirt1, -2 and -3 are deacetylating enzymes for lysine 37 of Ran, whereas lysine 71 is specifically deacetylated by Sirt2. The enzymatic acetylation of Ran by the acetyltransferases Tip60, p300 and CBP was shown by immunoblotting and mass-spectrometrical analysis and lysines 37, 134 and 142 were identified as the major acetyl-acceptors of Ran. Taken together, these results suggest a strong regulatory potential of Ran-acetylation depending on the cellular context.

Contents

List of Figures

List of Tables

Chapter 1

Introduction

1.1 The Ras superfamily

Cellular signal transduction enables prokaryotic and eukaryotic cells to react to extracellular stimuli- a prerequisite for survival. G-proteins (guanine nucleotide binding proteins, GNBPs) are key players in signal transduction. Based on sequence- and structure-similarities, GNBPs are divided into two major classes: the TRAFAC (translation factors) and the SIMIBI (signal recognition particle, MinD and BioD) class. More than twenty families are organized in both classes together, which are further subdivided into 57 subfamilies (Leipe et al., 2002). TRAFAC-GNBPs are involved in signal transduction, translation, cell migration and intracellular transport processes. The translation factor superfamily (e.g. EF-Tu), the Ras superfamily (e.g. Ras, Rho, Ran) and the myosin-kinesin superfamily (e.g. myosin) are well known examples. SIMIBI proteins are involved in protein targeting and -localization and their biological function is associated with homo- or heterodimerization. The signal recognition-associated GTPase superfamily (SRP and its receptor) is one example for the SIMIBI class. Based on their biological function GNBPs can be divided into:

1. α-subunits of heterotrimeric G-proteins (G_αs)
2. Translation factors (e.g. EF-Tu, IF-2)
3. Ras superfamily (e.g. Ras, Rho, Ran)
4. SRP and SRP-receptor
5. Large GNBPs (e.g. Dynamin, GBP)

Table 1.1: Subfamilies of the Ras superfamily (after (Rojas et al., 2012))

	Ras	**Rho**	**Rab**	**Arf**	**Ran**
Members	39	22	65	30	1
Function	differentiation proliferation apoptosis	cytoskeleton cell growth	vesicle transport	vesicle transport	nucleocytoplasmic transport mitotic spindle formation nuclear envelope formation
Examples	(H/K/N)-Ras Rap1A Rap1B RalA Rit1/2 Rhes	Rho(A/B/C) Rnd(1/2/3) Rac(1/2) CDC42 TC10 Rif	Rab1A Rab1B Rab2 Rab3A Rab3B Rab10	Arf1-6 Arl1-10	Ran

The Ras superfamily comprises more than 150 human small GNBPs with a molecular weight of 20 to 25 kDa. The prototypical member of the superfamily, Ras (rat sarcoma), was first identified in 1979 as the product of a gene later characterized as a proto-oncogene (Chien et al., 1979; Langbeheim et al., 1980; Shih et al., 1979). 20 - 30 % of all human tumors carry mutations in the RAS proto-oncogene (Prior et al., 2012). Based on functional- and sequence similarity the Ras superfamily is further subdivided into five main-families: Ras, Rho, Rab, Arf and Ran (Rojas et al., 2012). Ras family proteins play important roles in cell differentiation, -proliferation and apoptosis. Rho-proteins (ras-homologous) are involved in cytoskeleton organization, cell growth and regulation of gene expression. Members of the Rab (ras-like proteins from brain) and Arf (ADP-ribosylation factor) families regulate the generation and transport of vesicles. Ran (ras-related nuclear) is crucial for nucleocytoplasmic transport, mitosis and formation of the nuclear envelope.

The importance of G-proteins in signal transduction is based on the ability to adopt two different states: the GTP-bound "on"-state and the GDP-bound "off"-state. The two states differ in the conformation of the highly conserved core domain of the G-proteins, the G-domain. Downstream targets, so called effector proteins, are only able to bind to the GTP-bound conformation, defining this as the active state. The fact that both conformational states are interconvertible by nucleotide exchange, predestines G-proteins to act as molecular switches. The hydrolysis of GTP to GDP results in the inactivation of the G-protein, which terminates the signal transduction and prevents permanent "on"-signaling.

With the exception of the Ran and Rad subfamilies, all small G-proteins are post-translationally modified by lipidation. This lipid anchor is crucial for targeting specific subcellular membranes and, consequently, for regulation of the biological activity of the GNBPs. Ras- and Rho-proteins are farnesylated and/or

geranylgeranylated by specific farnesyltransferses and geranylgeranylases, respectively (Lowy and Willumsen, 1989). The lipid-anchor is attached to the C-terminal CaaX-consensus sequence (C: Cysteine, a: aliphatic, X: any amino acid) by thioetherbond-formation with the cysteine side chain (Hancock et al., 1989). Following lipidation, the farnesyltransferase catalyzes the proteolytic cleavage after the cysteine and methylation thereof (Dai et al., 1998; Schmidt et al., 1998). For N- and H-Ras additional palmitoylation was reported. In that case, one or two cysteines N-terminal to the CaaX-Box are modified by a reversible thioesterbond. A constant cycle of palmitoylation/depalmitoylation drives the rapid exchange of Ras between the plasma membrane and the golgi (Rocks et al., 2005). K-Ras, in contrast, is not palmitoylated. Instead, a polybasic domain consisting of multiple lysines targets K-Ras to the plasma membrane independent of the secretory pathway (Hancock et al., 1990). Furthermore, Rab-proteins are geranylgeranylated and Arf-proteins were found to be N-terminally myristoylated. For lipidated Rho- and Rab-proteins additional regulatory proteins were identified. The guanine-nucleotide dissociation inhibitors (GDIs) bind to the switch regions of the GDP-state and accommodate the lipid-anchor in a hydrophobic pocket (Figure 1.2). Thereby the activation by GEF-action is prevented and the protein is solubilized from biomembranes. Moreover, PDEδ (Phosphodiesterase 6 subunit δ) solubilizes a broad spectrum of farnesylated cargoes (Chandra et al., 2012; Ismail et al., 2011).

1.1.1 The G-domain

The G-domain of Ras, with 166 residues and a mass of approximately 20 kDa, can be regarded as the minimal signaling unit in all G-proteins (Vetter and Wittinghofer, 2001). It is characterized by a mixed six-stranded β-sheet flanked by five helices (Figure 1.1). This α, β protein fold is typical for nucleotide binding proteins, although variations in the number of sheets and helices are possible. Four to five conserved sequence elements (Table 1.2), all located in loop domains, are lined up along the nucleotide binding pocket and mediate the high-affinity binding of guanine nucleotides (Figure 1.4.a) (Bourne et al., 1991; John et al., 1990; Schmidt et al., 1996; Via et al., 2000). The P-loop contacts the β- and γ-phosphate of the nucleotide and, hence, makes the major contribution to high-affinity nucleotide binding (Saraste et al., 1990). Mutations of S/T to N result in dominant negative small GTPases with a drastically reduced nucleotide affinity (Farnsworth and Feig,

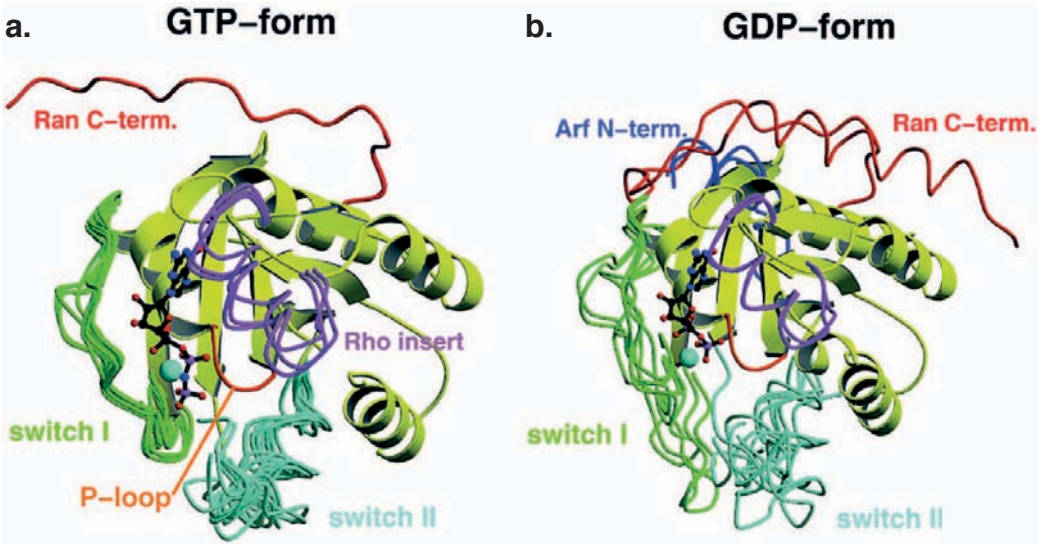

FIGURE 1.1: **Structure of the G-domain of GNBPs.** Superimposition of several GNBPs of the Ras superfamily on the G-domain in the GTP- (a) and GDP-conformation (b). The switch regions adopt a rigid conformation in the GTP-form and exhibit a high degree of exibility in the GDP-form. Extra elements in the structures of Rho (insert helix, magenta), Ran (C-terminal extension, red) and Arf (N-terminal helix, blue) are highlighted. Taken from (Vetter and Wittinghofer, 2001)

1991; Feig, 1999; John et al., 1993; Klebe et al., 1995a). The switch I and II regions primarily contact the -phosphate of the bound nucleotide. Removal of this phosphate during GTP-hydrolysis leads to conformational changes in both loops and consequently controls e ector binding (Spoerner et al., 2001; Wittinghofer and Pal, 1991). The bifurcated H bond between an Asp side chain in G4 and the nucleotide base as well as a main chain interaction between an invariant Ala in G5 (SAK motif) and the guanine oxygen are the determinants of the speci city for guanine.

TABLE 1.2: Motifs of the G-domain

Motif	Sequence	Function	Ras	Ran
G1 , P-loop	GxxxxGK(S/T)	- contacts - and -Phosphate - coordinates Mg^{2+}	^{10}GAGGVGKS^{17}	^{17}GDGGTGKT^{24}
G2, switch I	T	- hydrogen bond to -Phosphate - hydrogen bond to Mg^{2+}	^{30}DEYDPTIE^{37}	^{32}TGEFEKKYVATLG^{44}
G3, switch II	DxxG	- contacts -Phosphate (G) - coordinates Mg^{2+} (D)	^{57}DTAGQEEYSAM^{67}	^{65}DTAGQEKFGGLRDG^{78}
G4	NKxD	- contacts guanine base (speci city)	^{116}NKCD^{119}	^{122}NKVD^{125}
G5	SAK	- contacts guanine base (speci city)	^{145}SAK^{147}	^{150}SAK^{152}

1.1.2 Regulatory cycle

The existence of two nucleotide-dependent interconvertible conformational states is the basis for the relevance of small GNBPs as molecular switches. The GTP-bound state adopts a rigid conformation (Figure 1.1.a) which is recognized by effector proteins and activates downstream signaling cascades. Hydrolysis of the bound GTP releases switch I and switch II from this conformation, since the interactions to the γ-phosphate are lost. In the GDP-bound state the switch regions are highly flexible and, thus, not recognized by effector proteins or, if so, only with very low affinity. This "inactive" protein state is, however, interacting with regulatory proteins such as exchange factors. This cycle of activation and inactivation is depicted in scheme 1.2.

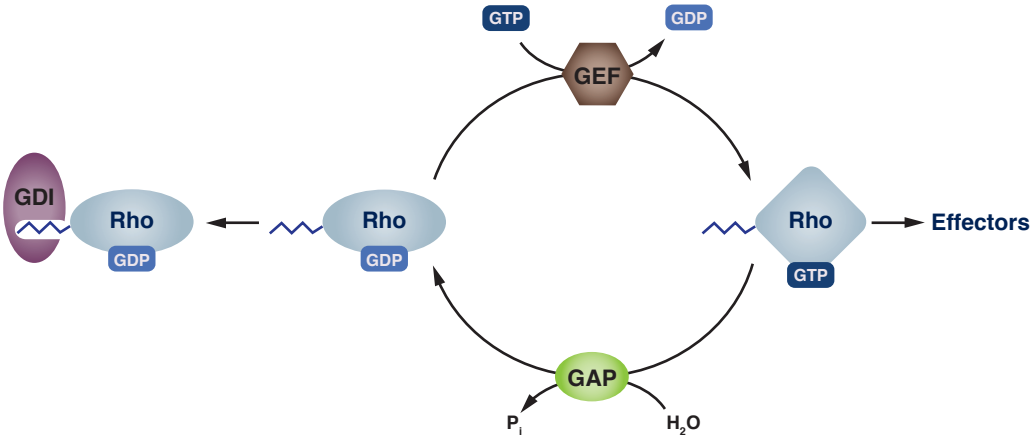

FIGURE 1.2: **Regulatory cycle of GNBPs of the Ras superfamily.** Small G-proteins (e.g. Rho) are regulated by guanine-nucleotide exchange factors (GEF) and GTPase-activating proteins (GAPs). Lipidated Rho- and Rab-proteins are, furthermore, regulated by guanine-nucleotide dissociation inhibitors (GDIs).

The basic machinery for interconversion of both states, by nucleotide hydrolysis and nucleotide exchange, is provided by the G-protein itself. However, intrinsic rates for GTP-hydrolysis as well as nucleotide exchange are too slow to be of physiological relevance. Hence, both processes are accelerated 10^5-fold by GTPase-activating proteins (GAPs) and guanine-nucleotide exchange factors (GEFs).

GAPs of small GNBPs are not conserved and they often approach the catalytic site from different directions. Furthermore, different catalytic mechanisms are utilized to accelerate GTP-hydrolysis (Scheffzek et al., 1997; Seewald et al., 2002). In most cases, the insertion of a positively charged residue by the GAP (either arginine

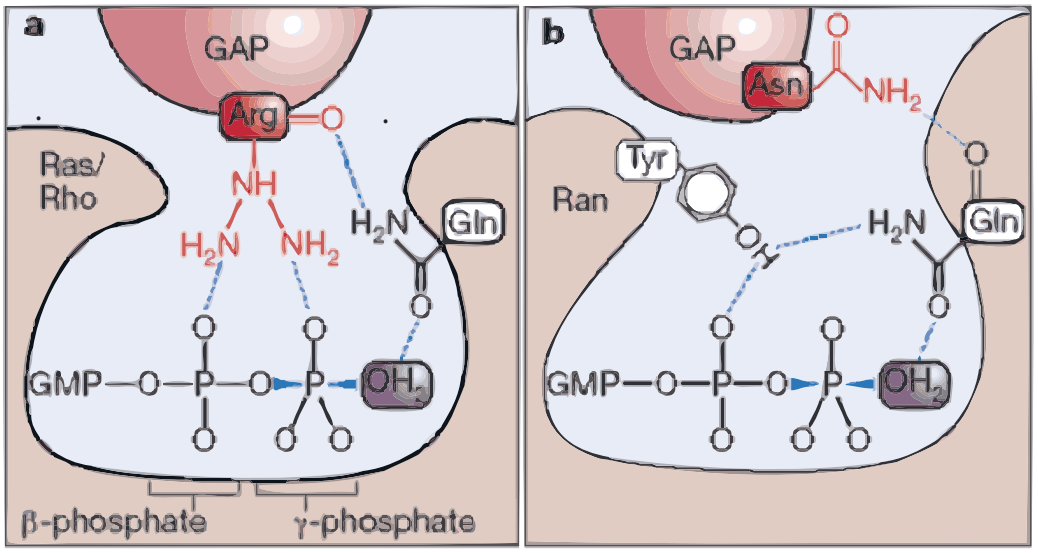

FIGURE 1.3: **Molecular basis for GAP-accelerated GTP-hydrolysis.** (a)Insertion of an arginine of RasGAP into the active site of Ras to position the catalytic glutamine. (b) RanGAP provides an asparagine to disrupt an inhibitory state created by tyrosine 39. Modified after (Rehmann and Bos, 2004)

or asparagine) stabilizes the catalytic machinery and lowers the activating energy of the catalytic step. Ras- and Rho proteins contain a conserved glutamine in switch II (Glu61 Ras/Rac/CDC42, Glu63 Rho) which positions a catalytic water molecule for nucleophilic attack on the the γ-phosphate of GTP (Resat et al., 2001). Ras- and RhoGAPs insert an arginine residue into the active site, the so called arginine-finger, to position the catalytic glutamine and to neutralize the developing negative charge in the hydrolysis step (Figure 1.3.a) (Ahmadian et al., 1997).

RanGAP provides an asparagine instead of the arginine-finger to accelerate the intrinsic GTP-hydrolysis. Furthermore, tyrosine 39 of Ran holds the catalytic glutamine (Glu69) and the water in an anti-catalytic position. Asparagine 131 of RanGAP displaces Tyr39 and allows for rapid hydrolysis by disruption of the inhibitory state (Figure 1.3.b) (Brucker et al., 2010). The GTP-hydrolysis of Rap is based on, yet, another mechanism, independent of a catalytic glutamine and the arginine-finger. In fact, a threonine residue without a detectable role in catalysis is found in the position of the catalytic glutamine. However, the missing glutamine in Rap is replaced by an asparagine in trans, the Asn-thumb, which is inserted into the active site by RapGAP and occupies exactly the same position as the catalytic glutamine in the other G-proteins (Scrima et al., 2008).

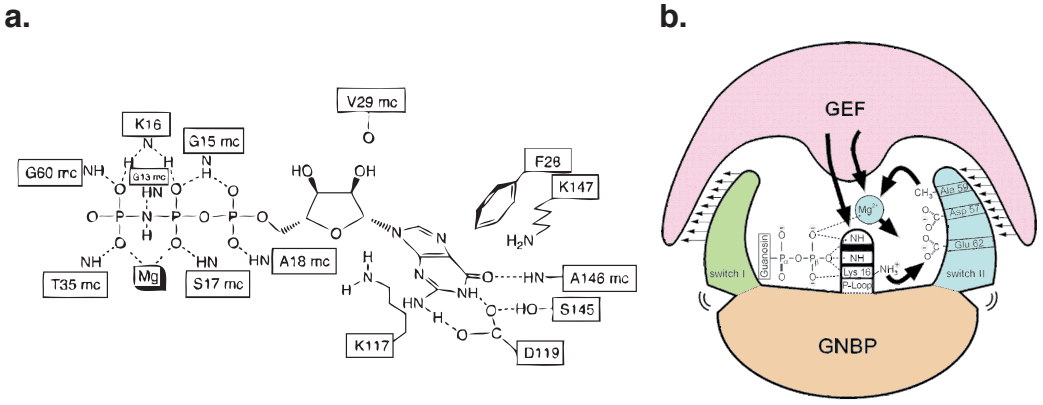

FIGURE 1.4: **Schematic presentation of nucleotide binding and GEF-mechanism.**(a) Schematic presentation of molecular contacts between GppNHp (a GTP-analogon) and residues of Ras (Wittinghofer and Waldmann, 2000). (b) Schematic diagram of the push-and-pull mechanism for GEF-induced nucleotide dissociation. Insertion of GEF-residues into/close to the magnesium-binding site and the P-loop disturbs nucleotide binding and reduces the nucleotide affinity. Switch I is pushed out and switch II pulled towards the nucleotide binding site (Vetter and Wittinghofer, 2001).

G-proteins bind GDP/GTP with low nanomolar to picomolar affinities and consequently exhibit very slow intrinsic nucleotide dissociation rates. GEFs accelerate these rates by several orders of magnitude by reducing the affinity for the nucleotide. The catalytic domains of various GEFs and also the specific binding sites differ throughout the Ras superfamily. However, GEF-binding always induces conformational changes in the switch regions and the P-loop, which sterically perturb the magnesium binding site (Lenzen et al., 1998). This mechanism is referred to as "push-and-pull mechanism", since switch I is pushed out of its normal position, whereas switch II is pulled toward the nucleotide binding site (Figure 1.4.b)(Vetter et al., 1999). Insertion of GEF-residues close to or into the P-loop and Mg^{2+}-binding area disturbs the nucleotide binding and drastically reduces the nucleotide affinity. The fact that the P-loop lysine (Lys16 in Ras), formerly contacting negative charges of the phosphates, is reoriented and interacts with either the invariant Asp (Asp^{57} in Ras) or the conserved Glu (Glu^{62} in Ras) of switch II, furthermore favors nucleotide release (Gasper et al., 2008). The stable nucleotide-free complex of GTPase and GEF is dissociated by subsequent rebinding of nucleotide. Noteworthy, the GEF-activity does not influence the binding selectivity regarding GDP or GTP. Rebinding of GTP, instead of GDP, is simply favored by a higher cellular GTP-concentration.

1.2 The small GTPase Ran

Ran was originally isolated with a Ras-like sequence from a human teratocarcinoma cell line (Drivas et al., 1990). Ran is a highly abundant and strongly conserved small GNBP, which is ubiquitously expressed in all eukaryotic cells (Ren et al., 1993). During interphase it shows predominantly nuclear localization, whereas it is widely distributed throughout the cell during mitosis. As a family member of the Ras superfamily, Ran features the characteristic G-domain and passes through the regulatory cycle (Scheffzek et al., 1995). In addition to the G-domain, Ran exhibits a C-terminal extension consisting of an unstructured linker followed by a 16 residue α-helix. In the GDP-bound state this extension contacts the protein core opposite of the switch I. In the GTP-bound state the unstructured C-terminus is extending away from the core, exposing the switch region for effector recognition and -binding. In contrast to the majority of small GTPases, Ran does not bind to biomembranes and, thus, is not post-translationally modified by prenylation. Ran carries an acidic C-terminus (-DEDDDL) which stabilizes the GDP-bound state and mediates interactions with RCC1, RanGAP, and RanBP1 (Richards et al., 1995).

Ran is involved in a variety of essential cellular processes. It is a key player in the transport of proteins in and out of the nucleus and also RNA is exported from the nucleus in a Ran-dependent process (Köhler and Hurt, 2007; Weis, 2002). Ran, furthermore, controls the cell cycle in yeast, regulates several mitotic processes and is involved in nuclear envelope formation (reviewed in (Clarke and Zhang, 2008)). Most of the functions of Ran are based on a gradient of Ran∗GDP/Ran∗GTP which is established by differential localization of the two regulating proteins RanGAP (cytosolic) and RCC1 (nuclear).

1.2.1 Nucleocytoplasmic transport

The nucleus of eukaryotic cells is delimited by the nuclear envelope, consisting of an inner nuclear membrane and an outer nuclear membrane. The outer nuclear membrane is continuous with the endoplasmatic reticulum. The inner nuclear membrane is lined by the nuclear lamina, a fibrillar network out of intermediate filaments and membrane associated proteins. The exchange of proteins, RNA and

small molecules between the cytosolic and the nuclear compartment is a prerequisite for survival of every eukaryotic cell. The translocation processes of these molecules are regulated with varying stringency. To this end, the nuclear envelope is perforated by nuclear pores - channels connecting inner and outer membrane and harboring the nuclear pore complexes (NPCs). NPCs are large multimeric protein assemblies out of 30 - 60 different proteins (nucleoporins) reaching a size of around 120 MDa in mammalian cells (Grossman et al., 2012; Reichelt et al., 1990; Rout and Aitchison, 2000). Phenylalanine-Glycine-(FG)-rich repeats (consensus sequence: FG, FxFG or GLFG) of nuclear pore proteins form a three-dimensional meshwork with hydrogel-like properties, which enables passive diffusion of molecules smaller than 25 - 40 kDa (Frey and Görlich, 2009; Frey et al., 2006). Larger molecules either possess the intrinsic capacity to interact with the NPC or the translocation is facilitated by association with specific transport receptors. These import- (importins) and export-receptors (exportins) recognize specific nuclear localization signals (NLS) and nuclear export signals (NES), respectively. From *in vitro* studies and single-molecule imaging experiments, an import rate capacity of 1000 molecules per second and NPC was estimated (Ribbeck and Görlich, 2001; Yang et al., 2004). Only facilitated, energy-dependent transport permits such an efficient translocation. However, the translocation process itself does not require energy. Rather, the energy consumption enables a directed transport against a concentration gradient. And in fact, transport-associated GTP-hydrolysis takes place after translocation trough the nuclear pore.

The cycling of Ran between its GDP- and GTP-bound state is crucial for nucleocytoplasmic transport (reviewed in (Cautain et al., 2014)). The spatial separation of Ran∗GTP-generation in the nucleus and GTP-hydrolysis in the cytosol generates the Ran∗GDP/GTP-gradient, which provides directionality to the nucleocytoplasmic transport (Kaláb et al., 2006). RCC1, the GEF of Ran, binds to chromatin and catalyzes the nucleotide exchange to generate Ran∗GTP in the nucleus. The mechanism of action of Ran∗GTP with transport receptors is different for import- and export processes (Figure 1.5). In the case of protein import, binding of Ran∗GTP dissociates import-complexes in the nucleus (Görlich et al., 1996). These complexes are formed in the cytosol and consist of a cargo molecule, an adaptor protein (e.g. Importin-α) and the import-receptor (e.g. Importin-β). The cargo protein carries a specific nuclear localization signal (one or two short stretches of positively charges amino acids) which is recognized and bound by Importin-α. Importin-β, the actual transport receptor, binds to the complex and

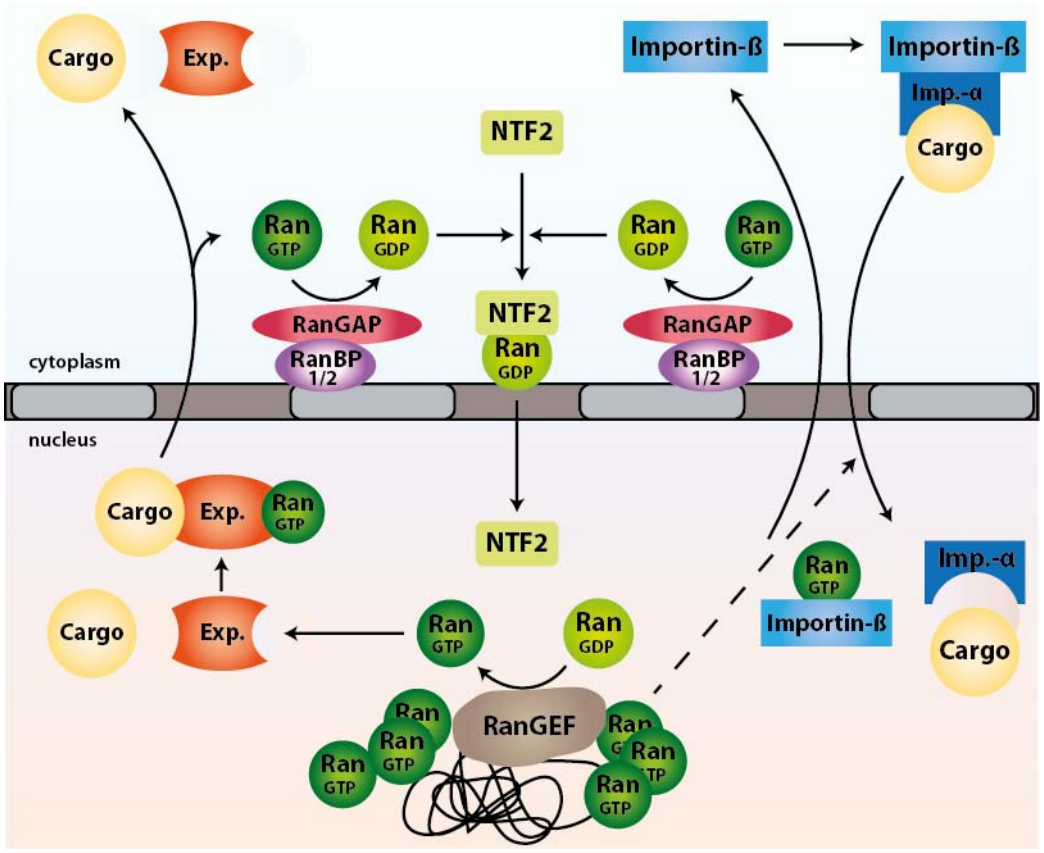

FIGURE 1.5: **The nucleocytoplasmic transport cycle.**Schematic presentation of the Ran-mediated nucleocytoplasmic transport cycle. Ran∗GTP is generated by the RanGEF (RCC1) at the chromatin, whereas hydrolysis of Ran∗GTP is accelerated by RanGAP at the cytosolic side of the nuclear pore complex. Protein export by export receptors (Exp.) as well as the classical import pathway, involving Importin-α (Imp-α) and Importin-α, are depicted.

facilitates translocation trough the NPC. The binding of Ran∗GTP to Importin-β in the nucleoplasm results in the dissociation of the import-complex and the release of the cargo molecule. Subsequently, the Importin-β-Ran∗GTP-complex passes the NPC and dissociates as a consequence of RanGAP-catalyzed GTP-hydrolysis in the cytosol.

In contrast to import processes, nuclear Ran∗GTP-binding to an exportin (e.g. Crm1) initiates export-complex formation by enhancing cargo binding. The ternary complex is exported through the NPC and dissociates upon GTP-hydrolysis by RanGAP. The cytosolic Ran-binding proteins (RanBPs) RanBP1 and RanBP2 co-stimulate the GAP-reaction. Both transport cycles, import and export, are closed by re-import of Ran∗GDP into the nucleus. This process is mediated by

the nuclear transport factor 2 (NTF2), which binds specifically to GDP-bound Ran.

1.2.2 Mitotic spindle assembly

Several observations suggested a participation of Ran and Ran-interacting proteins in mitosis. Expression of dominant mutants of Ran disrupted cell cycle progression and cell cycle defects were also observed when other components of the Ran-system were perturbed (Ren et al., 1994; Sazer and Nurse, 1994). Premature chromatin condensation after loss of RCC1 in a temperature-sensitive hamster cell line (tsBN2), furthermore, suggested a pivotal role for RCC1 during mitosis (Nishimoto et al., 1978; Uchida et al., 1990). Ran influences many different processes during mitosis. It promotes the nucleation of microtubuli at the centrosomes and plays a role in chromatin-directed nucleation (Carazo-Salas et al., 1999; Kalab et al., 1999; Ohba et al., 1999; Zhang et al., 1999). Moreover, Ran affects mitotic motor proteins involved in spindle assembly, regulates the microtubulin-flux during mitosis and stabilizes microtubuli (Carazo-Salas et al., 2001; Wilde et al., 2001).

In most cases, Ran acts by releasing mitotic spindle assembly factors (SAFs) from inhibitory complexes with Importin-α and/or Importin-β. Since Ran$*$GTP is the active species, able to bind to importins, the detachment of SAFs is linked to the Ran$*$GDP/GTP-gradient and, consequently, to Ran$*$GTP-generation by RCC1

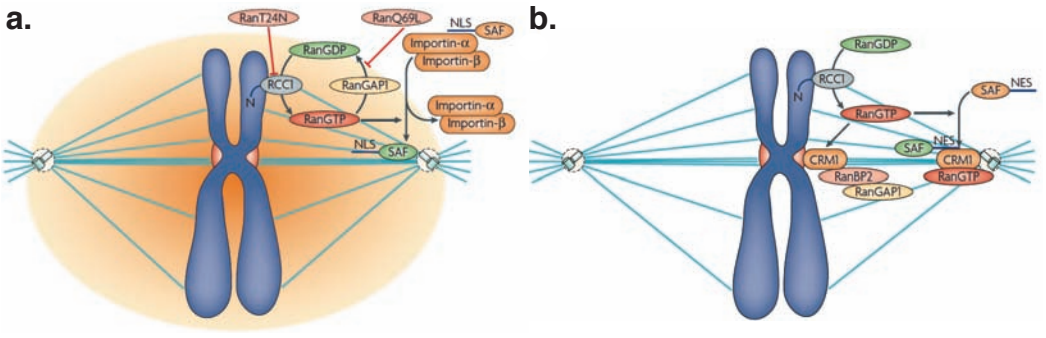

FIGURE 1.6: **Ran is involved in mitotic spindle formation.** (a) Release of spindle assembly factors (SAFs) from inhibitory complexes is coupled to Ran$*$GTP-generation by RCC1. (b) Localization of SAFs via their NES by a Crm1-Ran$*$GTP-dependent pathway. (modified after (Clarke and Zhang, 2008))

close to the chromatin. For example, the inactivation of TPX2 (target protein for Xklp2) by association of Importin-α is abolished by Ran∗GTP-mediated complex dissociation. TPX2 is a microtubuli-associated protein targeting motor proteins to the minus-ends of microtubuli (Wittmann et al., 2000). It, furthermore, activates the Aurora A kinase which is crucial for proper centrosome separation after the mitotic spindle has been formed (Eyers and Maller, 2004). On the other hand, NuMA (nuclear mitotic apparatus protein) is released from an inhibitory complex with Importin-β to regulate microtubuli organization in the spindle.

TABLE 1.3: Mitotic targets of RanGTP in spindle assembly

SAF	Mitotic function	Exp. system	Karyopherin	References
Direct targets				
TPX2	MAP, MT bundling	XEE, CMCs	Importin-α	(Gruss et al., 2001)
				(Trieselmann et al., 2003)
NuMA	MAP	XEE	Importinβ	(Nachury et al., 2001)
				(Wiese et al., 2001)
Kid	Chromokinesin	HCE, CMCs	Importin-α, -β	(Trieselmann et al., 2003)
				(Tahara et al., 2008)
XCTK2	Kinesin, MAP	XEE	Importin-α, -β	(Ems-McClung et al., 2004)
RAE1	MAP, RNA binding	XEE	Importin-β	(Blower et al., 2005)
NuSAP	MAP, MT stabilization/bundling	XEE, CMCs	Importin-α, -β, -7	(Ribbeck et al., 2006)
HURP	MAP, k-fibre stabilization/tension	XEE, CMCs	Importin-β	(Koffa et al., 2006)
				(Silljé et al., 2006)
Lamin B	Mitotic matrix formation	XEE	Unknown	(Tsai et al., 2006)
CDK11	MT stalibization	XEE	Importin-α, -β	(Yokoyama et al., 2008)
CRB3-CLPI	Polarized membrane targeting	Epithelial cells	Importin-β	(Fan et al., 2007)
Indirect targets				
TACC/Maskin	MT stabilization	XEE	Importin-α?	(Albee et al., 2006)
				(Sato and Toda, 2007)
XMAP215	MAP	XEE	Unknown	(Wilde et al., 2001)
				(Koffa et al., 2006)
Aurora A	Mitotic kinase	CEE, HCE	Importin-α, -β	(Trieselmann et al., 2003)
				(Tsai et al., 2003)
XRHAMM	MT nucleation	XEE	Unknown	(Groen et al., 2004)
BRCA1-BARD1	Mitotic spindle assembly	XEE, CMCs	Unknown	(Joukov et al., 2006)
Crm1-dependent				
RanBP2	K-fibre formation	CMCs	Crm1	(Arnaoutov et al., 2005)
RanGAP1	K-fibre formation	CMCs	Crm1	(Arnaoutov et al., 2005)
CPC	K-fibre attachment,	CMCs	Crm1	(Knauer et al., 2006)
	checkpoint signaling			

Abbreviations: XEE (Xenopus laevis egg extract), CMC (cultured mammalian cells), HCE (human cell extract), MT (microtubuli), MAP (microtubuli-associated protein), K-fibre (kinetochore-fibre), Kid (kinesin-like DNA binding protein), XCTK2 (Xenopus carboxy-terminal kinesin 2), RAE1 (ribonucleic acid export 1), NuSAP (nucleolar- and spindle-associated protein), HURP (hepatoma upregulated protein), CDK11 (cyclin-dependent kinase-11), CRB3-CLPI (Crumbs homolog 3 ending in CLPI), TACC (transforming acidic coiled-coil-containing protein 1), XMAP215 (X microtubuli-associated protein 215), XRHAMM (Xenopus receptor for hyaluronic acid-mediated motility), BRCA-1 (breast cancer type-1 susceptibility protein), BARD-1 (BRCA-associated RING domain protein), CPC (chromosome passenger complex); Table modified after (Clarke and Zhang, 2008)

Apart from the Importin-dependent recruitment of factors, some proteins are also localized via their NES by a Crm1-Ran∗GTP-dependent pathway, analogous to the protein export during interphase. Another way of regulatory influence of Ran

on mitotic processes, especially mitotic spindle assembly, involves the APC/C (anaphase-promoting complex). APC/C promotes the ubiquitination and subsequent degradation of several SAFs, namely BARD1, HMMMR, HURP and NuSAP (Song and Rape, 2010). Importin-β was shown to inhibit the APC/C-dependent ubiquitination of these factors. Thus, the interplay of APC/C and the Importin-β-Ran$*$GTP pathway regulates mitotic spindle assembly by controlling the amount of SAFs. Table 1.2.2 lists mitotic targets of Ran$*$GTP in the process of spindle assembly.

1.2.3 Nuclear envelope formation

Besides its importance for nucleocytoplasmic transport and regulation of mitotic spindle assembly, Ran is required for nuclear envelope reformation at the end of mitosis and for post-mitotic NPC assembly (Hetzer et al., 2000; Ryan et al., 2003; Zhang and Clarke, 2000). Bead-immobilized Ran was able to induce the formation of nuclear envelope-like structures in cell-free *Xenopus* egg extracts. Surprisingly, these structures contained NPCs. Furthermore, Hetzer *et al.* showed the necessity of RCC1 and Ran for the early stages of nuclear envelope formation. The molecular mechanisms of post-mitotic NPC-assembly are not yet fully understood, however, the involvement of Ran, Importin-β and the Nup107-Nup160-complex is clear (Harel et al., 2003; Walther et al., 2003). While an excess of Importin-β inhibits nuclear membrane fusion and NPC-assembly, Ran$*$GTP stimulates these processes. Most likely, Importin-β acts as a negative regulator by refraining the nucleoporins Nup107-Nup160 from the chromatin surface. In analogy to the releasing effect on SAFs, Ran$*$GTP overcomes this effect of Importin-β by dissociating the inhibitory complexes.

1.2.4 Ran-interacting proteins

Guanine-nucleotide exchange factor (GEF)

RCC1 (regulator of chromosome condensation 1) localizes to chromatin and is the only GEF acting on the small GNBP Ran (Bischoff and Ponstingl, 1991a,b; Ohtsubo et al., 1989). The yeast protein Mog1 stabilizes the nucleotide-free conformation of Ran, however, true GEF-activity could not be shown, therefore Mog1 was postulated to be a nucleotide-release factor (Steggerda and Paschal, 2000, 2001).

The exible N-terminal region (NTR) of RCC1 is responsible for chromatin binding (Moore et al., 2002). Deletion thereof disperses RCC1 from mitotic chromosomes, resulting in spindle abnormalities due to the disturbance of the Ran GTP localization. The NTR, furthermore, carries a bipartite NLS recognized by Importin- / 3 and is subject to post-translational modi cation. The N-terminal methionine is removed and serine two is mono-, di- or tri-methylated (Chen et al., 2007a). This methylation is required for chromatin interaction but is not regulated during the cell cycle. In contrast to the stable methylation, phosphorylation at serine two and eleven by CDK1/cyclin B1 is restricted to mitosis. Phosphorylation disrupts the binding of Importin- / 3 to the N-terminal NLS and thereby preserves the mobility of RCC1 during metaphase (Hutchins et al., 2004; Li and Zheng, 2004).

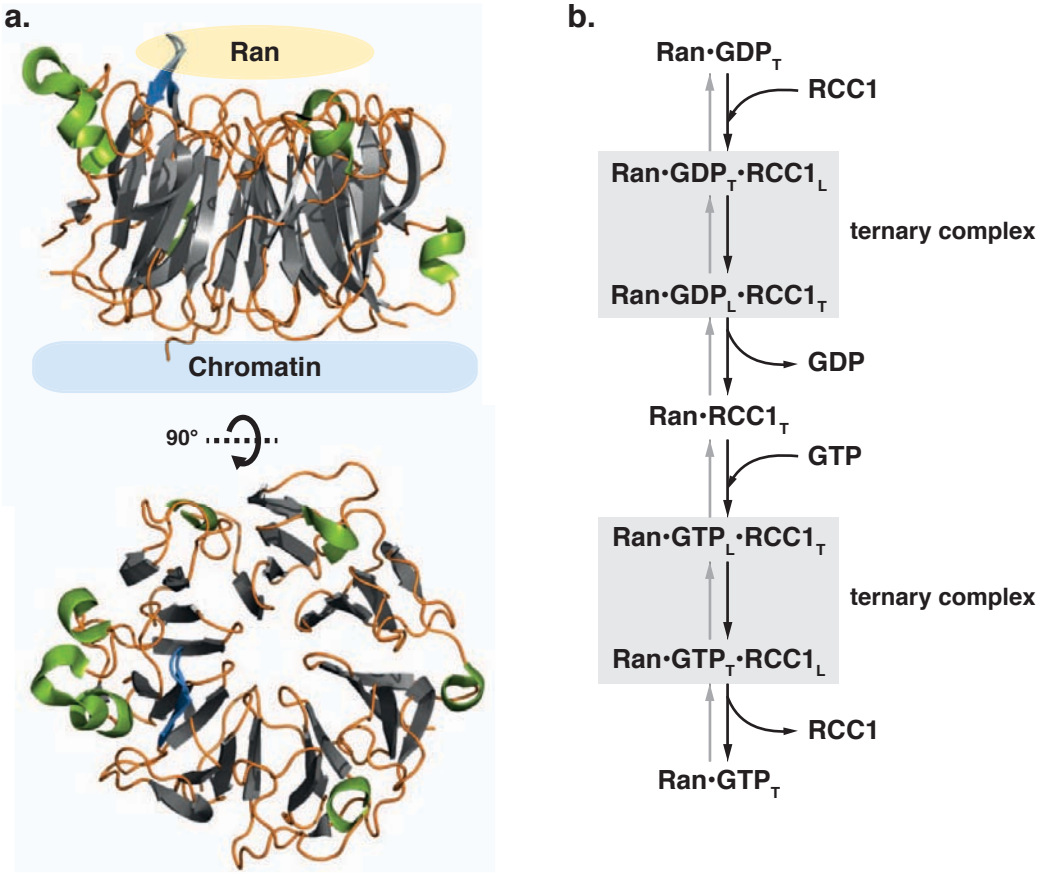

FIGURE 1.7: **Crystal structure and mechanism of action of RCC1.** (a) Cartoon-presentation of the -propeller-fold of RCC1 from two di erent angles (PDB:1I2M). Secondary structure elements are colored in grey (sheets), green (helices) and orange (loops) and the Ran- (yellow) and chromatin-binding site (light-blue) are indicated. (b) Multi-step mechanism of RCC1-catalyzed nucleotide exchange on Ran. The observed ternary complex comprises two intermediates, which change from tight (T) to loose (L) binding of RCC1 or nucleotide and *vice versa*.

Alternative splicing of the single RCC1-gene in animal cells results in three RCC1 isoforms (RCC1α/ β/ γ) which exhibit different expression levels in specific tissues (Hood and Clarke, 2007). The β- and γ-isoforms contain short inserts in the NTR, resulting in altered chromatin binding properties, molecular interactions and slightly different regulation by phosphorylation.

The crystal structure of RCC1 revealed a seven bladed β-propeller with seven 51 - 68 residue repeats (Figure 1.7.a) (Renault et al., 1998). Ran-interaction buries a large solvent-accessible surface area but otherwise entails only minor structural alterations (Renault et al., 2001). Ran contacts all seven propeller blades of RCC1. The binding-interface is relatively flat, except for a protruding β-sheet in blade three (residues 146 - 153 of RCC1), the so called β-wedge. Structural changes in the Ran structure upon binding of RCC1 involve switch II, the helices α3 and α4, as well as the region around the NKxD base-binding motif. Ran, furthermore, adopts the GDP-conformation - with an extra β-strand in the switch I region. The C-terminal extension is not visible in the complex-structure, indicating a high degree of flexibility.

RCC1 has the highest binding affinity for nucleotide-free Ran but binds to both nucleotide-states of Ran with similar (lower) affinity (Ran$*$GDP $1.3{\cdot}10^5 M^{-1}$; Ran$*$GTP $1.8{\cdot}10^5 M^{-1}$)(Klebe et al., 1995a). In the course of RCC1-catalyzed nucleotide exchange a ternary complex Ran$*$GXP$*$RCC1 is formed, which indicates that GXP and RCC1 claim spatially distinct or partially overlapping binding sites. A simple mechanism of facilitated dissociation is accepted for the reaction meaning that the high-affinity binding is the product of several low-affinity interactions (Klebe et al., 1995a; Prinz and Striessnig, 1993). In other words, the low-affinity binding of RCC1 to Ran$*$GXP is followed by a competition between RCC1 and GXP for weak interactions and results in a number of small conformational changes. As a result of this process, a ternary complex with low nucleotide affinity and high RCC1 affinity is formed, which allows fast dissociation of GXP and formation of a tight binary Ran$*$RCC1 complex. The rebinding of nucleotide, in turn, displaces RCC1 in an analogous manner - via the formation of a ternary complex (Figure 1.7). Notably, RCC1-action does not influence the binding characteristics (affinities or on/off-rates) of GDP or GTP on Ran. The net generation of Ran$*$GTP is solely due to a 10-fold higher concentration of GTP over GDP in the cell. The RCC1-mediated catalysis of nucleotide exchange on Ran results in

a 10^5-fold increased nucleotide exchange rate (from $1.8\text{x}10^{-5}\,s^{-1}$ to $2.1\,s^{-1}$)(Klebe et al., 1995a).

Ran GTPase activation protein (RanGAP)

The Ran GTPase-activating protein (RanGAP) was first reported as rna1, a mutant defective in mRNA processing and -transport in *S.cerevisiae* (Hartwell, 1967; Hopper et al., 1978). RanGAP is exclusively cytosolic during interphase, however, a fraction is tethered to the cytosolic face of the NPC. The localization to the nuclear pore is mediated by SUMO-1-modification at the C-terminus and binding to the Ran binding protein 2 (RanBP2) and the E2-conjugating enzyme Ubc9 (Mahajan et al., 1997; Matunis et al., 1996, 1998; Werner et al., 2012).RanGAP stimulates the GTP-hydrolysis on Ran 10^5-fold from $1.5\text{x}10^{-5}\,s^{-1}$ to $5.0\,s^{-1}$ (Klebe et al., 1995a). RanBPs are able to co-stimulate the GAP-reaction (Bischoff et al., 1995; Villa Braslavsky et al., 2000). RanGAP-catalyzed hydrolysis either takes place in the cytosol or on the cytoplasmic fibrils of the NPC and is independent of the translocation process trough the nuclear pore (Ribbeck and Görlich, 2001). In contrast to RasGAPs and RhoGAPs, RanGAP does not utilize an arginine finger to complement and stabilize the catalytic machinery of the G-protein (Seewald et al., 2002). In fact, the catalytic machinery is exclusively provided by Ran itself. However, RanGAP assists in positioning the catalytic glutamine Q69 and by shielding the active site from the solvent. Please refer to section 4.2 for mechanistic details.

Importin-β

Importin-β belongs to the karyopherin-β superfamily, which is also named Importin-β superfamily after the first receptor identified. The karyopherins are subdivided into importins and exportins to specify the direction of transport. The superfamily counts 14 members in yeast and more than 20 in humans. Proteins carrying an NLS or NES are bound by the respective karyopherin and transported through the NPC. A small number of proteins is able to pass the NPC directly (e.g. β-catenin) and also mRNAs use a different pathway (Köhler and Hurt, 2007).

Importin-β is the most prominent member of the family, which is also reflected by a high intracellular concentration of approximately $3\,\mu$M (Kutay et al., 1997). Import cargo recognition and protein import is mediated by adaptor proteins, which bind the cargo-NLS and Importin-β simultaneously. Up to eleven adaptor proteins are known so far and each heterodimer exhibits a different cargo specificity (Fried and Kutay, 2003; Jäkel et al., 2002). In the classical import pathway the

NLS of cytoplasmic cargoes is rst recognized and bound by Importin- , which then associates with Importin- via its N-terminal Importin- -binding (IBB) domain. The ternary complex (NLS/Importin- /) translocates trough the NPC and dissociates upon Ran GTP binding to Importin- in the nucleus.

Importin- is the typical structure of the superfamily (Figure 1.8). Two antiparallel -helices joined by a turn form the basic HEAT-repeat (Huntingtin, elongation factor 3, protein phosphatase 2A, and the yeast kinase TOR1) element. The overall protein consists of 19 such HEAT-repeats forming a short superhelix with an N-terminal Ran-binding domain (Cingolani et al., 1999; Vetter et al., 1999). Comparison of the seven available crystal structures of Importin- complexes (Importin- , 1QGK; Ran, 1IBR; FxFG-Nucleoporin, 1F59; SREBP-2, 1UKL; Nup1P, 1BPT; Snurportin, 2P8Q; Snail1, 3W5K) reveals individual binding sites and modes of interaction for every interaction partner. The Importin exhibits a high degree of exibility, creating binding sites by opening up repeats or wrapping the superhelix around the binding partner (Stewart, 2003).

The passage through the nuclear pore is regulated by the NPC, which prevents passive di usion of proteins larger than 40 kDa. The central tunnel of the NPC is lined by FG (phenylalanine-glycine)-rich repeat-containing nucleoporins. Members of the Importin- superfamily interact with these FG-repeats and facilitate translocation without direct energy consumption. One transport model suggests a gradient of increasing a nity through the pore, with the highest a nity of the transport complex for the last nucleoporin (Ben-Efraim and Gerace, 2001; Pyhtila and Rexach, 2003). The identi cation of two FG-repeat-binding regions on

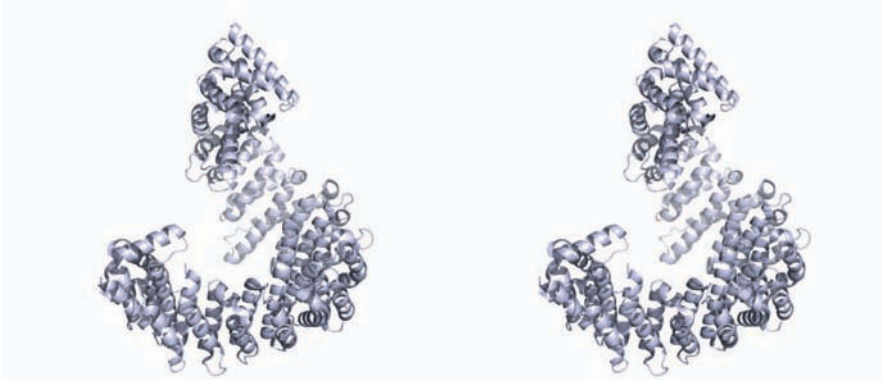

FIGURE 1.8: **Crystal structre of Importin- .**Stereo-view of the -helical structure of Importin- , forming a superhelix.

Importin-β initiated speculations about a multistep translocation process (Bednenko et al., 2003). The importin could step from one nucleoporin to the adjacent one by alternating detachment of one FG-binding site.

Apart from nucleocytoplasmic transport processes, Importin-β is involved in mitotic spindle assembly and nuclear envelope formation (refer to subsections 1.2.2, 1.2.3). Furthermore, Importinβ/α were reported to be part of the second, delayed signaling wave after axonal injury (Guzik and Goldstein, 2004; Hanz et al., 2003). Jakel *et al.* also assigned a cytoplasmic chaperone function to the Importin-β/-7-complex (Jäkel et al., 2002) which, by shielding basic domains, prevents aggregation of certain proteins (e.g. histone 1) in the cytosol.

Nuclear transport factor 2 (NTF2)

The Ran-binding protein NTF2 was identified as an essential protein in yeast (Corbett and Silver, 1996; Nehrbass and Blobel, 1996; Paschal et al., 1996). It is a homodimer able to bind to Ran and FG-repeat-containing nucleoporins (Isgro and Schulten, 2007). Since NTF2 transports Ran$*$GDP back into the nucleus, it is crucial for Ran-dependent nucleocytoplasmic transport (Ribbeck et al., 1998; Smith et al., 1998). Mutants defective in Ran-binding disrupt protein-transport and proper cell-cycle progression (Clarkson et al., 1997; Stewart et al., 1998).

The crystal structure of NTF2 shows a cone-shaped fold forming a distinctive hydrophobic cavity surrounded by negatively charged residues (Bullock et al., 1996). This specific fold is common to the members of the NTF2-like superfamily. Due to the fact that this fold can accommodate many different sequences, this superfamily comprises proteins without a common sequence motif and with or without enzymatic activity. Examples for the NTF2-like superfamily are SnoaL polyketide cyclase, scytalone dehydratase and Mba1 (multi-copy Bypass of AFG3).

NTF2 specifically binds Ran$*$GDP and the interaction primarily involves the switch II region (residues 65 - 78 of Ran), to a lesser extend switch I (39 - 43)(Stewart et al., 1998). The binding to the switch region explains the nucleotide-specificity of NTF2. The aromatic ring of Phe72 of Ran is buried in the hydrophobic cavity of NTF2. This corresponds to 22% of the buried binding surface and is a major contribution to complex formation. Furthermore, three salt bridges have been reported to be essential for the interaction: Glu42^{NTF2} - Arg76^{Ran} and D92/94^{NTF2} - Lys71^{Ran}. Mutation of these residues results in the loss of interaction between NTF2 and Ran (Kent et al., 1999; Stewart et al., 1998).

1.3 Protein lysine acetylation

Post-translational modification of proteins is a diverse and powerful regulatory tool of living cells. The spectrum includes anorganic (e.g. phosphorylation) and organic functional groups (e.g. acylation, glycosylation), proteins (e.g. ubiquitylation, SUMOylation), lipids (e.g. prenylation) and alterations of bonds or conformations (e.g. disulfide bonds, peptidy-prolyl-*cis/trans*-isomerization). Protein acetylation is a kind of acylation taking place at the ϵ-amino group of lysines or at the α-amino group of the N-terminal amino acid. Most eukaryotic proteins are co-translationally acetylated at the N-terminus by a family of N-terminal acetyltransferases (NATs) (Arnesen et al., 2009; Brown and Roberts, 1976). In contrast to lysine acetylation, N-terminal acetylation is an irreversible PTM. It is involved in the regulation of protein degradation via the N-end rule (Scott, 2011), protein targeting (Hwang 2010), metabolism and apoptotic processes (Hwang et al., 2010; Scott et al., 2011).

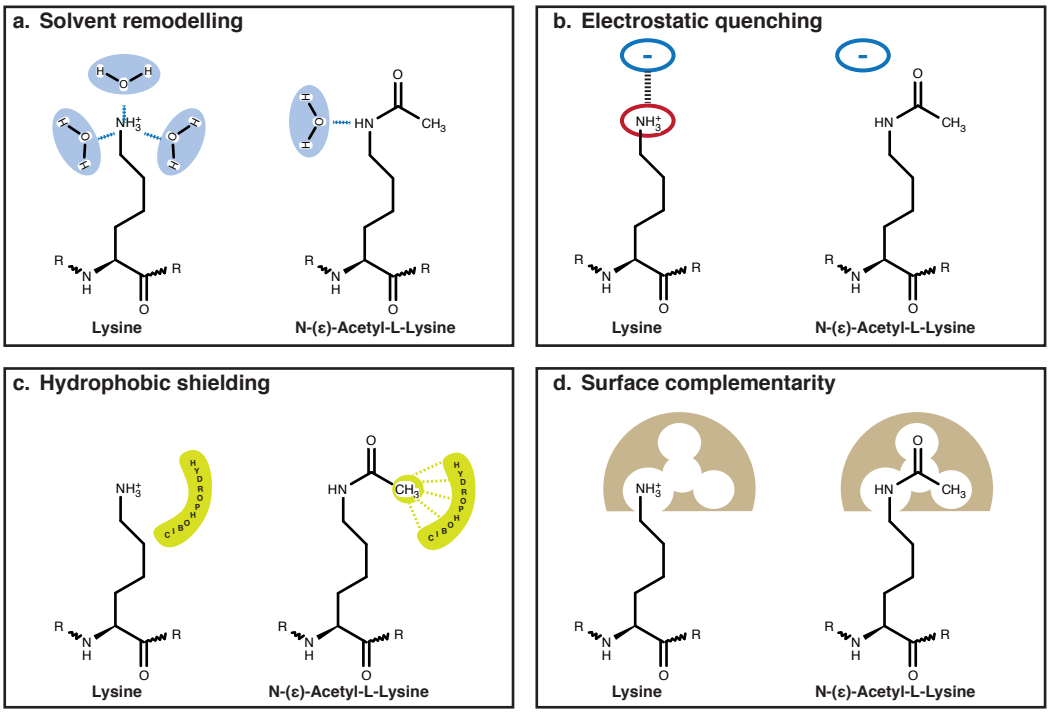

FIGURE 1.9: **Impact of lysine acetylation.**Comparison of chemical characteristics of lysine and acetyl-lysine regarding (a) solvent remodeling, (b) electrostatic and (c) hydrophobic interactions and (d) surface complementarity.

Reversible acetylation at the ϵ-amino group of lysines was first identified on histones by Allfrey *et al.* in 1964 (Allfrey et al., 1964). It took more than twenty

years until the first non-histone target of acetylation was discovered: the cytosolic α-tubulin (L'Hernault and Rosenbaum, 1983). The tumor suppressor p53 and the HIV transcriptional regulator Tat followed another decade later (Gu and Roeder, 1997; Ott et al., 1999). By now the existence of lysine acetylation in all organisms, from bacteria to humans, is established knowledge (Kim and Yang, 2011; Soufi et al., 2012).

The molecular effects of this relatively small modification on the lysine side chain are diverse and provide a broad spectrum of regulatory modes of action (Figure 1.9). The effect of electrostatic quenching might be the most dominant effect. Acetylation of the lysine side chain neutralizes the prominent positive charge, which can entail drastic consequences for protein structure or protein-protein interactions, e.g. by disrupting an essential salt bridge. The altered spacial demand of acetyl-lysine is, furthermore, relevant for the surface complementarity of two interaction partners, e.g. enzymes and substrate. The modification can either create or disrupt a complementary interaction surface and consequently facilitate/strengthen or disrupt/weaken binding, respectively. The acetylation also changes chemical characteristics of the side chain and thereby affects the hydrophobicity and the solvent-interaction (solvent remodeling) of the lysine residue.

1.3.1 Characteristics and regulation of lysine acetylation

Lysine acetylation is a reversible post-translational modification (PTM). The dynamics of this system originate from the existence of enzymes which generate (writers) and remove (erasers) the modification in a regulated manner. The recognition of the lysine acetylation by specific proteins (readers) allows for the signaling function in several cellular processes.

Lysine deacetylases

The removal of the acetyl-moiety by hydrolysis is catalyzed by lysine deacetylases (KDACs). There are 18 human KDACs, subdivided into four classes (KDAC I - IV): classes I, II and IV utilize a Zn^{2+}-dependent mechanism, whereas KDAC class III uses nicotinamide adenine dinucleotide (NAD^+) as a cofactor. Enzymes of KDAC class III are referred to as sirtuins- named after the yeast homolog Sir2 (silent information regulator), which was originally identified as a regulator of transcriptional silencing of mating-type loci, telomeres and ribosomal DNA (Shore et al., 1984). Based on sequence-based phylogenetic analysis mammalian sirtuins

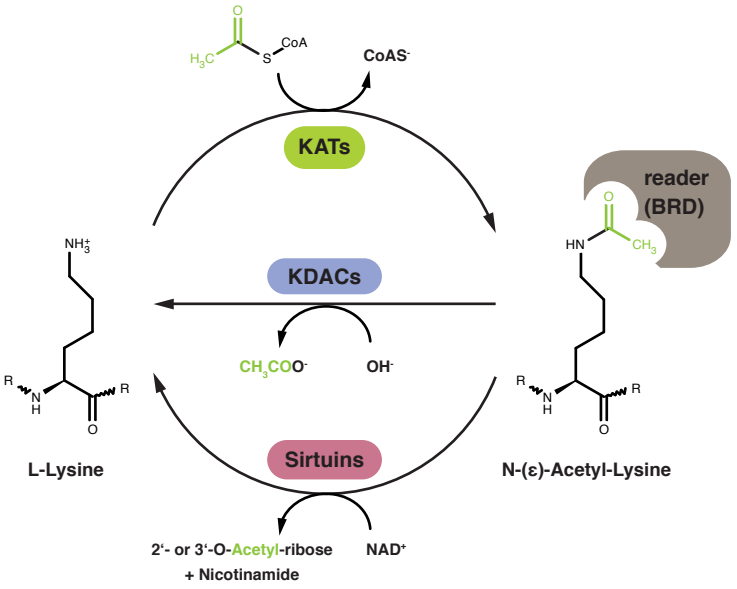

FIGURE 1.10: **Regulation of lysine acetylation.**Lysine-acetylation at the -amino group is a reversible post-translational modi cation which is regulated by acetyltransferases (KATs) and deacetylases (KDACs and sirtuins). Proteins with a bromodomain (BRD) can speci cally recognize and bind acetyl-lysine.

can be further subdivided into four classes (I - IV)(Table 1.4). Despite their function as transcriptional regulators, sirtuins are also regarded as energy sensors, since their NAD^+-dependence establishes a direct link to the cell metabolism (Imai et al., 2000). The activation of sirtuins was reported to be bene cial for metabolism-related diseases (e.g. diabetes 2, obesity), neurodegenerative diseases (Alzheimers, Parkinsons) and the stimulation of mitochondrial activity (reviewed in (Houtkooper et al., 2012)). Of the seven human sirtuins only three (sirtuins 1, 2 and 3) exhibit a decent deacetylase activity, whereas the other members of

TABLE 1.4: Sirtuins

Sirtuin	Class	Localization	Activity	Target	Refs.
Sirt1	I	Nucleus, cytosol	Deacetylation	FOXO1, p53, Notch, NF- B, SREBP-1c	(Daitoku et al., 2011; Lee and Gu, 2013) (Guarani et al., 2011; Kauppinen et al., 2013) (Ponugoti et al., 2010)
Sirt2	I	Cytosol	Deacetylation	Tubulin, PEPCK, FOXO1, PAR3	(Jiang et al., 2011; North et al., 2003) (Beirowski et al., 2011; Daitoku et al., 2011)
Sirt3	I	Mitochindria	Deacetylation	GDH SOD2, IDH2	(Lombard et al., 2007) (Qiu et al., 2010; Someya et al., 2010)
Sirt4	II	Mitochondria	ADP-ribosylation	GDH	(Haigis et al., 2006)
Sirt5	III	Mitochondria	Deglutarylation, demalonylation, desuccinylation		(Park et al., 2013)
Sirt6	IV	Nucleus	Deacetylation, demyristoylation	H3K9, H3K56	(Pan et al., 2011)
Sirt7	IV	Nucleolus	Deacetylation	H3K18	(Barber et al., 2012)

the family have to be regarded as deacylating enzymes catalyzing demalonylation, desuccinylation, deglutarylation or demyristoylation and ADP-ribosylation (Table 1.4)(Choudhary et al., 2014).

Lysine acetyltransferases

Lysine acetyltransferases (KATs) are "writers" of lysine acetylation by transferring an acetyl-group from the co-factor acetyl-CoA to the ϵ-amino group of the target lysine. So far, 22 different KATs were identified in human and mouse (reviewed in (Lee and Workman, 2007; Roth et al., 2001)). Based on sequence- and structural divergence these can be subdivided into five subfamilies: HAT1, Gcn5/PCAF, MYST (MOZ, Ybf2, Sas2, Tip60), p300/CBP and Rtt109 (Friedmann and Marmorstein, 2013). All subfamilies share a structurally conserved core region comprised of a three-stranded β-sheet and a helix, which is flanked by divergent regions.

Interestingly, little to no sequence homology is present between the subfamilies and, in conformity with this fact, all subfamilies employ different chemical strategies for catalysis (Yuan and Marmorstein, 2013). However, they all need acetyl-CoA as a cofactor to act as acetyl-donor and to stabilize the fold of the acetyltransferase domain (Yuan and Marmorstein, 2013). Figure 1.11 depicts the basic mechanisms of the Gcn5-related- and the MYST-family KATs. Both families utilize a conserved glutamate as general base to either directly (MYST) or indirectly (via catalytic water, Gcn5-related KATs) activate the target lysine for the nucleophilic attack on the thioester bond. In the case of MYST family KATs, this step is preceded by the formation of an acetylated cysteine as a covalent intermediate. Whereas no general base/acid was identified for Rtt109-transferases, p300/CBP use a tyrosine as general acid.

KATs are regulated by a variety of different mechanisms. Changes of the subcellular localization can shift the substrate spectrum without affecting the molecular substrate specificity. The ubiquitin-dependent degradation of KATs is another way of controlling KAT-levels and -activities. Furthermore, acetyltransferases are often active in multiprotein-complexes and activity as well as substrate specificity has been observed to be influenced by the associated subunits (Shahbazian and Grunstein, 2007). KATs are also subject to regulation by post-translational modifications such as acetylation, phosphorylation or SUMOylation. Especially activation by autoacetylation is a common phenomenon in the KAT superfamily.

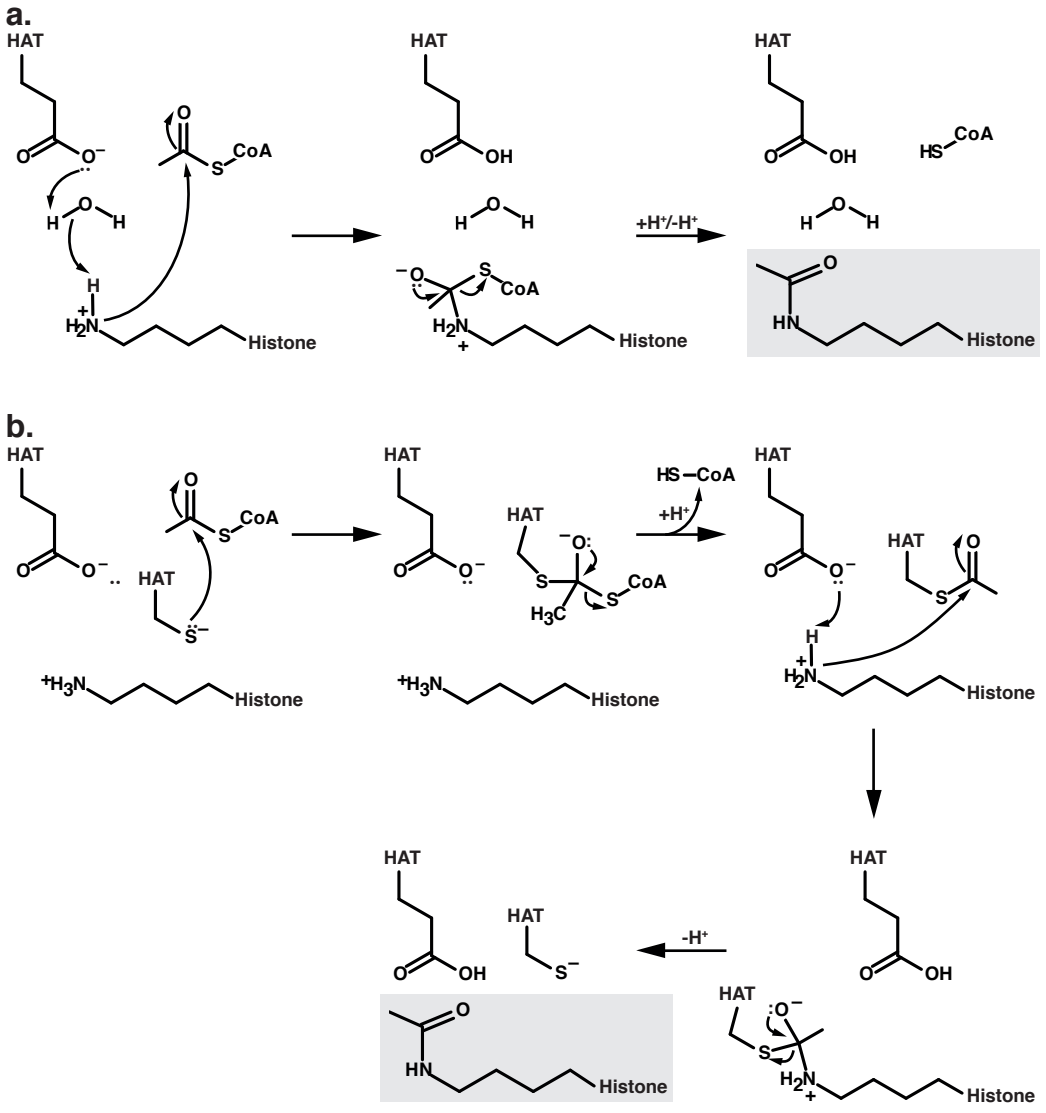

FIGURE 1.11: **KATs utilize a direct attack mechanism of acetylation.** The catalytic mechanism is depicted for (a) Gcn5-related and (b) MYST family acetyltransferases. Both families utilize a general base to catalyze the nucleophilic attack of the lysine amine on the thioester bond. MYST KATs form a covalent cysteine-intermediate before the acetyl-moiety is transferred to the lysine side chain.

Bromodomain-containing proteins

Acetylated lysines are specifically recognized and bound by bromodomain-containing proteins, also referred to as "readers" of this PTM. The bromodomain was named after the *Drosophila* protein brahma (Haynes et al., 1992; Tamkun et al., 1992). The conserved domain consist of around 120 amino acids arranged in an all-α-protein fold: a bundle of α-helices forming a hydrophobic pocket (Figure .1.12).

Bromodomains are often found in KATs and proteins involved in gene transcription (Jeanmougin et al., 1997). 46 acetyl-lysine-binding, bromodomain-containing proteins are predicted to be encoded in the human genome (Filippakopoulos et al., 2012).

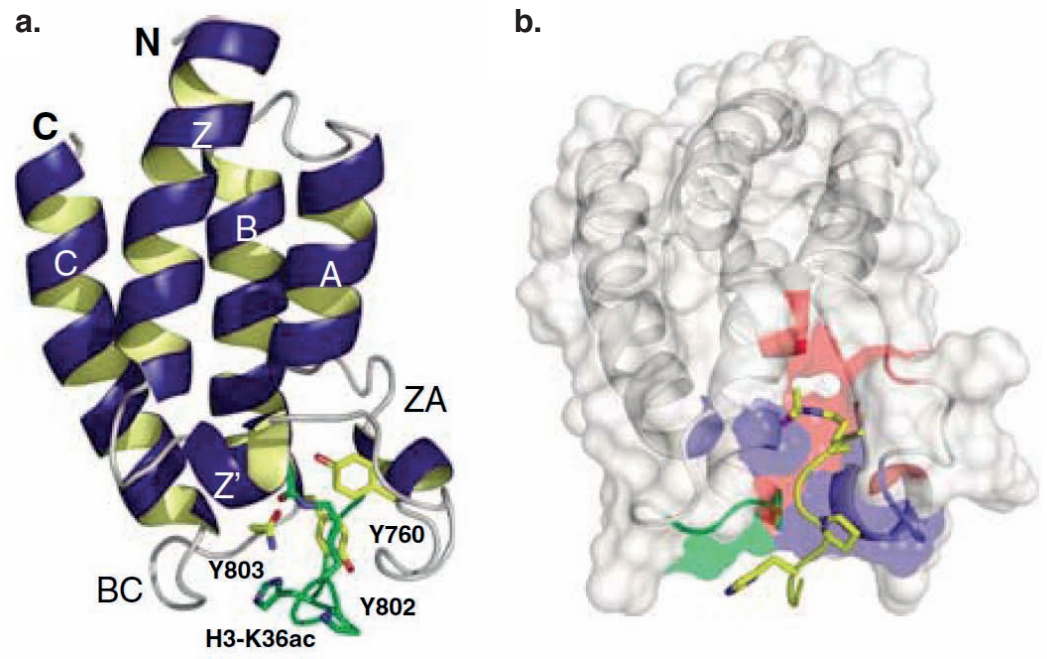

FIGURE 1.12: **Structure and acetyl-lysine recognition of the PCAF bromodomain.** (a) Cartoon presentation of the PCAF bromodomain bound to a lysine-acetylated peptide derived from histone H3 lysine 36. (b) The three main ligand contact sites, important for the recognition of the acetyl-lysine, are color-coded in red, blue and green. Modified after (Mujtaba et al., 2007)

1.3.2 Lysine acetylation as an emerging PTM

The rapid advances in high-resolution mass spectrometry (MS)-based proteomics result in an overwhelming amount of acetylome data sets, screening a broad spectrum of organisms and conditions and identifying an increasing number of acetylated proteins and acetylation sites. The regulatory potential of lysine acetylation in combination with the increasing number of identified acetylation sites prompted the hypothesis of acetylation as a PTM with a relevance rivaling that of phosphorylation (Kouzarides, 2000). While the functions of histone-acetylation are well studied, the roles of lysine acetylation are unclear for the majority of non-histone proteins identified in the acetylome screens (Khan and Khan, 2010). However,

due to the large number of analyzed organisms and conditions, several general conclusions can be drawn by now.

The comparison of the acetylome of different organisms reveals, that acetylation sites are frequently conserved across diverse organisms (Beltrao et al., 2012; Weinert et al., 2011; Zhang et al., 2009). Despite the fact, that histone-acetylation is well characterized, the majority of acetylation events occur on non-nuclear proteins (Choudhary et al., 2009; Kim et al., 2006; Zhao et al., 2010). Although quantification by MS-based proteomics is challenging, recent studies suggest a low overall stoichiometry for the majority of sites under the conditions tested (Baeza et al., 2014; Weinert et al., 2014). Interestingly, particularly mitochondrial proteins comprise a large proportion of the identified acetylation sites. The fact that this also applies to bacterial proteins is in agreement with the endosymbiotic theory (van Noort et al., 2012; Zhang et al., 2009).

An emerging body of evidence supports the theory of strong non-enzymatic protein acetylation in mitochondria and bacteria (Guan and Xiong, 2011; Newman et al., 2012). In mitochondria no acetyltransferase was identified so far, rather, does the higher pH of the mitochondrial matrix increase the reactivity of lysine side chains. Since the mitochondrial matrix is the primary site of acetyl-CoA metabolism, the highly reactive lysines come in contact with high levels of reactive acetyl-donors, such as acetyl-CoA. Mitochondrial levels of acetyl-CoA were reported to be 20- to 30-fold higher than cytosolic levels in yeast and rat, reaching up to millimolar levels in mitochondria (Garland et al., 1965; Weinert et al., 2014). Non-enzymatic lysine acetylation under these conditions is very likely. In fact, reproducing mitochondrial conditions *in vitro* resulted in non-enzymatic acetylation of mitochondrial and non-mitochondrial proteins (Wagner and Payne, 2013). The observation that mitochondrial acetylation always exerts an inhibitory effect led to the hypothesis of acetylation being a response to carbon stress and mitochondrial sirtuins (especially Sirt3) acting as detoxifying enzymes in protein-quality control (Wagner and Hirschey, 2014). Similar conditions were observed in bacteria (Weinert et al., 2013). Protein acetylation correlates with the abundance of the reactive metabolic intermediate acetyl-phosphate, e.g. increases in growth-arrested cells. The acetylation seems to be independent of the only *E.coli* acetyltransferase YfiQ (Pat in *Salmonella enterica*) and the sole sirtuin-class deacetylase, CobB, regulates only a small subset of sites (Lima et al., 2011; Starai and Escalante-Semerena, 2004).

Furthermore, incubation of proteins under the bacterial conditions *in vitro* also resulted in the acetylation of all sites identified *in vivo*.

Functional roles of lysine acetylation include:

1. Regulation of nucleic acid binding and protein-protein-interactions
2. Crosstalk with other PTMs
3. Regulation of enzymatic activity
4. Regulation of subcellular localization

1. Nucleic-acid binding and protein-protein interactions

The acetylation of histone-tails regulates the compaction of chromatin and, consequently, transcription (Tse et al., 1998). While histone-tails are hyperacetylated in euchromatin, they were found to be hypoacetylated in heterochromatin. The interplay of (reversible) histone acetylation and -methylation regulates transcriptional activation/inactivation. Another well established example is the acetylation of Tat by the acetyltransferase p300, which functions as a molecular switch between two Tat-activities and is the rate-limiting step for viral replication (Figure 1.13.a). Non-acetylated Tat binds to TAR (transactivating response element)

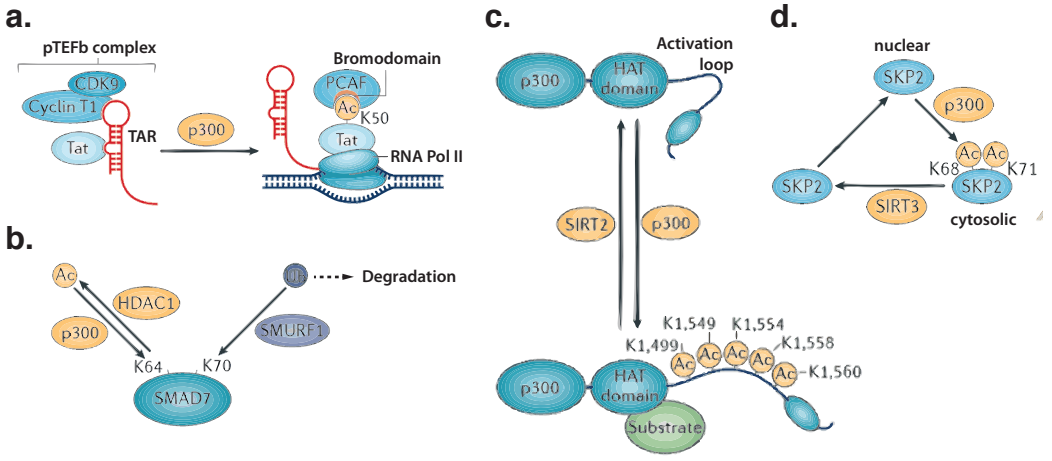

FIGURE 1.13: **Functional roles of lysine acetylation.** (a) Tat-acetylation regulates protein-protein interactions and functions as a molecular switch. (b) Crosstalk between acetylation and ubiquitylation regulates SMAD7 (Mothers against decapentaplegic homolog 7) stability. (c) Autoacetylation of p300 stimulates its catalytic activity. (d) The subcellular localization of the E3-ubiquitin ligase SKP2 (S-phase kinase associated protein 2) is controlled by acetylation/deacetylation of the NLS by p300/Sirt3. (modified after (Choudhary et al., 2014)

RNA, whereas acetylated Tat (on K50) binds the transcriptional coactivator PCAF via its bromodomain which promotes association with the elongating RNA polymerase II and HIV gene transcription elongation (Dorr et al., 2002; Mujtaba et al., 2002).

2. Cross-talk with other PTMs

The combination of several PTMs in one protein provides a different level of regulation. The cross-talk between two modifications can either be competitive, due to mutually exclusive modification sites, or non-competitive, if independent residues are modified. In the case of ubiquitylation or SUMOylation a competitive crosstalk is possible, since both modifications target lysine side chains. And actually one third of all acetylation sites in human cells were also found to be ubiquitylated (Wagner et al., 2011).

One example for the competitive cross-talk of acetylation and ubiquitylation is the protein SMAD7 (Mothers against decapentaplegic homolog 7). Acetylation of lysines 64 and 70 of SMAD7 by p300 prevents ubiquitylation (by SMURF 1) and subsequent proteasomal degradation (Figure 1.13.b). Deacetylation by HDAC1, however, makes the lysines accessible for ubiquitylation and initiates the degradation process (Grönroos et al., 2002; Simonsson et al., 2005). The well characterized tumor suppressor p53 provides two examples of non-competitive cross-talk between two different kinds of PTMs. Firstly, acetylation of p53 prevents the C-terminus from ubiquitylation and thereby stabilizes the protein. Secondly, methylation of lysine 372, in response to DNA damage, promotes acetylation of the adjacent lysine 373 and leads to transcription of p21 and cell cycle arrest (Ivanov et al., 2007).

3. Regulation of enzymatic activity

Lysine residues are often found in catalytic sites of enzymes. Taking into account, that lysine acetylation impacts drastically on the chemical characteristics of the lysine side chain, this modification can easily regulate enzymatic activities. The stimulation of catalytic activity by autoacetylation is known for several members of the KAT-family, including Tip60, CBP, PCAF and Rtt109. P300, for example, exhibits a low basal activity in the hypoacetylated state. Autoacetylation at five lysines within the activation loop motif (K1499/1549/1554/1558/1560) stimulates the catalytic activity (Figure 1.13.c)(Thompson et al., 2004). This process is probably induced by dimerization and reversed by Sirt2 (Black et al., 2008).

4. Regulation of subcellular localization
Acetylation can also impact on the subcellular localization of proteins, since positively charged lysine residues are often part of subcellular localization signal domains, e.g. monopartite NLS with a loose consensus sequence of K(K/R)X(K/R) (Conti and Kuriyan, 2000; Fontes et al., 2000). The S-phase kinase associated protein 2 (SKP2) is a E3 ubiquitin ligase involved in cell survival and tumorigenesis. Acetylation of lysines in the NLS by p300 results in nuclear export and cytoplasmic retention of SKP2. The ubiquitylation of E-cadherin in the cytoplasm enhances cell migration. Deacetylation of the NLS by Sirt3 restores the original nuclear localization of SKP2 (Figure 1.13.d).

1.3.3 Tools to study lysine acetylation

Quantitative mass spectrometry to study lysine acetylation
The increased interest in lysine acetylation of non-histone proteins is primarily owing to major advances in high-resolution MS-based proteomics. Over the last decade high-throughput analyses of different species/conditions identified thousands of new acetylation sites and acetylated proteins. In contrast to serine- or threonine phosphorylation, lysine-acetylated peptides are stable during MALDI- and ESI-ionization and can be reliably identified by their specific marker ions at m/z 126.1 and 143.1 (Trelle and Jensen, 2008). Most studies utilize the bottom-up, or "shotgun", approach to analyze a complex mixture of proteins, e.g. cell lysates. This method is based on the digestion of all proteins in the complex mixture (cell- or tissue lysate) and subsequent, mostly antibody-based, enrichment of modified peptides, followed by liquid chromatography and tandem MS. In contrast to the top-down approach, which analyzes intact proteins, the peptide-based shotgun-method makes the assignment of protein isoforms and modification patterns difficult. The predominant use of trypsin as a protease, furthermore, limits the detection to trypsin-accessible acetylation sites. However, due to the lack of efficient protein fractionation techniques the top-down approach was so far not feasible for high-throughput acetylomics. Technical advances in the field, such as the four-dimensional separation system by Tran *et al.* will close this gap in the near future (Tran et al., 2011).

The generally low stoichiometry of lysine acetylation poses a high technical challenge for the identification of this PTM in complex protein mixtures. One way to

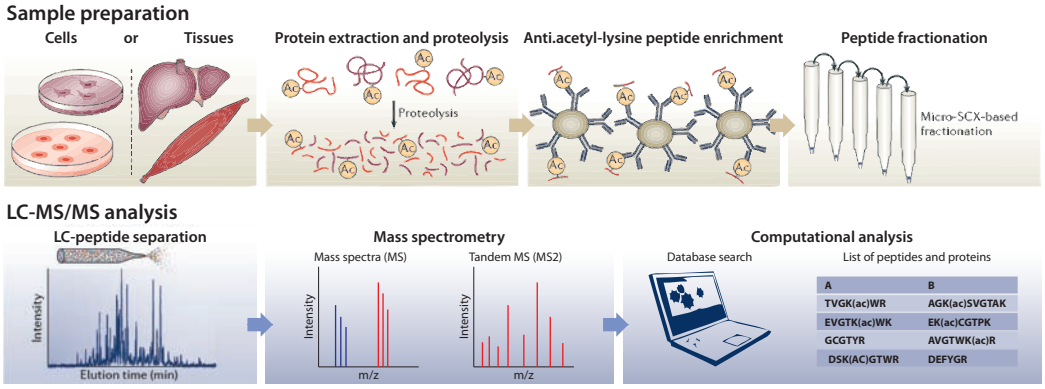

FIGURE 1.14: **MS-based global analysis of lysine acetylation.** Scheme of a typical bottom-up (shotgun) approach for large-scale acetylome studies. The procedure involves enzymatic digestion, peptide fractionation and liquid chromatography coupled to tandem MS. Software such as MaxQuant or ProteomeDiscoverer are used for the computational analysis. (modified after (Choudhary et al., 2014))

overcome this problem is the enrichment of acetylated peptides with acetyllysine-specific antibodies. This procedure is an inherent part of the described bottom-up approach, which drastically increases the number of identified acetylation sites. However, the dependence on specific antibodies also limits the reproducibility and complicates the interpretation of data, since target specificity, enrichment efficiency and batch-to-batch variations of the antibody directly influence the experimental outcome (Shaw et al., 2011). The reduction of sample complexity and increase of the dynamic range by fractionation also allows detection of low-abundant proteins/modifications at the expense of increased input material and measurement time. Fractionation is typically achieved by separating different cellular compartments, electrophoresis of proteins and/or chromatographic separation of proteins/peptides. The increased speed and sensitivity of new mass spectrometers reduces the importance of peptide enrichment and fractionation for the detection of low-abundance proteins or modification.

Quantification

The quantification of detected PTMs is crucial for the interpretation of the biological relevance, especially against the background of increasing evidence for non-enzymatic acetylation. The determination of absolute quantities is possible by comparing the amount of modified peptide to an injected labeled peptide standard (e.g. AQUA-method). Due to the label the standard peak can be distinguished from the peptide peak and absolute quantity can be calculated from the

peak ratios (Gerber et al., 2003). For high-throughput acetylome studies, relative quantification techniques such as metabolic or chemical labeling are used as routine in most labs. This approach can identify regulated acetylation sites by comparing the peptide intensities under two or more distinct condition, without providing an absolute stoichiometry. A schematic overview of the different quantification methods is shown in Figure 1.15.

Using metabolic labeling, or SILAC (stable isotope labeling by aminoacids in cell culture), up to three different conditions can be analyzed in parallel. The different cell populations are cultured in normal (light) medium and in medium containing amino acids (lysine or arginine) labeled with stable, non-radioactive isotopes (heavy). The incorporation of the isotopes results in chemically identical protein/peptides which can be attributed to the respective growth condition by the detected mass difference. Thus, lysates of the conditions are combined and analyzed together which reduces quantitative variability due to subsequent biochemical manipulation/sample handling. This principle can also be used to analyze *de novo* protein production. In that case, heavy medium is only added for a short period of time (pulsed SILAC).

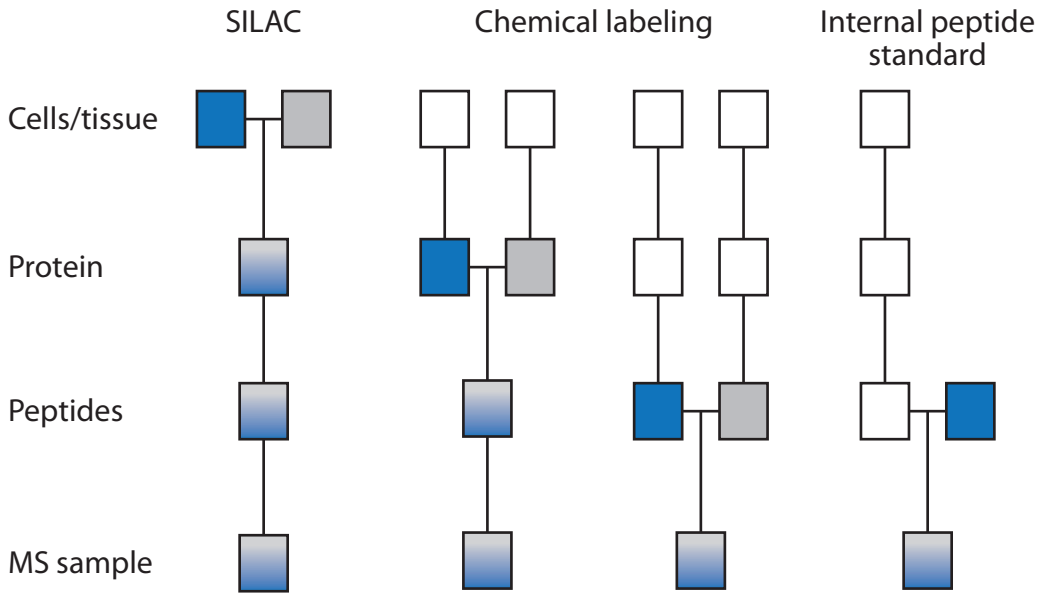

FIGURE 1.15: **Comparison of quantification strategies.** Comparison of quantification strategies based on labeling techniques or external standards. The reference (label or standard) can be introduced at different stages of the procedure.

The major advantage of chemical isobaric labeling compared to metabolic labeling, is the higher number of conditions/samples which can be analyzed in parallel. The different isobaric labeling techniques (TMT,Tandem mass tag; iTRAQ, isobaric tags for relative and absolute quantification) are based on isobaric mass tags, which are chromatographically indistinguishable but fragment into reporter ions with different masses during tandem MS. The number of analyzed conditions is merely limited by the number of available isobaric tags (currently 8-plex for iTRAQ). The samples are chemically labeled after proteolytic digestion and then combined to be measured and analyzed together. This procedure is more susceptible to variability and manipulations since the samples are combined much later than in the case of SILAC. Label-free quantification uses peptide intensities (and less often peptide counts) of two or more samples to determine relative abundances of modified peptides.

Acetylation mimics as tools

To study the molecular effects of lysine acetylation *in vitro*, site-specifically acetylated proteins are important tools. However, these are difficult to obtain. Chemical acetylation of recombinant proteins is not site-specific and does in most cases result in a mixture of acetylated species if several acetyl-donors are available. The use of recombinant acetyltransferases is an alternative to chemical acetylation. However, the enzyme-specific sites often unknown and the degree of modification is difficult to control and in most cases far from quantitative. Furthermore, the problem of site-specificity also applies to *in vitro* KAT-catalyzed acetylation, since the target specificity of KATs often depends on the formation of multi-protein complexes *in vivo*. Thus, often more than one lysine is targeted by the enzyme *in vitro*. Native chemical ligation introduces the acetyl-lysine by ligating a modified synthetic peptide with the recombinant protein core carrying an engineered N-terminus (reactive cysteine at the end) (Figure 1.16) (He et al., 2003). This strategy is not suitable to introduce acetyl-lysine in the core of the protein.

Acetylation mimics, such as glutamine and arginine, are often used to study the effects of lysine acetylation *in vivo* and *in vitro*. Usually, glutamine is regarded as the residue representing the acetylated lysine, whereas arginine mimics the non-acetylated/acetylatable lysine. In terms of charge characteristics, this assignment might be appropriate, however, with respect to the steric properties arginine is the better mimic for acetyllysine.

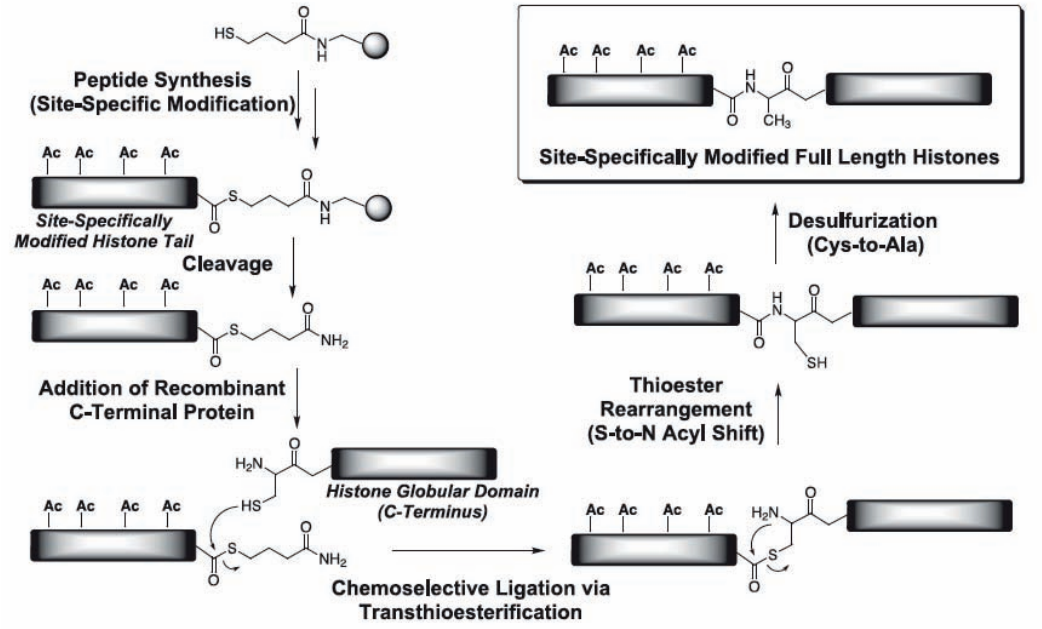

FIGURE 1.16: **Chemical ligation for the modification of C- or N-terminal domains.** The acetyl-lysine is incorporated into the synthetic terminal peptide, which is then ligated to the (recombinant) globular domain of the protein by transthioesterification. Thioester rearrangement followed by desulfurization results in the acetylated protein. (modified after (He et al., 2003))

Huang *et al.* presented MTCTK (methylthiocarbonyl-thiaLys) as an acetyl-lysine analog (Huang et al., 2010). To create this analog, the lysine of interest is replaced by cysteine, which is then used as reactive nucleophile for the subsequent alkylation (Figure 1.17). MTCTK, which was used for the functional characterization of acetylated CK2 protein kinase, was shown to be recognized by site-specific anti-acetyl-lysine antibodies and a bromodomain (Huang et al., 2010). A clear disadvantage of this technique is the need for removal of all additional cysteines from

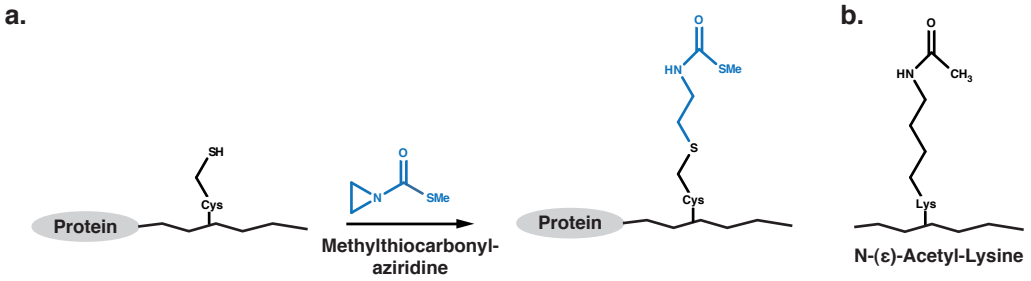

FIGURE 1.17: **Acetyl-lysine-analog by alkylation of cysteines.**(a)The alkylation of cysteine with Methylthiocarbonyl-aziridine yiels an acetyl-lysine analog. (b) In comparison to acetyl-lysine several chemical properties of the analog are altered by the carbon-sulphur-exchange.

the sequence. The replacement of one carbon by sulphur, furthermore, changes several chemical properties compared to acetyl-lysine (bond-length and -angle, pK_a of amine). At this point trifluoro-acetyl-lysine- and thio-acetyl-lysine-analogs of acetyl-lysines have to be mentioned, since they are valuable tools for deacetylase-structure determination and for the development of deacetylase inhibitors. However, the problem of site-specific incorporation into proteins remains.

1.3.4 Genetic code expansion concept

The co-translational incorporation of modified amino acids is an elegant method to study post-translationally modified proteins, such as acetylated proteins, *in vitro*. In contrast to the techniques described above (chemical ligation, mimics and cysteine-based analogs, chemical and enzymatic acetylation) the genetic code expansion concept (GCEC) provides quantitatively and site-specifically acetylated material. The incorporation is possible at any position of the protein and also double- or multi-acetylated proteins can be generated. The deficiencies of mimics and analogs are avoided and the lysine-acetylated material can even be used to assess the validity of indispensable mimics/analogs. This is especially valuable when it comes to *in vivo* experiments since the application of Q/R-mimics is still the easiest/established/prevalent way to study lysine acetylation in cells. However, over the last decade the GCEC was already extended to yeast, *D.melanogaster*, *C.elegans* and mammals/mammalian cells (Bianco et al., 2012; Greiss and Chin, 2011; Hancock et al., 2010; Kang et al., 2013; Wang et al., 2007).

Genetic code expansion is the artificial extension of the genetic code by one ore more codons to co-translationally incorporate non-proteinogenic amino acids at specific positions of a protein. Several prerequisites have to be fulfilled in order to make use of the GCEC:

- The amino acid to incorporate must not be among the encoded proteinogenic amino acids of the target organism.
- An unused codon has to be available to encode the desired amino acid. Often rare stop-codons or four-base codons (in combination with evolved ribosomes) are used. The amber codon (UAG), for example, is the least used codon in *E.coli* and therefore predestined for GCEC.

- The orthogonal tRNA has to speci cally recognize the target codon.
- An orthogonal tRNA-synthetase to load the speci c tRNA with the arti cial amino acid has to be introduced.

Most importantly, the orthogonal tRNA-synthetase/tRNA-pair must not cross-talk with endogenous tRNAs/tRNA-synthetases by still being functional with the endogenous translation machinery (e.g. ribosomes). The modi ed amino acid has to be provided to enable the incorporation, otherwise the translation stops at the corresponding codon. Often the endogenous transport machinery can be utilized to import the supplied amino acid from the culture medium. However, in the case of acetyl-lysine it is still unknown how the amino acid is taken up by *E.coli*. Alternatively, a biosynthetic pathway can be engineered or incorporated to produce the residue (Da Silva and Sheppard, 2015). Figure 1.18 illustrates the incorporation of acetyl-lysine into a recombinant protein in *E.coli*.

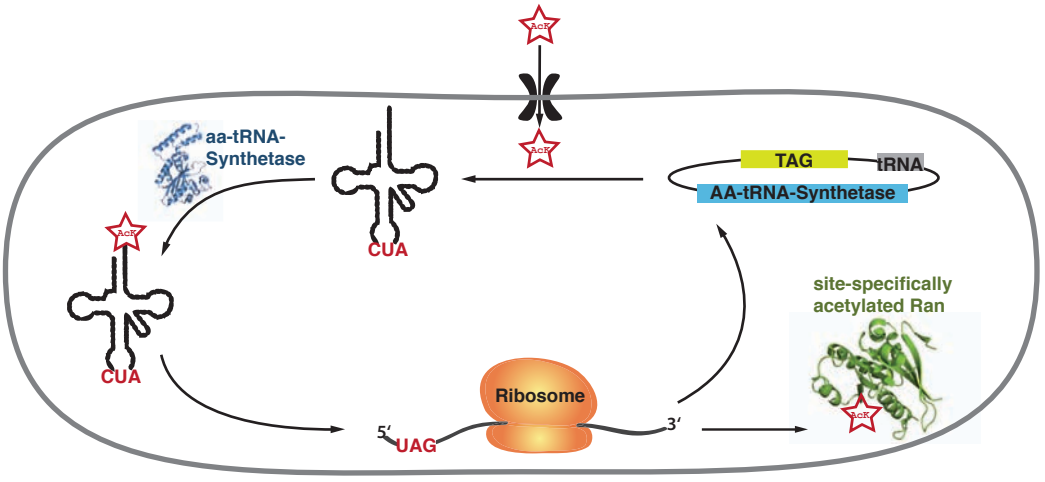

FIGURE 1.18: **Genetic-code expansion concept.**Schematic presentation of the incorporation of acetyl-lysine by expansion of the genetic code. Acetyl-lysine (AcK) is supplemented to the medium and taken up by *E.coli*. The orthogonal tRNA is charged with AcK by the orthogonal acyl-lysyl-tRNA-synthetase. The incorporation of the acely-lysine in response to the introduced amber-codon occurs co-translationally, resulting in a site-speci cally acetylated protein.

In 2008, Neumann et al. presented an orthogonal N-( )-acetyl-lysyl-tRNA-synthetase/$tRNA_{CUA}$-pair for the incorporation of acetyl-lysine in *E.coli* (Neumann et al., 2008). The synthetase and its cognate suppressor tRNA were derived from the pyrrolysyl-tRNA-synthethase from *Methanosarcina barkeri*. Based on the crystal structure of the homologous enzyme from *M.mazei* promising residues

of the active site were chosen for several rounds of selection for acetyl-lysine instead of pyrro-lysine. The proof of principle was provided one year later by successful acetylation of histone H3 at lysine K56 (Neumann et al., 2009). Furthermore, in 2010 Lammers *et al.* could solve the first crystal structure of a lysine-acetylated protein, CypA, and its complexes with HIV-1 capsid and cyclosporin (Lammers et al., 2010). This study demonstrated that this technique has the capacity to provide high yields of homogeneously acetylated protein, suitable for biophysical characterization and X-ray crystallography.

1.4 Acetylation of Ran

In 2009 the global human lysine acetylome was analyzed by high-resolution mass spectrometry (Choudhary et al., 2009). In three different human cell lines a sum of 3600 lysine acetylation sites on 1750 proteins were identified by a typical shotgun (bottom-up) approach. Furthermore, the effect of two deacetylase inhibitors on the acetylome was investigated/quantified. Metabolic labeling (SILAC) was used to enable quantification. After tryptic digest acetylated peptides were enriched with specific AcK-antibodies and isoelectric focussing was applied as an additional fractionation step.

The small G-protein Ran was found to be acetylated at five (out of eighteen) lysines: K37, K60, K71, K99 and K159. Close inspection of available crystal structures of Ran and Ran-complexes suggested a strong impact of acetylation on protein function or protein-protein interaction for several of the lysines. Two of the modified lysines, namely K37 and K71, are part of switch I and switch II, respectively, and thus located at the binding interface of Ran-effectors and -regulators (RCC1 and RanGAP). Especially K71 of Ran might be of major importance, since it is located in the switch II region of the G-domain of Ran. Due to the close proximity to Q69 (Q61 in Ras), which is important for positioning of the catalytic water molecule essential for GTP hydrolysis, acetylation may influence the hydrolysis of GTP by changing the orientation of Q69. Furthermore, steric effects or induced conformational changes could block the access to GDP/GTP. In addition, lysine 71 forms two essential salt bridges to D92 and D94 of NTF2. It is reported that disruption of these salt bridge abolishes NTF2-binding (Kent et al., 1999; Stewart et al., 1998).

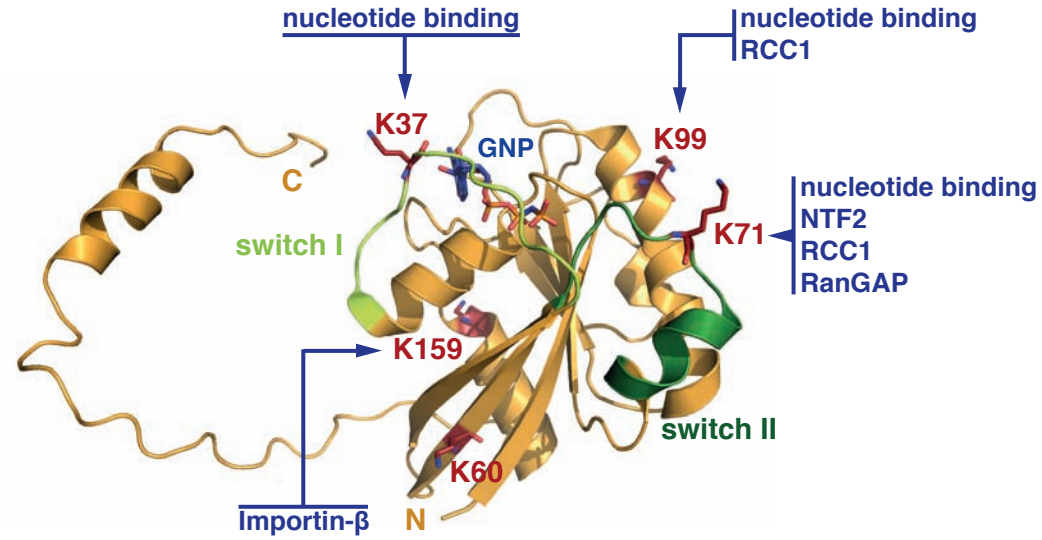

FIGURE 1.19: **Ran acetylation sites and possible effects.**Cartoon-presentation of Ran (yellow) with GppNHp (blue) bound (PDB: 1K5D). The switch regions are highlighted in green (switch I ligth-green, switch II dark-green) and the five reported acetylated lysines are shown as sticks (red). Possibly affected interactions/processes are named for each acetylation site.

As visible from the crystal structure of Ran and Importin-β (PDB:1IBR), lysine 159 interacts with a negatively charged, acidic patch of the import receptor. Acetylation of that residue could directly impact on the interaction and consequently influence thermodynamic or kinetic parameters of the interaction. Lysine 99 of Ran forms a salt bridge with D128 of RCC1, which might be influenced by electrostatic quenching upon acetylation.

1.5 Aim of this thesis

Ran was shown to be acetylated at five distinct lysines (K37, K60, K71, K99 and K159) in human cell lines. However, the physiological relevance of this post-translational modification of Ran is unclear. In order to judge the significance of Ran-acetylation in the biological context, the following questions regarding molecular effects, stoichiometry and regulation of Ran-acetylation had to be answered.

1. How does Ran-acetylation impact on Ran-function and -interactions?
I used the genetic code expansion concept to produce Ran site-specifically acetylated at each of the five identified acetylation sites. All acetylated Ran variants (AcKs) were compared to unmodified Ran (Ran wt) regarding intrinsic properties (stability, nucleotide binding), protein functionality (nucleotide exchange/-hydrolysis) and the interaction with Ran-interacting proteins *in vitro*. The RanGEF RCC1, the major import receptor Importin-β and the Ran-shuttling protein NTF2 were analyzed, since an effect of Ran-acetylation on these interactions was likely, as judged by available structural data. Protein-protein interactions were characterized by isothermal titration calorimetry (ITC) to obtain binding affinities and thermodynamic parameters (enthalpy, entropy, stoichiometry and free energy). Stopped-flow fluorescence spectroscopy was used to determine association kinetics for the Importin-β-Ran association and to compare the RCC1-catalyzed nucleotide exchange on Ran wt and all five Ran AcKs. Cell culture experiments with acetylation mimics (Q and R) provided information on acetylation-dependent alterations in Ran localization.

2. How abundant is this PTM of Ran in mammalian cells and under which conditions is up- or downregulation taking place?
The acetylation of Ran had to be verified on protein level by immunodetection after isolation from mammalian cell lysate. Either acetyl-lysine or Ran was used as target for affinity enrichment by specific antibodies (against acetyl-lysine) or Ran-specific binding proteins (RCC1). Another aim was the estimation of the stoichiometry of Ran-acetylation in mammalian cells and the influence of stress- or growth-conditions with on the acetylation dynamics.

3. How is this modification regulated on the cellular level?
Finally, I wanted to identify Ran-specific acetyltransferases and deacetylases to gain insight into the regulation of Ran-acetylation.

Chapter 2

Material and Methods

2.1 Materials

2.1.1 Primer

Table 2.1: Cloning primer

Name	sequence (length)	Enzyme
GEXRanflfoB	CGGGATCCATGGCTGCGCAGGGAG (24)	BamHI
RanflrevE	CGGAATTCCGTTACAGGTCATCATCCTC (28)	EcoRI
GEXRan8foB	CGGGATCCCAGGTCCAGTTCAAAC (24)	BamHI
RSFRan1foB	CGCGGATCCCGGAATGGCT GCGCAGGGAGAGC (32)	BamHI
RSFRan8foB	CGCGGATCCCGGACAGG TCCAGTTCAAAC (29)	BamHI
Ran213revE	CGGAATTCCGTTAATCCTCATCCGGGAGAGC (31)	EcoRI
Ran177revE	CGGAATTCCGTTAAACAAATTCCAAGTTAG (30)	EcoRI
RSFRan1foB	CGCGGATCCCGGAATGGCTGCGCAGGGAGAGC (32)	BamHI
RSFRan8foB	CGCGGATCCCGGACAGGTCCAGTTCAAAC (29)	BamHI
EGFPRan1foE	CCGGAATTCCATGGCTGCGCAGGGAGAGCC (30)	EcoRI
EGFPRan216revB	CGCGGATCCCAGGTCATCATCCTCATCCGGG (31)	BamHI
GEXImp1foB	CGCGATCCATGGAGCTGATCACCATTC (28)	BamHI
GEXImp862revN	TTTAGCGGCCGCATTCTTATTTAAGCTTGGTTCTTCAGTTTC (42)	NotI
GEXRCC149foB	CGGGATCCAAGGTCTCACACAGGTCC (26)	BamHI
GEXRCC1444revX	CCGCTCGAGCGGTTATTCTTTGTCCTTGAC (39)	XhoI
GEXNTF2revX	CCGCTCGAGCGGTCAGCCAAAGTTGTGC (28)	XhoI
GEXNTF2foE	CCGGAATTCCGGATGGGAGACAAGCC (26)	EcoRI

Table 2.2: Quick change primer

QCRan37amber	GGTGAATTTGAGTAGAAGTATGTAGCCACCTTGGG	35
QCRanK37Q	GGTGAATTTGAGCAGAAGTATGTAGCCACCTTGGG	35
QCRanK37R	GGTGAATTTGAGAGGAAGTATGTAGCCACCTTGGG	35
QCRanK60amber	CAACAGAGGACCTATTTAGTTCAATGTATGGGAC	34
QCRanK60Q	CAACAGAGGACCTATTCAGTTCAATGTATGGGAC	34
QCRanK60R	CAACAGAGGACCTATTAGGTTCAATGTATGGGAC	34
QCRanK71amber	CACAGCCGGCCAGGAGTAGTTCGGTGGACTGAGAG	35
QCRanK71Q	CACAGCCGGCCAGGAGCAATTCGGTGGACTGAGAG	35
QCRanK71R	CACAGCCGGCCAGGAGAGATTCGGTGGACTGAGAG	35
QCRanK99amber	GAGAGTTACTTACTAGAATGTGCCTAACTGG	31
QCRanK99Q	GAGAGTTACTTACCAGAATGTGCCTAACTGG	31
QCRanK99R	GAGAGTTACTTACAGGAATGTGCCTAACTGG	31
QCRanK159amber	GTAACTACAACTTTGAATAGCCCTTCCTCTGGCTTGC	37
QCRanK159Q	GTAACTACAACTTTGAACAGCCCTTCCTCTGGCTTGC	37
QCRanK159R	GTAACTACAATTTGAAAGGCCCTTCCTCTGGCTTGC	37

2.1.2 Vectors

The expression vector for GST-tagged protein expression, pGEX4T5 TEV, is based on the commercially available pGEX4T1 (GE healthcare). However, a TEV (tobacco etch virus) protease cleavage site was inserted between the Thrombin cleavage site and the first restriction site of the multiple cloning site (MCS). The Thrombin cleavage site as well as the reading frame were not affected by the insertion.

The commercially available pRSF-Duet-1 (Novagen) was modified as follows (refer to Appendix...): The evolved acetyl-lysyl-tRNA-synthethase AcKRS-3 (AcKRS of *M.barkeri* with mutations: L266M, L270I, Y271F, L274A, C313F) was cloned under the control of an *glnS* promoter/terminator using SphI (Neumann et al., 2008). It also contains the PylT gene under the control of an *lpp* promoter and a *rrnC* terminator. For additional information on the sequence and cloning of the synthetase/tRNA please refer to Appendix A.1. Furthermore, the His_6-tag sequence was modified ($MGSSH_6$- to $MPSSH_6$-) by Quickchange PCR to prevent α-N-6 phosphogluconoylation of the tag (Referenz, Geoghegan 1999). Target protein genes (Ran AcKs) carrying the amber codon were cloned with BamHI/EcoRI, utilizing MCS I and II.

2.1.3 Buffers and solutions

GSH-affinity chromatography

Buffer GST I	25 mM	Tris/HCl, pH 8.0
	500 mM	NaCl
	5 mM	$MgCl_2$
	5 mM	β-ME
	100 μM	PMSF
Buffer GST II	25 mM	Tris/HCl, pH 8.0
	250 mM	NaCl
	5 mM	$MgCl_2$
	5 mM	β-ME
Buffer GST III	25 mM	Tris/HCl, pH 8.0
	100 mM	NaCl
	5 mM	$MgCl_2$
	5 mM	β-ME
Buffer GST IV	25 mM	Tris/HCl, pH 8.0
	100 mM	NaCl
	5 mM	$MgCl_2$
	5 mM	β-ME
	30 mM	GSH

Ni-affinity chromatography

Buffer His I	25 mM	Tris/HCl, pH 8.0
	500 mM	NaCl
	5 mM	$MgCl_2$
	10 mM	Imidazole
	2 mM	β-ME
	100 μM	PMSF
Buffer His II	25 mM	Tris/HCl, pH 8.0
	1 M	NaCl
	5 mM	$MgCl_2$
	10 mM	Imidazole
	2 mM	β-ME
Buffer His III	25 mM	Tris/HCl, pH 8.0
	300 mM	NaCl
	5 mM	$MgCl_2$
	10 mM	Imidazole
	2 mM	β-ME
Buffer His IV	25 mM	Tris/HCl, pH 8.0
	300 mM	NaCl
	5 mM	$MgCl_2$
	500 mM	Imidazole
	2 mM	β-ME

Buffer V	50 mM	Tris/HCl, pH 7.5
(size-exclusion chromatography)	100 mM	NaCl
	5 mM	$MgCl_2$
	2 mM	β-ME
Assay-buffers		
Phosphate buffer	30 mM	KP_i
(measurement buffer)	5 mM	$MgCl_2$
	2 mM	β-ME
HPLC-buffer	100 mM	KP_i, pH 6.4
	10 mM	TBAB
	2% (v/v)	Acetonitrile
	(20% (v/v)	Acetonitrile for mant-nucleotides)
KDAC-assay buffer	25 mM	Tris/HCl, pH 8.0
	137 mM	NaCl
	2.7 mM	KCl
	1 mM	$MgCl_2$
	0.1 mg/ml	BSA
	0.5 mM	NAD^+
KAT-assay buffer	50 mM	Tris/HCl, pH 7.3
	50 mM	KCl
	0.1 mM	EDTA
	1 mM	DTT
	5% (v/v)	Glycerol
SDS-PAGE and immunoblotting		
SDS-PAGE Running buffer	25 mM	Tris/HCl, pH 8.3
	192 mM	Glycine
	2% (w/v)	SDS
Sample buffer	50 mM	Tris/HCl, pH 6.8
	50% (v/v)	Glycerol
	500 mM	DTE
	10% /w/v)	SDS
	0.5% (w/v)	Bromphenolblue
Staining solution	40% (v/v)	Methanol
	10% (v/v)	Acetic acid
	0.4% (w/v)	Coomassie blilliant blue R-250
	0.4% (w/v)	Coomassie blilliant blue G-250
Destaining solution	20 % (v/v)	Ethanol
	10% (v/v)	Acetic acid
Transfer buffer	25 mM	Tris, base
(semi-dry)	150 mM	Glycine
	10% (v/v)	Methanol

Media, Antibiotics, Inhibitors

LB-medium (1l)	10 g	NaCl
	10 g	Tryptone
	5 g	Yeast extract
	stock	end concentration
Ampicillin	100 mg/ml	0.1 mg/ml
Kanamycine	25 mg/ml	0.025 mg/ml
PMSF	100 mM	0.1 mM
Trichostatin A (TSA)	5 mM	1 μM
SAHA	10 mM	2 μM
Butyrate	1 M	1 mM
Nicotinamide	2 M	10 mM

2.2 Biomolecular methods

2.2.1 Cloning

Fragments were amplified with Phusion Polymerase (NEB) using the manufacturers protocol. The used oligonucleotide-primers provided the neccessary consensus sequence for the restriction enzymes (Table 2.1). Inserts were amplified by PCR, purified by gel extraction (QIAquick Gel Extraction Kit), digested according to the manufacturers protocol (NEB) and subsequently purified by PCR-purification (QIAquick PCR purification Kit). Vector DNA was digested and furthermore dephosphorylated prior to purification. After ligation by T4 DNA Ligase (NEB), plasmids were transformed into NEB5α cells (NEB). The identification of positive clones was done by analytical PCR (colony PCR) using 5 Prime Mastermix (5Prime), scraped cells of the colony as template and primers specific for the target vector. The amplified fragment was separated by agarose gelelectrophoresis and stained with SybrSafe (ThermoScientific).

2.2.2 Purification of DNA

Plasmid-DNA was purified using commercially available kits from Qiagene. Either the QIAprep Spin Miniprep kit or the QIAGEN Plasmid Midi kit was used.

2.2.3 Transformation

100 μl of chemocompetent *E. coli* cells (NEB5α or BL21 (DE3)) were incubated with 20-100 ng Plasmid-DNA or 10-20 μl ligation mix for 30 min on ice. Following a heatshock for 2 min at 42 °C, 800 μl LB-medium were added and the cells were allowed to recover for 45 min at 37 °C. Cells were pelleted and plated on agar plates containing the selection-antibiotics.

2.3 Biochemical methods

2.3.1 Preparative expression of recombinant proteins

Four to five colonies were picked from the agar plate and transfered to 200 ml LB-medium containing the appropriate antibiotic. After growth over night at 37 °C and 140 rpm, this pre-culture was used to inoculate 10 l of LB medium at a ratio of 1:100. The expression culture was grown at 37 °C and 160 rpm until the optical density at 600 nm (OD_{600}) reached 0.5 and 0.8 for expression of acetylated and unacetylated proteins, respectively.

For unacetylated (GST-tagged) proteins the protein expression was induced by addition of 100 μM IPTG to the culture at an OD_{600} of 0.8. To incorporate acetyllysine into the target protein, the temperature was decreased to 20 °C at an OD_{600} of 0.5 and 10 mM of N-(ϵ)-acetyl-L-lysine (Chem-Impex Int.) and 20 mM nicotinamide (AppliChem) were added to the culture. After 30 min protein expression was induced with 100 M IPTG. After induction both cultures were grown over night at a reduced temperature of 20 °C and pelleted at 4000 x g for 20 min. The pellet was resuspendet in 150 ml of buffer I and stored at -80 °C.

2.3.2 Lysis of cells

The resuspended pellet was thawed and cells were lysed by sonicating 3 x 2 min. A Branson Sonifier 250 was used with 60% duty cycle and micro tip limit 8. The lysate was cleared from unsoluble components and cell debris by centrifugation at 50000 x g for 45 min.

2.3.3 Purification of recombinant proteins

To purify recombinant proteins ÄKTApurifier systems (GE healthcare) were used, providing constant flow and pressure conditions. The systems furthermore recorded the absorptions at 220 nm and 280 nm, which facilitates the monitoring of the purification procedure and the identification of elution fractions containing protein. All purification steps were carried out at 4 °C.

Table 2.4: Purification strategies for recombinant proteins

Protein	Vector	Resistance	Column	MWCO	Superdex
Ran wt	pGEX4T5 TEV	Amp	GST	10 kDa	S 75
Ran KxQ/R	pGEX4T5 TEV	Amp	GST	10 kDa	S 75
NTF2	pGEX4T5 TEV	Amp	GST	3 kDa	S 75
RCC1 49-444	pGEX4T5 TEV	Amp	GST	30 kDa	S 200
Importin-β	pGEX4T5 TEV	Amp	GST	30 kDa	S 200
Ran KxAcK	pRSFDuet	Kan	Ni-NTA	10 kDa	S 75

GSH-affinity chromatography

The cleared lysate was applied to a buffer-equilibrated GSH-column (buffer GST I), packed with 40 - 60 ml of PureCube Glutathion Agarose (Cube Biotech) material. The column-bound protein was washed with 5-10 column volumes (CV) wash buffer (buffer GST II), followed by 2 CV TEV-cleavage buffer (buffer III). TEV-protease was added and circulated over night at 4 °C. The cleaved protein was eluted with buffer GST III. Depletion of the His-tagged TEV-protease was achieved by affinity capture using Ni-Sepharose 6 Fast Flow (GE healthcare). The protein was concentrated by ultrafiltration with AmiconUltra centrifugal filter devices with appropriate pore sizes (molecular weight cut-off 3, 10 or 30 kDa). Subsequently a size-exclusion chromatography (Superdex S75 or S200, GE healthcare) was carried out with buffer V. The pure protein was concentrated again, flash frozen in adequate aliquots and stored at -80 °C.

Ni-affinity chromatography

The cleared lysate was applied to a buffer-equilibrated Ni-NTA column (buffer His I), packed with 40 - 60 ml of Ni-Sepharose 6 Fast Flow (GE healthcare) material. The column-bound protein was washed with 5-10 column volumes (CV) high salt buffer (buffer His II) followed by 2 CV buffer His III. To elute the protein from

the column a gradient from 10 mM to 500 mM imidazole (buffer His III to IV) over 10 CVs was applied and the eluate collected in 4 ml-fractions. The fractions containing the target protein were identified by SDS-PAGE and pooled for ultrafiltration. Subsequently a size-exclusion chromatography was carried out with buffer V. The pure protein was concentrated again, flash frozen in adequate aliquots and stored at -80 °C.

Regeneration of column material
GSH-columns were flushed with 2 CV GSH-containing buffer (buffer GST IV) to elute the TEV-cleaved GST and uncleaved GST-fusion protein, still bound to the column. A sample of this step was also applied to SDS-PAGE to quantify the cleavage efficiency. The column was furthermore flushed with 3 CV water, 2 CV guanidinium hydrochloride and finally 5 CV water.
Ni-NTA columns were treated with 1 CV 3 M Imidazole, followed by 3 CV water, 2 CV guanidinium hydrochloride and 5 CV water. For long term storage all columns were equilibrated with 20% (v/v) ethanol.

2.3.4 Analytical size-exclusion chromatography

150 μM protein (Ran wt/AcK71/K71Q and NTF2) in phosphate buffer was applied to a Superdex S75 10/300 column at a flow-rate of 0.6 ml/min. Eluting protein was detected by absorption at 280 nm. Equimolar mixtures (Ran wt/AcK71/K71Q-NTF2) were incubated on ice for 30 min to allow complex formation prior to size exclusion chromatography.

2.3.5 Determination of protein concentration

To determine protein concentrations the absorption at 280 nm was measured and the Lambert-Beer law was applied.

$$A = \epsilon \cdot c \cdot l \tag{2.1}$$

with the absorbance A, the absorption coefficient ϵ ($M^{-1}cm^{-1}$), the protein concentration c (M) and the path length l (cm).
Due to the absorption of the bound nucleotide at 280 nm, the concentration of

Ran could not be determined by the Lambert-Beer law. Instead the BradfordUltra assay (Expedeon) was used. In this assay the colorimetric reaction of Coomassie brilliant blue G-250 with amino acid side chains is used as a read-out at 595 nm. The quantification was based on standard curves with bovine serum albumin (BSA).

2.3.6 SDS-Polyacrylamide gelelectrophoresis (SDS-PAGE)

Denaturing, discontinuous SDS-polyacrylamide gelelectrophoresis according to Laemmli was used to separate protein mixtures. Tris-Glycine gels with 5% stacking gel and 12-15% separation gel were run for 45 - 60 min at 200 V. All proteins were stained with staining solution and destained with an ethanol/acetic acid mixture (see buffers).

2.3.7 Western blotting and immunodetection

Following SDS-PAGE, protein transfer onto a methanol-activated PVDF membrane (GE Healthcare) was achieved by semidry electrotransfer in transfer buffer at 150 mA for 45 min. 3% (w/v) milk powder in PBST was used as blocking solution (30 min). Primary antibodies were diluted in blocking solution according to the manufacturers protocol and incubated with the membrane over night at 4 °C (Table 2.5). The membrane was washed three times 10 min with PBST. HRP-coupled secondary antibodies were used as 1:10000 dilution in blocking solution and incubated with the membrane for 30 - 60 min at room temperature. After three washes with PBST, 5 min each, signal development was done with RotiLumin (Roth) in the darkroom.

To strip the PVDF-membrane of antibodies for subsequent detection with a different antibody, 0.2 M NaOH was applied for 2 x 10 min. After three washing steps with PBST, the immunodetection procedure was repeated, starting with the blocking step. Used PVDF membranes could be stored in a dried state and reactivated by a short incubation in methanol.

Table 2.5: Antibodies

Antigen	Catalog nr.	Species	Dilution
Ran	ab4781	rabbit	1:2500
AcK	ab21623	rabbit	1:1500
His_6-tag	ab18184	mouse	1:2000
NTF2	ab137192	rabbit	1:1500
Sirt2	ab75436	rabbit	1:500
Myc	ab24740	rabbit	1:1000
GST	71097 (Novagen)	mouse	1:1000
rabbit-IgG (HRP)	ab6721	goat	1:10000
mouse-IgG (HRP)	ab6728	rabbit	1:10000

2.3.8 Nucleotide exchange on Ran protein

Nucleotide exchange on the small GTPase Ran was done in buffer V. 3 - 10 mg protein were incubated with a 5-fold molar excess of nucleotide (GTP, GppNHp, GTPγS and mant-labelled nucleotides) in the presence of catalytic amounts of GST-RCC1. If a non-hydrolyzable nucleotide was to be loaded, 1 μl of calf intestinal phosphatase (CIP, NEB) was added to the reaction to hydrolyze GDP/GTP. GST-RCC1 was removed with Glutathion-Agarose beads and Ran was separated from excess nucleotide by size-exclusion chromatography. All nucleotides were purchased from Jena Biosciences. Alternatively, the nucleotide was exchanged by addition of a 2-fold molar excess of EDTA in the presence of desired nucleotide (similar ratios as for RCC1-method). After 2 h on ice, a 1.5-fold molar excess of $MgCl_2$ over the EDTA-concentration was added to stabilize the nucleotide binding. In analogy to the other method, Ran was separated from excess nucleotide by size-exclusion chromatography.

2.3.9 High pressure liquid chromatography (HPLC)

The identity of bound nucleotides was determined by reversed-phase high pressure liquid chromatography (RP-HPLC) with buffer containing tetrabutylammonium bromide (TBAB, Sigma) at a flowrate of 2 ml/min. As solid phase a Chromolith-Performance RP-18e 100 - 4.6 mm column (Merck) was used. The protein (30 μl) was denatured at 95 °C for 5 min and subsequently pelleted at 13,000 x g. The supernatant was applied to the RP-HPLC. TBAB interacts with phophates and thereby increases the hydrophobicity of nucleotides dependent on the number of

available phosphates. Consequently GDP elutes earlier than GTP. Eluting nucleotides were detected by absorption at 254 nm. 20% (v/v) acetonitrile (instead of 2%) were used for mant-labeled nucleotides since these are more hydrophobic and do not elute from the column with 2% (v/v) acetonitrile. The column was washed and stored in 20% (v/v) acetonitrile.

2.3.10 Activity Test for Deacetylases

Deacetylases were purchased from Biomol or Sigma (Table 2.6). All deacetylases were recombinantly expressed either in *E.coli* (sirtuins 1 - 5) or in a baculovirus expression system (HDACs 1 - 11, sirtuins 6 and 7). 1000 pmol Fluor-de-Lys substrate (fluorogenic HDAC substrate 2a or 3, Biomol, see Table 2.6) were incubated with buffer (background) or HDAC 1 - 11 in triplicates for 30 min at 37 °C. Developing solution (trypsin, Sigma) was added and after incubation for 10 min at RT the fluorescence intensities were determined (exc. 350 nm, em. 450 nm). For the sirtuin activity assay 250 pmol fluorogenic Sirt2 substrate (Sigma) were used. The amount of enzyme per well corresponded to a turnover of 1000 pmol/h (HDACs) and 250 pmol/h (sirtuins), as specified by the manufacturer.

2.3.11 KDAC-Screen

The KDAC-screen was done in KDAC-assay buffer. 100 pmol recombinant Ran (wt or AcK) was incubated with deacetylase or buffer (negative control) for 3 h at 25 °C. Each condition was set up as triplicates in 20 μl in a 96-well-plate. As read-out, a dot-blot procedure with 1 μl per well on a nitrocellulose membrane was performed, followed by immunodetection with the anti-acetyl-lysine antibody (AcK, see Table 2.5). Equal loading was verified by immunodetection of the His_6-tag of Ran. The AcK-fluorescence intensities were normalized based on the His-background. The amounts of enzyme used for the screen were adjusted based on the enzymatic activity determined in the preceding activity test: amount was normalized to correspond to 40-fold intensity increase over the background. This experiment was conducted together with P.Knyphausen.

Table 2.6: Human KDACs

KDAC (Biomol)	Construct	Affinity-tag	Activity (pmol / min / μg)	Conc. (mg/ml)
HDAC1	full-length	C-term. His/Flag-tag	460	0.56
HDAC2	full-length	C-term. His-tag	675	0.75
HDAC3	full-length	C-term. His-tag	3000	1.1
HDAC4	627 - 1084	N-term.GST-,C-term.His-tag	103255	0.24
HDAC5	657 - 1123	C-term. His-tag	2521	1.65
HDAC6	full-length	N-term. GST-tag	219	1.5
HDAC7	518 - end	N-term. GST-tag	26437	0.04
HDAC8	full-length	C-term. His-tag	298	1.56
HDAC9	604 - 1066	C-term. His-tag	3137	1.76
HDAC10	1 - 481	N-term.GST-, C-term.His-tag	2.4	0.13
HDAC11	full-length	N-term. GST-tag	3.7	0.09
Sirt1	193 - 741	N-term. GST-tag	30.1	0.2
Sirt2	50 - 356	C-term. His-tag	1	0.26
Sirt3	102 - 399	N-term. GST-tag	6.5	0.07
Sirt4	25 - 314	N-term. GST-tag	-	0.32
Sirt5	full-length	N-term. GST-tag	3.6	0.94
(Sigma)			(RLU/min/ng)	
Sirt6	full-length	His-tag	120	0.1
Sirt7	full-length	His-tag	140	0.1

2.3.12 Deacetylase (KDAC)-Assays

Deacetylase assays were done in KDAC-assay buffer. 100 pmol of acetylated Ran were incubated with catalytic amounts of KDACs (refer to respective figure legends) for the indicated time at 25 °C. The reaction was stopped by adding sample buffer and heating the samples for 5 min at 95 °C. Acetylation was detected by western blotting and immunodetection with an acetyl-lysine specific anibody (Table 2.5). This experiment was conducted together with P.Knyphausen.

2.3.13 Acetyltransferase (KAT)-Assays

120 pmol Ran were incubated with 1 μl recombinant acetyltransferase purchased from Biomol: full length CBP, Gcn5 and Tip60, as well as p300 (aa 965-1810) and pCAF (165 aa from HAT domain). Except for CBP (mouse), all enzymes were of human origin. The KAT-assays were done in KAT-assay buffer supplemented with

100 μM acetyl-CoA. The reaction was stopped by adding sample buffer and heating the samples for 5 min at 95 °C. The enzyme activities were tested using known histone substrates (recombinant, BPS Bioscience), namely 0.75 g H3 (for p300, CBP and Gcn5) and 7.5 μg H4 (for pCAF and Tip60). Acetylation was detected by western blotting and immunodetection. For analysis by mass spectrometry 10 μg Ran wt (10 μM in 40 μl) were incubated with 1 μl transferase in KAT-buffer for 4 h at 25 °C.

2.3.14 Pull-down of endogenous Ran

All centrifugation steps with GSH-agarose beads were conducted with max. 500 x g. GSH-Agarose beads (100 μl slurry per condition/sample) were washed three times with buffer V and subsequently incubated with purified, recombinant GST-RCC1 (0.5 mg/condition) for 30 min at 4 °C. Unbound GST-RCC1 was removed by three washing steps with buffer V. In a fourth washing step buffer V supplemented with KDAC-inhibitors (buffer V+I) was used. Cells were lysed by sonication (3 x 30 sec, duty cycle 4%, tip limit 2) in buffer V+I. The lysate was cleared by centrifugation (1000 x g, 10 min) and the supernatant was incubated with 100 μl RCC1-loaded GSH-beads (rotating, 1 h, 4 °C). The beads were pelleted and the supernatant (lysate after incubation) removed. The beads were washed three times with 1 ml buffer V+I. Finally, protein was eluted by three subsequent incubations (5 min each) with 100 - 150 μl buffer V+I supplemented with 30 mM GSH. The three eluates were pooled and concentrated with centrifugal concentrators (Vivaspin500, MWCO 10 kDa, SartoriusStedim) at 15000 x g. At a final volume of 25 -40 μl sample buffer was added and the samples were analyzed by western blotting and immunodetection for acetyl-lysine and Ran.

2.4 Cell culture

2.4.1 Cultivation of cell lines

HeLa cells were cultivated at 37 °C and 5% CO_2 in DMEM (Gibco) supplied with 10% (v/v) fetal calf serum (PAN) Biotech, 1% (v/v) Penicillin/Streptomycin and 1% (v/v) non-essential amino acids (both Gibco). Cells were split by trypsination (0.25% trypsin-EDTA-solution, Sigma) at a confluency of more than 70%. Cells were stored at 80 °C in culture medium supplied with 10% (v/v) DMSO.

2.4.2 Transfection

For transfection approx. 40000 cells were seeded on cover slips in a 24-well plate. After 20 h cells were transfected with 0.25 g DNA (Ran-acetylation mimetics with N-terminal EGFP) using Lipofectamine LTX Plus (Invitrogen) according to the manufacturers protocol.

2.4.3 Immunocytochemistry

HeLa cells transfected with EGFP constructs on cover slips were fixed with 3% (w/v) Paraformaldehyde for 20 min at room temperature. After three washes with ice cold PBS, DNA was stained by incubation with DAPI. for 30 - 60 min. After three washing steps cover slips were embedded in ProLongGold antifade reagent (Invitrogen) on microscope slides. The cover slips were sealed with varnish 24 h later and stored in the dark at 8 °C. Images were taken on a Zeiss Meta 510 Confocal Laser Scanning Microscope. Images were processed with ImageJ.

2.4.4 Pull-down of His_6-tagged Ran (*in vivo* KAT assay)

For pull-down of His_6-tagged Ran, HEK293T cells grown in 15 cm dishes were transfected with 10 μg of the respective KAT plasmid (all pCMV-C-Myc except for pTriEx-2-Tip60) and with 10 μg pcDNA3.1CnoK-Ran (from which all lysine

codons in the tag-region had been mutated to arginine codons) using Lipofectamine 2000 (Invitrogen). 16 h after transfection cells were harvested and sonicated in 1.8 ml lysis buffer (10 mM Tris pH 8.0, 100 mM NaH_2PO_4, 300 mM NaCl, 2 mM β-Mercaptoethanol, 0.05% (v/v) Tween 20, 8 M Urea, and 10 mM Imidazole). Lysates were cleared by centrifugation for 10 min at 17500 x g and a 50 μl input sample was taken. Lysates were then incubated with 50 μl Ni^{2+}-NTA magnetic beads (5 Prime) over night at 4 °C with agitation. Beads were washed three times for 5 min with wash buffer (lysis buffer + 20 mM imidazole) and His_6-tagged proteins were eluted with 50 μl binding buffer containing 250 mM imidazole for 20 min at room temperature.

2.5 Biophysical methods

2.5.1 Mass spectrometry

Sample preparation and digestion

Samples of *in vitro* KAT-assays and pull-downs of His_6-tagged Ran from HEK cells transfected with KAT-plasmids were digested with trypsin based on a filter-aided sample preparation (FASP) protocol (Wisniewski et al., 2009).

UHPLC and Mass Spectrometry

Peptides were separated using a binary buffer system of A (0.1% (v/v) formic acid in H_20) and B (0.1% (v/v) formic acid in acetonitrile) on an Easy nano-flow LC 1000 system (Thermo Fisher Scientific). A linear gradient from 4 to 30 % B in 40 min followed by 95% B for 10 min and re-equilibration to 5% B within 5 min on a 50 cm column (75 μm ID) in-house packed with C18 1.8 μm diameter resin. The flow rate was set to 250 nL/min. To control the column temperature we used an in-house made column oven at 45 °C. The UHPLC was coupled via a nano-electrospray ionization source (Thermo Fisher Scientific) to the quadrupole based mass spectrometer QExactive Plus (Thermo Fisher Scientific). MS spectra were acquired using $3{\cdot}e^6$ as an AGC target at a resolution of 70,000 (200 m/z) in a mass range of 350-1650 m/z. The maximum injection time was set to 60 ms for ion accumulation. In a data dependent mode MS/MS events were measured for the ten most abundant peaks (Top10 method) in the high mass accuracy Orbitrap after HCD (Higher energy C-Trap Dissociation) fragmentation at 25 collision energy in

a 100-1650 m/z mass range. The resolution was set to 35,000 at 200 m/z combined with an injection time of 120 ms and an AGC target of $5{\cdot}e^5$.

Data analysis

All raw files were processed with MaxQuant (version 1.5.2.8) using the implemented Andromeda search engine (Referenzen). For protein assignment ESI-MS/MS fragmentation spectra were correlated with the Uniprot *E.coli* database (for the *in vitro* assay) or the *H.sapiens* database (for pull-down from HEK cells) including the respective Ran-sequence (from pRSF-Duet for *in vitro*, from pcDNA for *in vivo* assay) and a list of common contaminants. Searches were performed with trypsin specificity allowing two missed cleavages and a mass tolerance of 4.5 ppm for MS and 6 ppm for MS/MS spectra. Carbamidomethyl at cysteine residues was set as a fixed modification. Acetylation at lysine residues, oxidation at methionine and acetylation at the N-terminus were defined as variable modifications. The minimal peptide length was set to 7 and false discovery rate (FDR) for proteins and peptides to 1 %. FDR for site modifications was calculated seperately using the revert algorithm in MaxQuant. The minimal peptide score cut-off was set to 0 and the minimal delta score to 0 and 6 for unmodified and modified peptides, respectively.

Data presentation

The peptide intensities originating from the MaxQuant search were processed for data visualization. To enable comparability intensities of acetylated peptides were normalized to correspond to a total-protein intensity (sum of all unmodified peptides) of $1{\cdot}10^{11}$ in all samples tested. Factors were determined based on the raw intensities (*in vitro* KAT assay) and LFQ (label-free quantification) intensities (*in vivo* KAT assay). For heat map presentation, normalized peptide intensities of two independent experiments were averaged.

Hierarchical clustering

Hierarchical clustering was done by Hendrik Nolte using heatmap.2 function. Distance was calculated by Euclidian method and linkage was performed in complete mode. Data are represented as raw intensities and missing values are shown in grey.

Random imputation of missing values for Volcano plot

In vitro KAT assays with CBP and without (-KAT) as a control, led to the identification of several acetylation sites. However missing values are a prominent

problem due to very low abundance or absence of acetylation sites. To overcome this problem and make sites accessible to statistical test, we imputated random data according to a 0.75 down-shifted Gaussian distribution (in log2 scale) with the standard deviation of all measured sites (e.g. 1.7 in $\log_2$ scale). Two sided t-test was utilized for calculation of p-values assuming equal variance. To estimate the FDR we repeated the resampling step 500 times and the averaged values for $\log_2$ fold change and $\log_{10}$ p value were used. Visualization and calculations were performed by Hendrik Nolte using statistical environment R.

2.5.2 Isothermal titration calorimetry (ITC)

Isothermal titration calorimetry was used to characterize protein-protein interactions thermodynamically and to determine binding affinities (Wiseman et al., 1989). This calorimetric method is based on the fact that every reaction is accompanied by a change in reaction enthalpy. A binding partner is titrated stepwise into the measurement cell filled with the protein of interest. The release (negative ΔH, exothermic) or uptake (positive ΔH, endothermic) of heat during the interaction is determined indirectly by monitoring the power necessary to keep the measurement cell at the same temperature as the water-filled reference cell (power compensation mode). This heating power per injection is plotted as a function of time until binding saturation is obtained. The binding isotherms are fitted to a one-site-binding model to determine the equilibrium association constant K_A, the stoichiometry and the reaction enthalpy ΔH directly. Based on the correlation

$$\Delta G = \Delta H - T\Delta S = -RTlnK_A \tag{2.2}$$

the reaction entropy ΔS and the Gibbs free energy ΔG of the protein-protein interaction can be derived.

We used an ITC_{200} (Malvern Instruments). For a typical experiment 2 - 3 μl of protein in the syringe (0.1 - 0.3 μM) was injected into the cell containing protein B in concentrations of 10 - 50 μM depending on the interaction analysed. The standard measurement temperature was 25 °C and all measurements were conducted in phosphate buffer. Furthermore, a differential power (DP) of 6, initial

delay and spacing of 120 sec (Importin-β 180 sec) and a stirring speed of 1000 rpm (Importin-β 700 rpm) were set for all experiments. For applied concentrations and measurement temperatures of individual measurements please refer to the corresponding figure legends.

We used the standard EDTA-$CaCl_2$ sample tests as described by MicroCal to assess the statistical significance of individual observations. These gave values within the manufacturers tolerances of $\pm 20\%$ for K_A values and $\pm 10\%$ in ΔH. The data analysis was done with the software provided by the manufacturer.

2.5.3 Fluorescence spectroscopy

Fluorescence spectroscopy takes advantage of the fact that the fluorescence of a fluorophore depends primarily on its environment. This is based on fluorescence quenching: fluorescence energy is transmitted from the fluorophore to molecules in close proximity (for example solvent molecules such as H_2O) and is subsequently released by radiationless transitions, such as translation- or rotation-processes. For an interaction (protein-protein, protein-ligand) quenching results in an increase or decrease of fluorescence intensity when the environment of the fluorophore becomes more hydrophobic or hydrophilic, respectively.

For the characterization of interactions of the Ran protein mant-labeled nucleotides were used as fluorophors. The mant-(2‘/3‘-O-(N-Methyl-anthraniloyl)-fluorophor is coupled to the ribose moiety of GDP or GppNHp (see Figure 2.1). The Ran

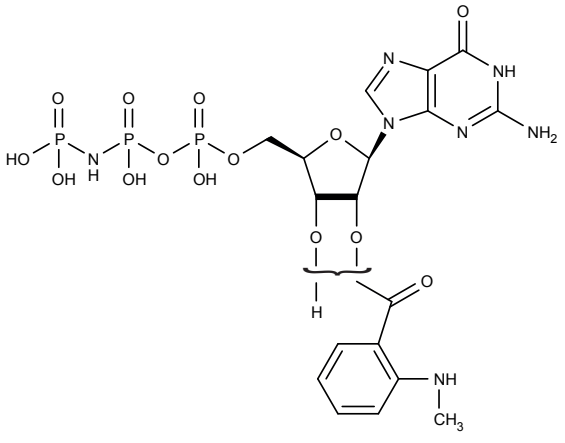

FIGURE 2.1: Structure of 2‘/3‘-O-(N-Methyl-anthraniloyl)-GppNHp

protein is loaded with labeled nucleotids by nucleotide exchange. Due to its spectroscopic properties the mant-group can either be excited directly at 355 nm or an indirect excitation by FRET (fluorescence resonance energy transfer) from tryptophanes is employed. Accordingly, either the change of the fluorescence signal of the tryptophanes (which is quenched by FRET) or the emission of the man-group can be used as reaction read-out.

Stopped-flow kinetics

Fast interaction kinetics were characterized by stopped-flow. The technique is suitable to record the fluorescence signal of a reaction down to a microsecond-timescale (dead time approx. 2 - 3 msec.). Two solutions containing the interaction partners are shot into the reaction chamber. As the solution fills the stopping syringe, the plunger hits a block, causing the flow to be stopped instantaneously. Stopped-flow experiments were done in phosphate buffer at 25 °C using an SX20 Applied Photophysics spectrometer (Leatherhead, UK). The photomultiplier voltage was adjusted to the respective experimental condition. For a reaction of two interaction partners (A and B) forming a complex (AB)

$$A + B \rightleftharpoons AB \tag{2.3}$$

the rate of complex formation is given by

$$\frac{d[AB]}{dt} = k_{on}[A][B] - k_{off}[AB] \tag{2.4}$$

Assuming that the concentration of one reaction partner A is constant, due to a high excess over the other, pseudo-first-order conditions are fulfilled and the second-order reaction $v = k[A][B]$ can be handled as $v = k_{obs}[B]$.

$$\frac{d[AB]}{dt} = k_{obs}[B] - k_{off}[AB] \tag{2.5}$$

with $k_{obs} = k_{on}[A]$. The solution of the differential equation yields

$$[AB] = \frac{k_{obs}[B]_0}{k_{obs} + k_{off}} - \frac{k_{obs}[B]_0}{k_{obs} + k_{off}} \cdot e^{-t(k_{obs}+k_{off})} \tag{2.6}$$

The fit of the primary traces to an exponential function provides k_{obs} which, under the assumption of a pseudo-first-order reaction, is given by

$$k_{obs} = k_{on}[A] + k_{off} \tag{2.7}$$

The plot of k_{obs} over the concentration of A results in a linear curve with the slope k_{on} and the intercept k_{off}. However, the dissociation rate constants determined by this method are often inaccurate and should be verified by direct determination. GraFit 7.0 was used for data analysis.

The association of Ran∗mantGppNHp and Importin-β was monitored by using an excitation of 350 nm and an emission cut-off filter of 420 nm, thus monitoring the mant fluorescence directly. 200 nM (final 100 nM) of Ran∗mantGppNHp were titrated with increasing concentrations of Importin-β (1 - 8 μM; final 0.5 - 4 μM). The increase in fluorescence was monitored over time and fitted to a single-exponential function to give the observed rates (k_{obs}). The plot of the k_{obs}-values (3 - 5 individual time courses per Importin-β concentration) over the Importin-β concentration resulted in a linear curve. All data points were fitted to a linear function applying explicit (user defined) weighting based on the error of the primary exponential fit of every individual trace.

To determine RCC1-catalyzed nucleotide exchange rates, mant-labeled Ran was excited at 295 nm and the fluorescence energy transfer from tryptophane to the mant-group was measured by using a 420 nm cut-off filter. A constant concentration of 1 μM (final 500 nM) Ran∗mantGDP was titrated with increasing concentrations of RCC1 (0.039 - 80 μM; final: 0.0195 - 40 μM) in the presence of excess GTP (50 μM; final: 25 μM). The fluorescence signal was plotted over time and fitted to a single-exponential function to give the observed rates (k_{obs}) for each RCC1-concentration. The plot of the k_{obs}-values (3 - 5 individual time courses per RCC1 concentration) over the RCC1 concentration resulted in a hyperbolic curve. By fitting to a hyperbolic function (Equation 2.8) the maximal rate of nucleotide

dissociation from the ternary complex, k_{-2}, and the equilibrium constant of the Ran∗mGDP-RCC1 interaction, K_1, were obtained.

$$k_{obs} = \frac{k_{-2}K_{-1}[RCC1]}{K_{-1}[RCC1] + 1} \tag{2.8}$$

2.5.4 Data visualization

Images were processed using ImageJ and Adobe Photophop CS5.1. Figures were created with Abobe Illustrator CS 5.1. For the presentation of structural data based on crystallography Pymol was used.

Chapter 3

Experimental results

3.1 Protein purification and identification

Until now, five out of eighteen lysine residues of Ran were found to be acetylated in human samples. In mouse and rat even up to eleven lysines were found do be modified. To gain a fundamental understanding of the impact of lysine acetylation on the protein integrity and function, a site-specific characterization of the acetylated protein is inevitable. The use of the genetic code expansion concept circumvents most of the shortcomings of acetylation mimetics, chemical modification or synthetic peptides. I therefore used this method to incorporate acetyl-lysine co-translationally and site-specifically into the recombinant Ran protein. After purification and quality control (SDS-PAGE, immunoblotting, mass spectrometry), the proteins were used to study the acetylation sites separately *in vitro*. All unacetylated proteins (namely Ran wt and Q/R-mutants, RCC1, NTF2 and Importin-β) were expressed as GST-fusion proteins. This strategy is less time consuming and provides high yields of pure protein. The GST-tag is furthermore beneficial for the stabilization of proteins that tend to aggregate during expression. However, for the incorporation of acetyl-lysine a His_6-tag proved beneficial, resulting in higher yields.

3.1.1 Purification of acetylated Ran

Acetylated Ran was expressed in *E.coli* transformed with an expression vector carrying the mutated Ran-(amber)-sequence, the evolved acetyl-lysyl-tRNA-synthethase and the corresponding amber-tRNA. The bacteria were grown at 37 °C up to an OD_{600} of 0.6. At that point 10 mM N-(ϵ)-acetyl-lysine and 20 mM nicotinamide were added and cells were grown for another 30 min at 20 °C before induction. The addition of acetyl-lysine is crucial to prevent translation stops due to the lack of modified amino acid. If no acetyl-lysine is added, the translation stops at the amber stop codon, yielding shortened proteins/peptides specific for the incorporation site. We observed that, even without addition of acetyl-lysine, a small proportion of protein is still expressed in full length and acetyl-lysine is incorporated. In this case the modified lysine probably originates from peptone or yeast extract included in the luria broth. The supplemented nicotinamide inhibits the single characterized *E.coli* deacetylase CobB. The addition of both components 30 minutes prior induction ensures sufficient uptake and minimizes the accumulation of translation stop fragments. After induction the protein was expressed for 16 to 24 h at 20 °C, the cells were pelleted and lysed by sonication. The following centrifugation step separated the soluble fraction from insoluble aggregates, cell debris and intact cells. The supernatant was applied to a Nickel-affinity (Ni-NTA) column to bind the His-tagged target protein. High salt buffer with 10 mM imidazole was applied to remove proteins binding unspecifically to either Ran or the Ni-NTA-column. By applying a gradient of imidazole to elute the protein, even stronger binding impurities were removed. Fractions containing recombinant full length Ran were pooled and concentrated (MWCO 10 kDa) to a volume appropriate for size exclusion chromatography (1-4 ml). After size exclusion chromatography Ran containing fractions were pooled, concentrated to approximately 20 mg/ml, flash frozen in liquid nitrogen and stored at -80°C. An exemplary SDS-PAGE with samples of all stages of the described procedure is shown in figure 3.1.

Recombinant Ran turned out to be very stable. Aggregation was neither observed during the purification procedure, nor after thawing. Furthermore, in only few cases we detected Ran in the exclusion peak of the size exclusion chromatography, which would indicate protein aggregation. By applying the described method yields of 8 mg to up to 60 mg of recombinant, acetylated Ran were obtained.

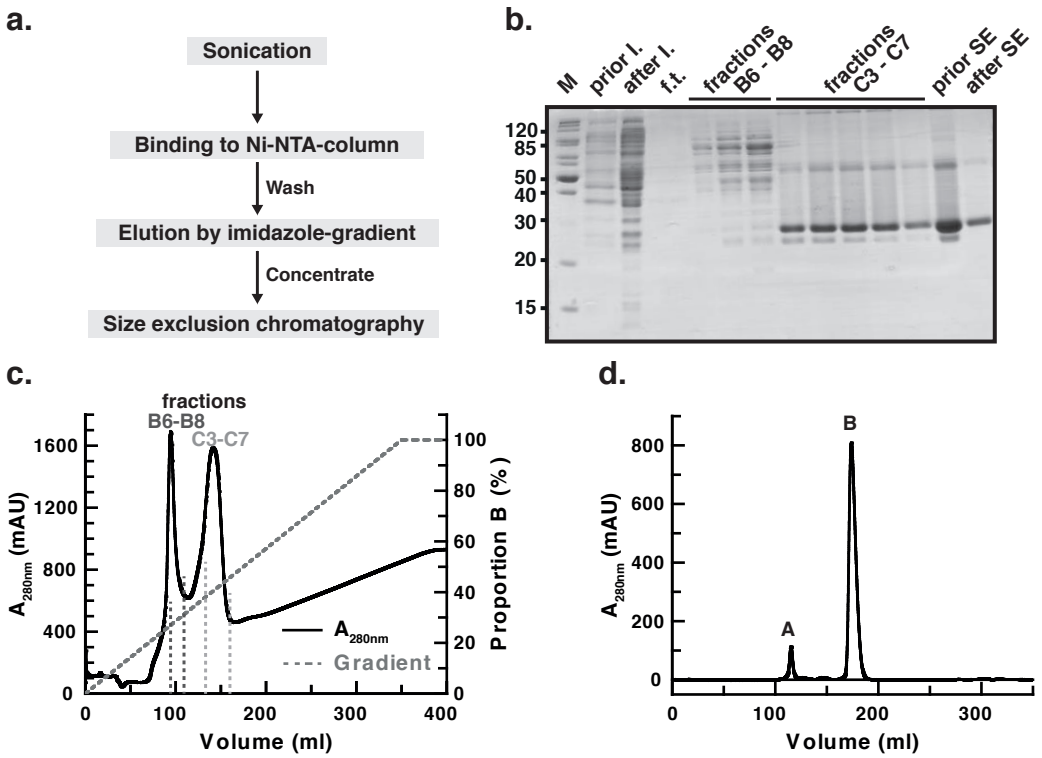

FIGURE 3.1: **Purification of Ran AcKs.** An exemplary purification of Ran AcK37 is shown. (a) Flow-scheme of the His_6-tag-based purification procedure.(b) Coomassie-stained SDS-PAGE of the purification showing marker(M), lysates prior/after induction (prior/after I.), flow-through (f.t.), eluted fractions of the imidazole-gradient and Ran AcK prio/after size-exclusion chromatography (prior/after SE). (c) Elution profile of the imidazole-gradient. Samples for SDS-PAGE were taken as indicated. (d) Chromatogram of the final size-exclusion chromatography using a Superdex S75 (26/60). Peak A corresponds to the exclusion volume, peak B contains the purified Ran AcK.

3.1.2 Quality control of acetylated Ran

All purified Ran variants exhibit a high degree of purity. The SDS-PAGE in figure 3.2 shows Ran wt and all five acetylated variants of Ran. In each lane 5 μg of protein were loaded. All protein bands are well defined and migrate in accordance with the molecular weight of full length Ran (24.6 kDa for Ran wt and 26 kDa for Ran AcK). The difference in molecular weight and migration behavior between Ran wt and the acetylated proteins is due to the absence of the His_6-tag in the case of Ran wt. Apart from the Ran band only minor impurities or degradation bands are visible on the gel, therefore a purity of $> 95\,\%$ can be assumed. For immunodetection 250 ng of protein were blotted onto a PVDF membrane and acetyl-lysine as well as Ran was detected using specific antibodies. The anti-Ran

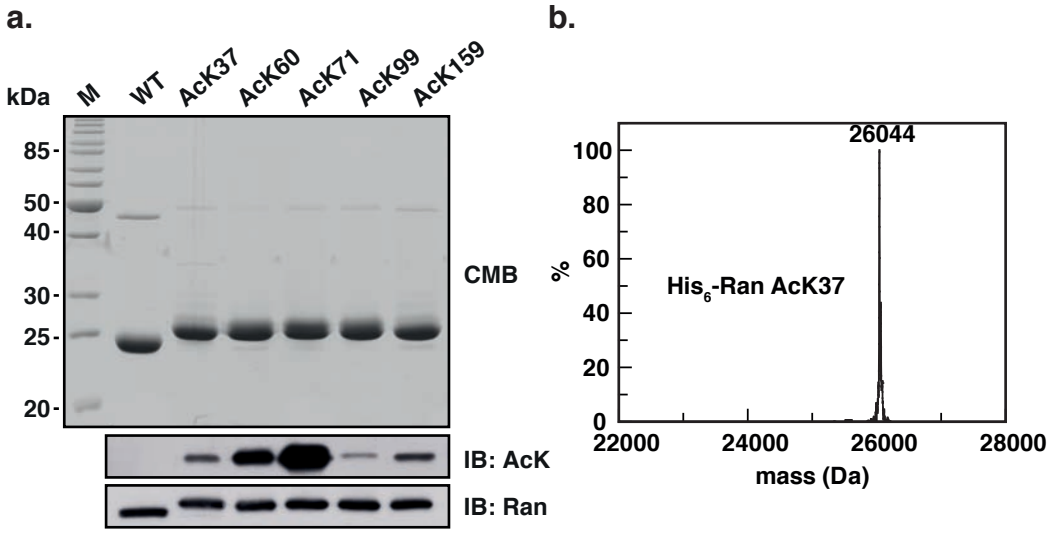

FIGURE 3.2: **Incorporation of acetyl-lysine into recombinant Ran.**(a) Coomassie-stained SDS-PAGE (CMB) and immunoblots (IB) probed with anti-AcK and anti-Ran antibodies for recombinant Ran-variants (wt and acetylated). (b) Quantitative incorporation of N-(ϵ)-acetyl-lysine into recombinant His-tagged Ran was verified by ESI-mass spectrometry. The calculated mass is 26043,6 Da

antibody detects one specific band for all Ran variants. No degradation products are detected. The immunodetection of acetyl-lysine confirms the incorporation of acetyl-lysine into the recombinant Ran protein. All five acetylated Ran variants are stained with the AcK-specific antibody. This blot also illustrates the specificity and selectivity of the used antibody. The unacetylated Ran wt, serving as a negative control, is not detected. Interestingly, the signal intensities of the five acetylated samples differ substantially, which indicates an epitope selectivity of the polyclonal primary antibody. An acetyl-lysine incorporated in position 71 of Ran results in a much stronger signal than the same modification at lysine 99.

The incorporation of acetyl-lysine was also confirmed by molecular mass determination by ESI-MS. Figure 3.2.b shows the ESI-MS spectrum of Ran AcK37, for the complete list refer to Appendix A.2. The detected mass of 26044 Da corresponds to the His-tagged full length Ran lacking the start-methionine and carrying one single acetyl-moiety.

3.1.3 Purification of Ran-interaction partners

For all unacetylated proteins (Ran wt, Ran Q/R, RCC1, NTF2 and Importin-β) the purification based on the GST-tag was favored. The GST-tag can be beneficial for the expression of demanding proteins, such as the 95 kDa Importin-β. The purification yields highly pure protein, even before size exclusion chromatography, and it can optionally be conducted as a batch purification. The use of the pGEX4T5 TEV vector, furthermore, allows for the easy cleavage of the GST-tag thereby providing a tag-free purification product.

GST-tagged proteins were expressed in *E.coli*. After induction at an OD_{600} of 0.8, cells were grown at 20 °C over night and harvested by centrifugation. The standard procedure for a GST-based purification is illustrated in the flowchart in figure 3.3.a. Following sonication, the cell lysate was cleared by centrifugation and applied to Glutathion-agarose/sepharose for protein binding. An extensive washing step with salt-rich buffer eliminated unspecifically bound proteins. The proteolytic cleavage of the column-bound GST-fusion protein by TEV-protease was done over night in buffer GST III. The cleaved target protein was depleted of TEV-protease by a short incubation with Ni-beads and concentrated to 1 - 4 ml prior to size exclusion chromatography. The protein specific peak fractions were pooled, concentrated to approx. 20 mg/ml and flash frozen in liquid nitrogen. Protein specific molecular weight cut-off sizes (MWCO) and achieved yields are listed in table 3.1.

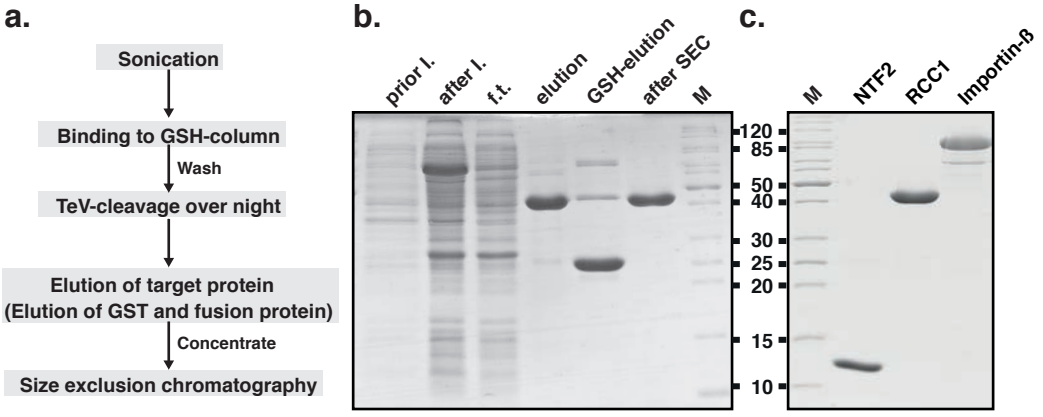

FIGURE 3.3: **Purification of Ran-binding proteins.** (a) Flow-scheme of the GST-tag-based purification procedure. (b) Exemplary SDS-PAGE of substeps of the purification of RCC1. (c) SDS-PAGE of the purified Ran-binding proteins used in this project, namely NTF2, RCC1 and Importin-β.

TABLE 3.1: Parameters for the purification of Ran-binding proteins

Protein	**MW (kDa)**	**MWCO (kDa)**	**Yield (mg/l)**
Ran (wt/Q/R)	24.6	10	2 - 10
RCC1	42.5	30	22
Importin-β	97.5	30	2.5
NTF2	15	3	1.4

To determine the cleavage efficiency and to recover uncleaved fusion protein, GSH-buffer was applied to the column to elute bound GST. The recombinant Ran-binding proteins have purities $> 95\,\%$ and SDS-PAGE (see figure 3.3.c) as well as size exclusion chromatography indicate homogeneity of the proteins. The obtained yields are protein dependent but sufficient for extensive biophysical characterization.

3.1.4 Nucleotide exchange on Ran

Ran-binding proteins distinguish between the different nucleotide-dependent conformational states of Ran. In contrast to effector proteins such as Importin-β, NTF2 binds predominantly to Ran$*$GDP. Since the nucleotide exchange factor RCC1 catalyzes nucleotide release to bind the nucleotide-free Ran with high affinity, it interacts with GDP- and GTP-bound Ran.

Recombinant Ran is purified from *E.coli* in the GDP-bound form. To be able to characterize the interactions of Ran$*$GTP and to introduce fluorescently-labeled nucleotides, GDP was exchanged for GTP, GppNHp or mant-nucleotides (mant-GDP, mantGppNHp). The nucleotide exchange was done after the purification. Either EDTA or catalytic amounts of RCC1 were used to accelerate the exchange reaction. EDTA acts as a chelator for the essential magnesium ion of Ran. Withdrawal of the ion results in a decrease of affinity and consequently release of the bound nucleotide (GDP). The re-addition of an excess of Mg^{2+} in the presence of an excess of nucleotide (GTP, GppNHp, mant-nucleotides) restores the nucleotide binding capability of Ran. Consequently, GDP and the nucleotide of interest are bound in the same ratio they were added. If a non-hydrolyzable nucleotide analog is to be exchanged, this ratio can be influenced by addition of calf intestine phosphatase (CIP), since the binding affinity for GMP is 10^6-fold lower compared to GDP/GTP (John et al., 1990; Rensland et al., 1995). As an alternative to the EDTA-method, catalytic amounts of GST-RCC1 were used in the presence of

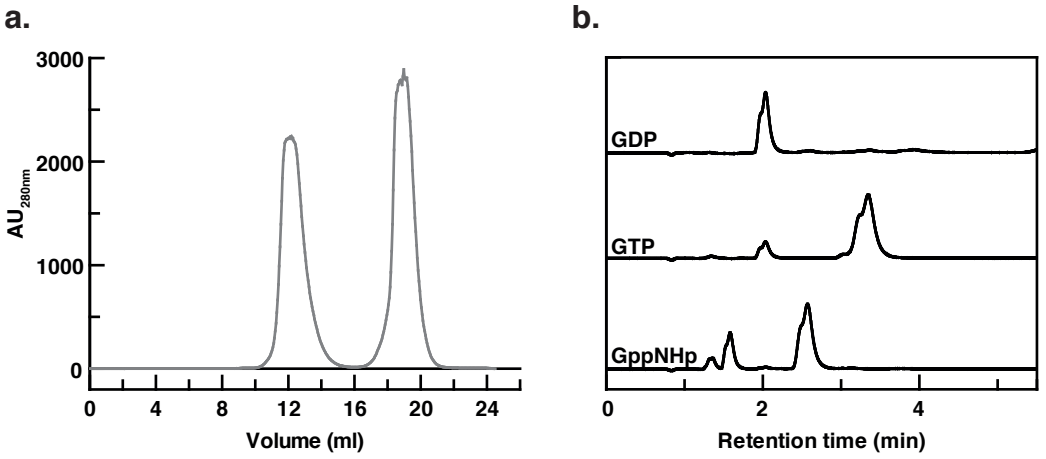

FIGURE 3.4: **Nucleotide exchange on Ran.** (a) Exemplary chromatogram of the size-exclusion chromatography (Superdex S75 10/300) after nucleotide exchange. Protein and nucleotide absorb at the detected wavelength of 280 nm. Ran elutes in one peak after 12 ml, whereas the excess of nucleotide elutes after 19 ml. (b) Chromatograms of Ran AcK37 prior (GDP) and after nucleotide exchange (GTP, GppNHp). The nucleotides absorb at 254 nm and elute after characteristic retention times, dependent on the number of phosphates.

excess of nucleotide and, if applicable, CIP. After one hour at room temperature GST-RCC1 was removed with buffer-equilibrated GSH-beads. After every nucleotide exchange a size-exclusion chromatography was done to remove unbound nucleotide. One exemplary chromatogram is shown in Figure 3.4.a. The free nucleotide, which also absorbs at 280 nm and 254 nm, elutes after Ran (Ran 12 ml, GXP 19 ml) and due to the small size close to the total column volume (24 ml). The elution behavior of Ran reflects the high quality of the purified protein. Ran elutes in one single, symmetrical peak and no protein is detected in the exclusion volume (8 ml), hence neither aggregates nor major impurities are present.

The efficiency of the exchange reaction was verified by reversed phase (RP)-HPLC with TBAB as mobile phase component (Tucker et al., 1986). TBAB interacts with phosphates and influences the elution from the used RP-column dependent on the number of phosphates. The elution is detected by absorption at 254 nm. The column was calibrated with nucleotide standards. The exemplary chromatogramms (Ran AcK37 after nucleotide-exchange) in Figure 3.4.b show that the retention time increases with the number of phosphates present in the analyzed nucleotide. The (early-eluting) additional peak for GppNHp originates from a heat-induced degradation product, which is also observed for GppNHp-standards after heating for 5 min at 95 °C.

3.2 Biophysical studies on the effect of Ran acetylation

To characterize the effect of the five different acetylation sites *in vitro*, three Ran interacting proteins were selected. NTF2 binds specifically to Ran∗GDP and is essential for the nucleocytoplasmic transport cycle. RCC1 is the guanine nucleotide exchange factor (GEF) for Ran and allows for the existence of the crucial Ran∗GDP - Ran∗GTP gradient. Hence, RCC1 plays an important role in mitosis and nucleocytoplasmic transport. Importin-β was chosen as the third interaction partner. It is the best-known import receptor and by binding exclusively to Ran∗GTP Importin-β is a true effector of Ran. Furthermore, the interaction with RanGAP (Ran GTPase activation protein), RanBP1 (Ran binding protein 1) and the major export receptor CRM1 was characterized by Philipp Knyphausen. All these proteins are pivotal for proper Ran function- especially in nucleocytoplasmic transport. The *in vitro* characterization of the effect of Ran acetylation on these proteins should indicate/point out/suggest the possible physiological relevance of this modification.

3.2.1 Effect of Ran-acetylation on NTF2 interaction

The binding of wildtype and acetylated Ran versions to NTF2 was investigated by ITC. Diminished binding could severely disrupt the cellular Ran gradient in interphase cells, since Ran∗GDP would not be shuttled back into the nucleus, where nucleotide exchange would take place. The consequence would be a cytosolic accumulation of Ran∗GDP and finally the arrest of Ran-dependent transport processes. The crystal structure of the Ran∗NTF2-complex indicates such a consequence for the acetylation of lysine 71, since an essential salt bridge could no longer be formed (Figure 3.8).

All ITCs with NTF2 were measured in phosphate buffer at 25 °C. The chosen standard concentrations were 300 μM Ran in the syringe and 30 μM NTF2 in the cell. The monitored power over molar ratio (syringe/cell) was fitted based on a single binding model. The determined binding affinities are in the nanomolar range and stoichiometries indicate one to one binding (Table 3.2). Please refer to Appendix A.3 for original ITC-curves and fitting results. While acetylation at four lysines have no effect on the binding of Ran and NTF2, Ran acetylated at

TABLE 3.2: Characterization of the Ran-NTF2 interaction by ITC

		ΔG (kcal/mol)	**ΔH (kcal/mol)**	**-TΔS (kcal/mol)**	**N**	**K_D (nM)**
Ran∗GDP	**WT**	-9.0	-3.7 ± 0.035	-5.3	1.0	**260** ± 29
(300 μM)	**AcK37**	-8.6	-4.2 ± 0.040	-4.4	0.9	**490** ± 46
NTF2	**AcK60**	-8.6	-5.8 ± 0.14	-2.8	1.1	**500** ± 110
(30 μM)	**AcK71**	n.b.				n.b.
	AcK99	-9.0	-5.0 ± 0.037	-4.0	0.9	**250** ± 23
	AcK159	-9.1	-3.9 ± 0.043	-5.2	0.8	**230** ± 31
	K71R	-7.4	-2.2 ± 0.066	-5.2	1.4	**4000** ± 660
	K71Q	n.b.				n.b.
	K99Q	-9.0	-3.5 ± 0.034	-5.5	0.7	**240** ± 28
	K99R	-8.9	-3.2 ± 0.031	-5.7	1.1	**280** ± 35

lysine 71 (Ran AcK71) shows no binding heat when titrated to NTF2. Since the reaction enthalpy is temperature dependent, the measurement was repeated at 10 °C and 30 °C. However, in contrast to Ran wt and the other acetylated versions of Ran, no binding can be detected for Ran AcK71 and NTF2 using ITC in the temperature range of 10 °C to 30 °C.

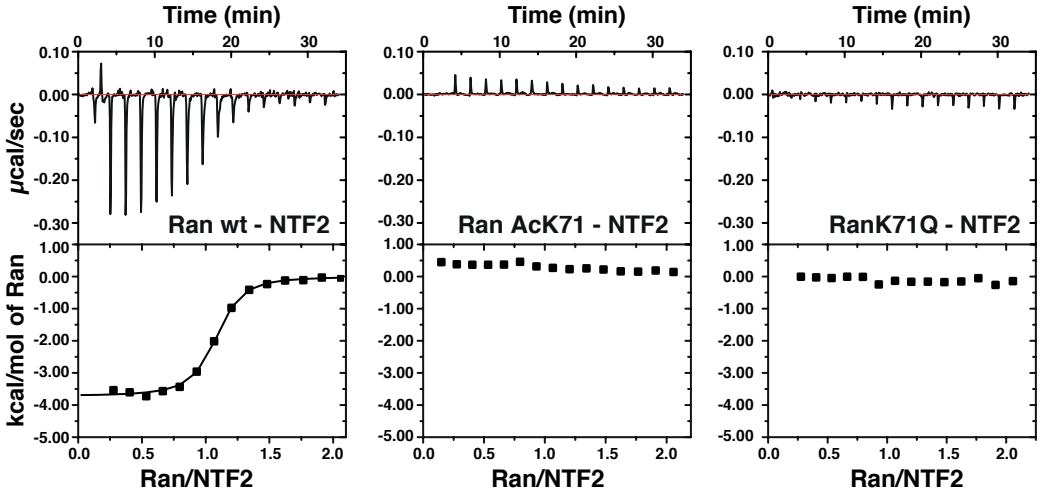

FIGURE 3.5: **ITC of NTF2 and Ran wt/AcK71/K71Q.** Representative ITC-titrations of 300 μM Ran (wt/AcK71/K71Q) to 30 μM NTF2. Ran wt binds NTF2 with a middle nanomolar affinity (K_D=260 nm ± 29 nm), no binding is detectable for Ran AcK71 and K71Q.

To confirm that NTF2 and Ran AcK71 do not form a complex, analytical gelfiltration runs were carried out, using the NTF2∗Ran wt complex as a reference. With a binding affinity in the nanomolar range, the complex is sufficiently stable to be separated from the monomeric fractions containing only Ran or NTF2. The analytical gelfiltration was done with a Superdex S75 10/300 column and phosphate buffer as mobile phase. The elution volumes of Ran wt, Ran AcK71 and NTF2 were determined in separate runs. Then mixtures of NTF2 with Ran wt and Ran AcK71 were preincubated on ice to allow complex formation and applied to the column. Figure 3.6 shows the chromatograms (absorption at 280 nm over elution volume) for all runs. The NTF2∗Ran wt complex elutes earlier than NTF2 and Ran wt alone and is well separated from the other elution peaks. A small shoulder in the chromatogram corresponds to unbound NTF2/Ran wt. In contrast, the elution profile of NTF2∗Ran AcK71 fully superposes with the peaks of NTF2 and Ran AcK71 and does not exhibit a smaller retention volume. This clearly confirms that acetylated Ran at lysine 71 is not able to bind do NTF2.

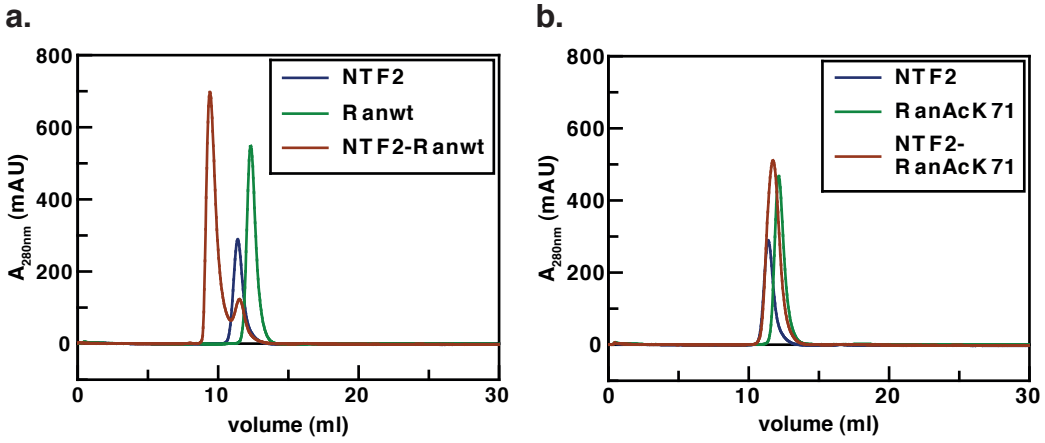

FIGURE 3.6: **Analytical size-exclusion chromatography of Ran-NTF2-complexes.** (a) The elution behavior of Ran wt, NTF2 and the preformed complex was analyzed by size-exclusion chromatography. 150 μM protein or the equimolar complex was applied to a Superdex S75 10/300 column at a flow-rate of 0.6 ml/min. Protein was detected by absorption at 280 nm. (b) The same procedure as described in (a) was applied to Ran AcK71.

In interphase cells, around 90 % of the endogenous Ran is localized in the nucleus (Ren et al., 1993). The fact that Ran AcK71 is not binding to NTF2 should result in the cytosolic accumulation of Ran. To test this hypothesis *in vivo*, HeLa cells were transfected with EGFP-constructs of the acetylation mimetics glutamine (Q) and arginine (R). The mimetics for lysine 71 were first evaluated regarding

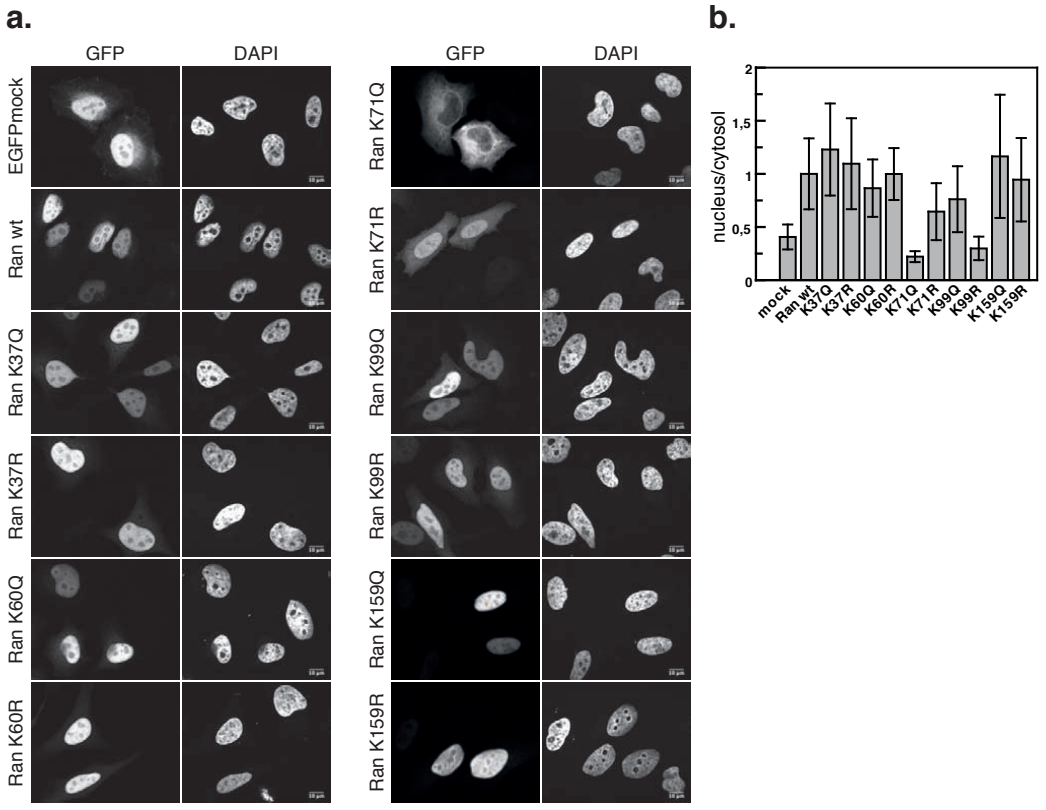

FIGURE 3.7: **Subcellular localization of acetylation mimetics.** (a) HeLa cells were transfected with Ran K to Q and K to R mutants with C-terminal EGFP-tag and additionally stained with DAPI. Cytosolic accumulation was observed for Ran K71Q/R and K99R. Scale bar 10 μm (b) Quantification of subcellular localization of Ran-EGFP-constructs. The ratio of nuclear to cytosolic EGFP-intensity was determined for at least 20 cells per condition. Shown is the mean $\pm$ s.d. relative to Ran wt.

their validity and applicability. Ran K71Q turned out to mimic the acetylated Ran in regard to NTF2 interaction, since ITC measurements as well as analytical gelfiltration verified the inability of complex formation. In contrast, Ran K71R still exhibits binding to NTF2, even though with a reduced affinity.

For the localization studies, HeLa cells were grown on cover slips and transfected with the C-terminal EGFP-constructs of Ran wt and all five acetylation sites. The ratios of the cytosolic and nuclear fluorescence signal were determined. As seen in figure 3.7.a, the C-terminal EGFP-tag does not interfere with the nuclear localization of Ran in interphase cells. Furthermore, the majority of acetylation mimetics (except for K71Q, K71R and K99R) also show a nuclear localization similar to the wildtype protein. This observation corresponds well to the affinities determined by ITC, which indicated normal NTF2 binding behaviour for all

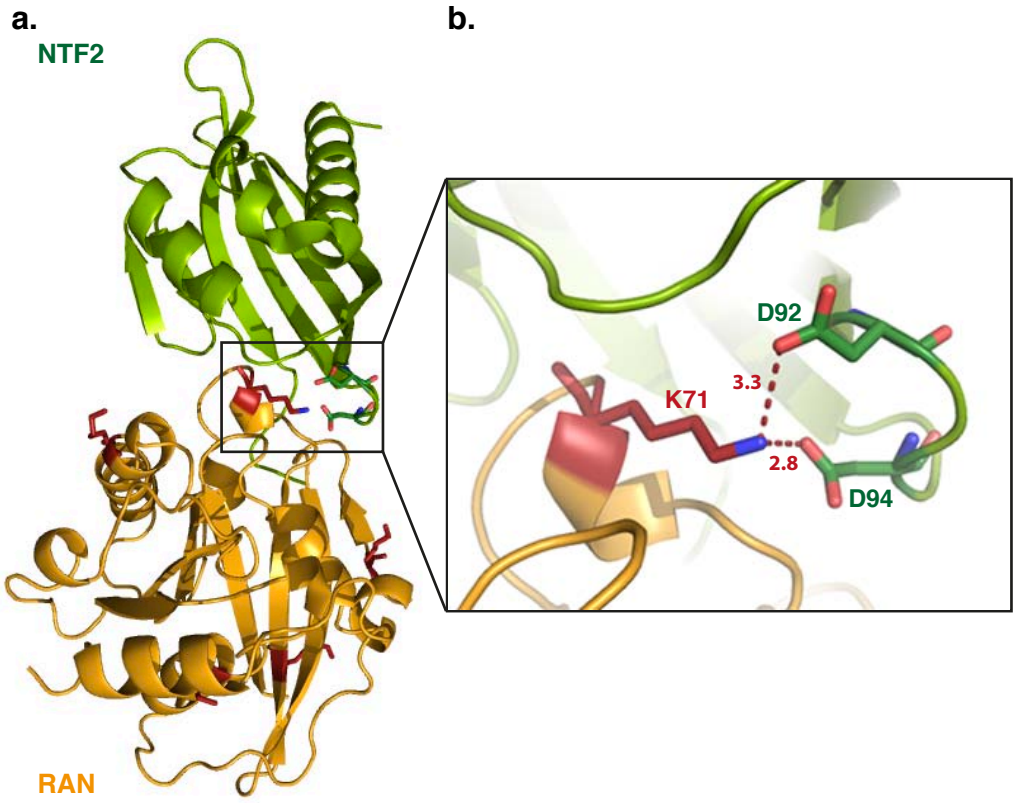

FIGURE 3.8: **Ran in comlex with NTF2.** (a) Ribbon-presentation of Ran (yellow) in complex with NTF2 (green) with the ve acetylation-sites studied here (red sticks) (PDB:1A2K). (b) Close-up of the binding interface with the two essential salt-bridges and corresponding interaction distances.

acetylated Ran versions except for AcK71. In agreement with the *in vitro* data Ran K71Q accumulates in the cytosol and is almost depleted from the nucleus, since it is restricted to enter the nucleus by di usion. Ran K71R, however, is almost evenly distributed between nucleus and cytosol, which is probably due to the reduced binding a nity of Ran K71R towards NTF2. The altered localization of Ran K99R has to be attributed to a disturbed process independent from NTF2-binding, since the determined a nity is similar to Ran wt. Acetylation of the other three lysine residues does neither a ect the binding a nities towards NTF2 nor the subcellular localization of the corresponding EGFP-constructs. The described ndings t well to the available structural data of the NTF2 Ran wt complex (pdb:1A2K)(Stewart et al., 1998)). Two of the major intermolecular contacts are two salt bridges formed between lysine 71 of Ran and aspartic acid residues 92 and 94 of NTF2 (see Figure 3.8). The disruption of the salt bridges by acetylation of the lysine side chain leads to the loss of binding, as shown by ITC and analytical gel ltration. Glutamine, mimicking the neutral charge of an acetylated lysine, is

not able to restore the salt bridges and consequently exhibits the same phenotype as Ran AcK71. The arginine substitution, in contrast, retains the charge characteristics of an unmodified lysine by simultaneously mimicking the steric features of acetylated lysine. This combination preserves the salt bridges and NTF2 binding, albeit with lower affinity due to steric reasons.

The characterization of the interaction of site-specifically acetylated Ran and NTF2 revealed that acetylated Ran at lysine 71 is not able to bind to NTF2. Since Ran AcK71 is then restricted to enter the nucleus by diffusion, it accumulates in the cytosol. Depending on the ratio/abundance of this acetylation this could severely derogate the nucleocytoplasmic transport machinery, by diminishing the level of actively cycling Ran.

3.2.2 Effect of Ran-acetylation on RCC1-interaction and nucleotide exchange

The existence of the Ran gradient is a prerequisite for several cellular processes, including mitotic spindle formation and nucleocytoplasmic transport. The slow intrinsic nucleotide exchange rate of Ran is accelerated by a Ran-specific guanine nucleotide exchange factor (RanGEF), namely RCC1. RCC1 is associated with chromatin and binds Ran∗GDP and Ran∗GTP likewise. The acetylation of Ran could influence the interaction of Ran and RCC1 or the catalyzed nucleotide exchange reaction. Both processes were analyzed separately. The binding affinities and interaction thermodynamics were determined by ITC, whereas the exchange reaction was monitored by stopped-flow.

Binding affinities determined by ITC

The binding affinities of RCC1 and Ran∗GDP and Ran∗GppNHp were determined by ITC. GppNHp was used as a non-hydrolyzable GTP-analog, to investigate the triphosphate state without disturbances by nucleotide hydrolysis. The nucleotide exchange was done with either catalytic amounts of RCC1-GST or by applying the EDTA-method. ITC measurements were done in phosphate buffer at 1000 rpm, differential power 6, 120 s initial delay and spacing and 2 μl injections. The standard setup comprised 293 μM Ran in the syringe and 37 μM RCC1 in the cell at 25 °C. Concentrations and measurement temperature were adjusted whenever necessary and changes are stated in the corresponding text.

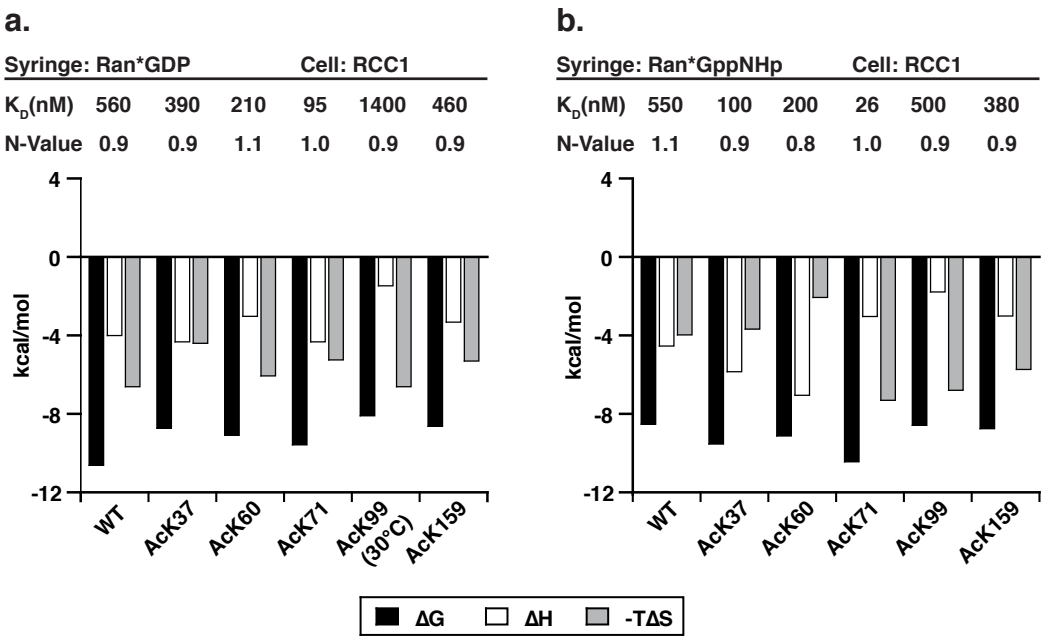

FIGURE 3.9: **Signature plots of the interaction of Ran and RCC1.**Signature plots showing free energy (ΔG), reaction enthalpy (ΔH) and reaction entropy (-TΔS) of the interaction of Ran (wt and AcKs) and RCC1 determined by ITC in KP_i at 25 °C. Determined K_D-values and stoichiometries are given in the upper panel. (a) Ran∗GDP (180 μM) was titrated to RCC1 (22 μM). (b) Ran∗GppNHp (300 μM) was titrated to RCC1 (37 μM).

Binding affinities of Ran wt as well as acetylated Ran towards RCC1 are in the medium nanomolar range (in phosphate buffer). Please refer to Appendix A.4 and A.5 for original ITC-curves and fitting results. All interactions are characterized by a favourable (exothermic) reaction enthalpy and a favourable reaction entropy. The resulting free energy (ΔG) is comparable for all interactions of Ran wt and acetylated Ran with RCC1. For Ran wt and most AcKs the bound nucleotide (GDP or GppNHp) does only marginally affect the binding affinities measured by ITC (see Figure 3.9). This observation is in agreement with the accepted binding model, suggesting a tight Ran-RCC1 complex after nucleotide release from a loose ternary Ran-GXP-RCC1 complex. Thus, RCC1 does not distiguish between the active (GTP) or inactive (GDP) nucleotide state of Ran and directionality of nucleotide exchange is rather dependent on prevailing concentrations. The determined affinities for RCC1 are 560 nM and 550 nM for Ran-GDP and Ran∗GppNHp, respectively. Taking the manufacturers tolerance of $\pm$ 20% for K_A into account, the determined binding affinities of AcK37∗GDP, and AcK159∗(GDP and GppNHp) are similar/comparable to the wildtype. Ran AcK60 binds RCC1

with a roughtly 2-fold reduced affinity which is also nucleotide-independent. Interestingly, the Ran AcK37 interactions are dependent on the bound nucleotide. Ran AcK37∗GDP binds with 390 nM, whereas the active, GppNHp-loaded protein binds with a 5-fold higher affinity (100 nM). However, how AcK37 mediates this effect on the molecular level is unclear. Acetylation on lysine 71 resulted in the most prominent alteration, increasing the RCC1-affinity 6- and 20-fold for AcK71∗GDP and -GppNHp, respectively.

The comparison of the thermodynamic profiles of all interactions sets Ran AcK99 apart from the other Ran AcKs. The interaction of AcK99 in both nucleotide states is characterized by a distinctly lower reaction enthalpy which is only partially compensated by a slightly higher entropic contribution. Due to the resulting weak heat signal, the measurement had to be conducted at 30 °C instead of 25 °C in the case of AcK99∗GDP. This clear difference in the thermodynamic profile indicates a different binding mechanism for this interaction.

RCC1-catalyzed nucleotide exchange reaction characterized by stopped-flow

The effects of Ran-acetylation on the RCC1-catalyzed nucleotide-exchange reaction were investigated by stopped-flow measurements (original traces and fits in Appendix A.6). The Ran-protein was loaded with fluorescently-labeled mantGDP and subsequently titrated with increasing concentrations of RCC1 in the presence of unlabeled GTP. The decrease in fluorescence was plotted against time and fitted to a single-exponential function to give the observed rates (k_{obs}) for each RCC1-concentration. The plot of the observed rates against the RCC1-concentration resulted in a hyperbolic curve (Figure 3.10.a). Fitting to equation 2.8 determined the maximal rate of nucleotide dissociation (k_{-2}) and the affinity constant for the binding of RCC1 to Ran∗mGDP (K_{-1})(Figure 3.10.b). For further details refer to Chapter 2.5.3.

For the reaction of Ran wt and RCC1 an affinity constant of 1.1 μM and a maximal nucleotide dissociation rate of 12.8 s^{-1} were determined. The dissociation constant is similar to published values also determined by stopped flow, namely 0.9 - 1.3 μM (Klebe et al., 1995b). The dissociation rate deviates noticeably from the published value (21 s^{-1}), however, this is probably due to differences in the experimental setup (exchange for GTP instead of GDP, slightly different Ran construct). Since the main focus of this investigation is the direct comparison of Ran

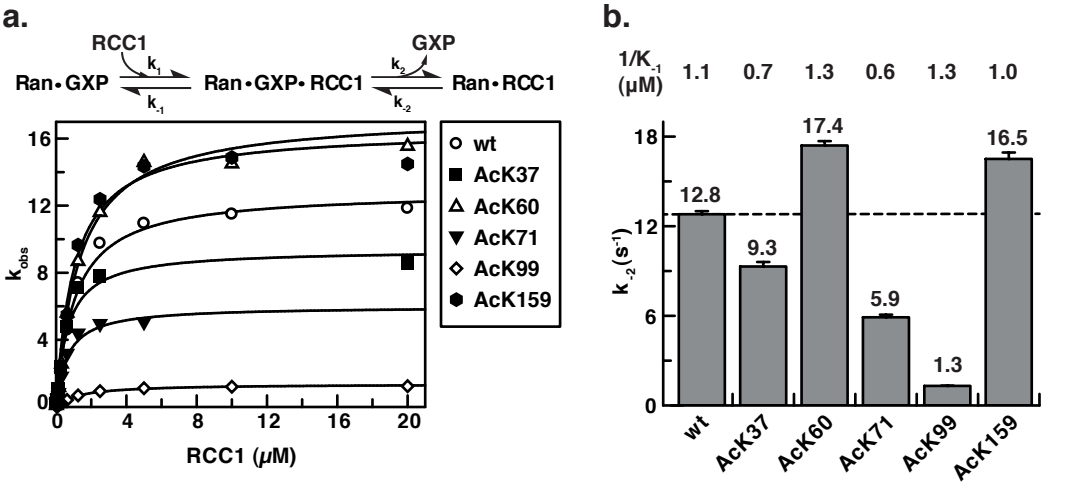

FIGURE 3.10: **RCC1-catalyzed nucleotide exchange measured by stopped-flow.**Ran∗mantGDP (1 μM) was titrated with RCC1 (0.039 - 80 μM) in the presence of GTP (50 μ). Tryptophanes were excited at 295 nm and mant-fluorescence was detected using a 420 nm-cut off filter. (a) Reaction scheme and hyperbolic plot of k_{obs} over the RCC1-concentration. (b) Determined nucleotide-dissociation rates (k_{-2}) and affinity constants ($1/K_1$) of RCC1 and Ran∗mantGDP.

wt with the acetylated Ran variants, these minor deviations are negligible/acceptable. Acetylation of Ran on lysines 60 and 159 results in a slight increase of the RCC1-catalyzed nucleotide dissociation rate and RCC1 affinities (K_D) similar to Ran wt. Ran AcK37, on the other hand, exhibits a slightly decreased dissociation rate in combination with a lower equilibrium dissociation constant ($1/K_{-1}$). The fact that these three Ran variants show only minor deviations from the Ran wt behavior, corresponds well to the thermodynamic binding characterization by ITC. In contrast acetylation of Ran at lysine 71 or 99 affects the RCC1-catalyzed reaction drastically. Ran AcK71 has a 2-fold decreased nucleotide dissociation rate, which could be due to the drastic increase in binding affinity (nucleotide-dependent 6- to 20-fold) as determined by ITC. However, the strongest impairment of the exchange reaction is exerted/caused by Ran-acetylation at lysine 99. The nucleotide dissociation is reduced by a factor of ten, whereas the RCC1 affinity is comparable to Ran wt.

Structure-based discussion of results

The crystal structure of the Ran-RCC1 complex (PDB: 1I2M) locates the Ran-binding site opposite to the chromatin binding site of the seven-bladed β-propeller of RCC1. The RCC1-structure does not change much upon Ran-binding, except

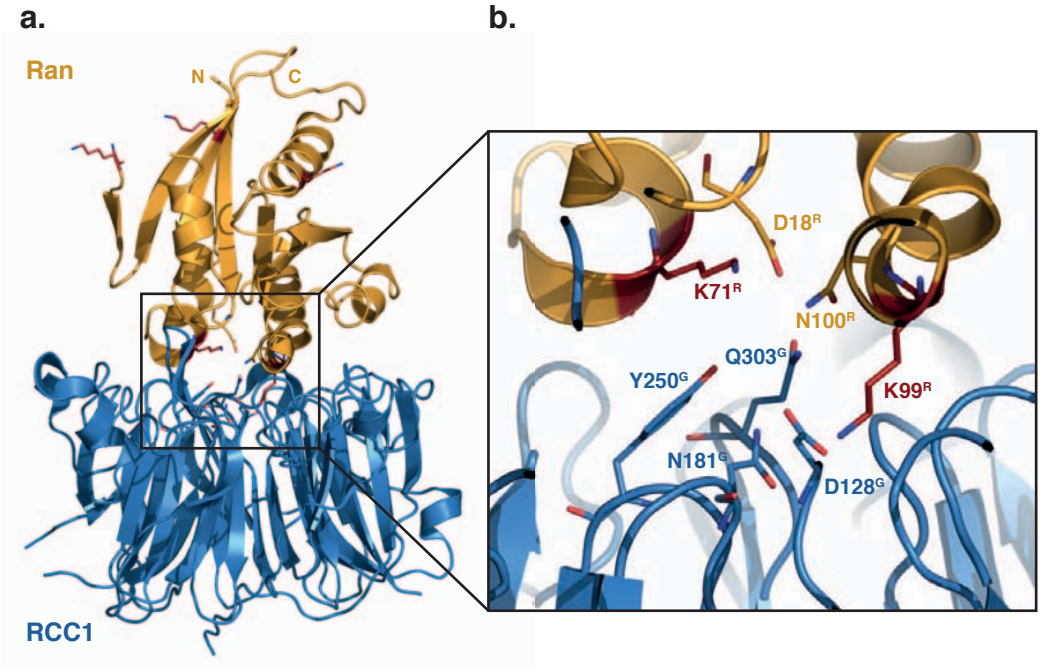

FIGURE 3.11: **Ran in comlex with RCC1.**(a) Ribbon-presentation of Ran (yellow) in complex with RCC1 (blue) with the ve acetylation-sites studied here (red sticks) (pdb:1I2M). (b) Close-up of the binding interface with the Ran lysines 71 and 99 as well as the RCC1 residues in interaction distance (blue sticks).

for a prominently protruding/exposed -sheet in blade three (146 - 153), the so called -wedge. In contrast, the Ran structure shows structural di erences in switch II, helices 3/ 4 and the ^{121}NKxD^{125} nucleotide base binding motif. The two acetylation sites with the strongest impairment of the RCC1-catalyzed exchange reaction, lysines 71 and 99, are both located in the binding interface of Ran and RCC1 (see gure 3.11.a and b). Lysine 71 is part of switch II, which rearranges upon RCC1-binding and interacts with N268 and H304 of RCC1. Lysine 71 is also in interaction distance of lysine 18 in the P-loop of Ran. Mutational studies in the past pointed towards K71 and F72 of Ran as very important for the interaction with RCC1 (Renault et al., 2001). This study shows that acetylation of K71 drastically increases the a nity towards RCC1, presumably by forming additional contacts. Furthermore, the nucleotide dissociation rate of Ran AcK71 is lowered by a factor of two compared to Ran wt. Since switch II is not directly involved in the nucleotide exchange reaction, this e ect is more likely due to the altered binding a nity. Acetylated Ran at lysine 99 exhibited a tenfold reduced RCC1-catalyzed nucleotide dissociation rate in combination with a changed thermodynamic interaction pro le determined by ITC. This is not surprising, given

that lysine 99 is located in helix α3, which forms the most extensive interactions with RCC1. Especially Ran lysine 99 relocates upon binding to be buried in a pocket close to the central tunnel of the RCC1-propeller structure. It furthermore interacts with D128 and N181 of RCC1. Acetylation of this residue results in a reduced reaction enthalpy, indicating a loss of hydrogen bonds, salt bridges or van-der-Waals interactions. The observed effects could either be due to drastically altered binding kinetics or an indirect structural interference with the nucleotide exchange reaction. Notably, the RCC1 mutations D182A and H304A significantly affect the k_{kat} of RCC1 (Renault et al., 2001). Structural data based on a complex of Ran AcK71 or AcK99 and RCC1 would provide valuable information regarding the molecular mechanisms of the acetylation effects. All crystallization attempts with recombinant Ran AcK 71/99 and RCC1 in different construct lengths failed, though.

3.2.3 Effect of Ran-acetylation on Importin-β interaction

In the nucleocytoplasmic transport cycle, Ran∗GTP binds to transport receptors to facilitate cargo-binding (export receptors) or -release (import receptors) in the nucleus. Importin-β, the classical import receptor, was chosen to investigate the effect of Ran-acetylation on import receptor binding. The binding affinities and thermodynamic parameters of the interaction were determined by ITC (Figure 3.12 and Appendix A.7). Furthermore, the association kinetics were analyzed by stopped-flow measurements. Due to the extremely low k_{off} rate for the high-affinity Ran-Importinβ-complex and protein stability issues, we desisted from analyzing the dissociation reaction, but derived them from the K_D and k_{on} values instead.

Since Importin-β does exclusively bind Ran∗GTP, ITC measurements were done with GppNHp-loaded Ran. For a standard binding experiment 268 μM Importin-β was titrated to 40 μM Ran∗GppNHp in 2.5 μl injection-steps. The titration was done at 25 °C in phosphate buffer at 800 rpm, differential power 6, 180 s initial delay and spacing.

Importin-β binds with an affinity of 160 nM to Ran wt∗GppNHp in phosphate buffer. In contrast, published affinities ,determined indirectly by competition assays or fluorescence-based determination of the kinetic constants, are in the low nanomolar to picomolar range (Görlich et al., 1996; Villa Braslavsky et al., 2000).

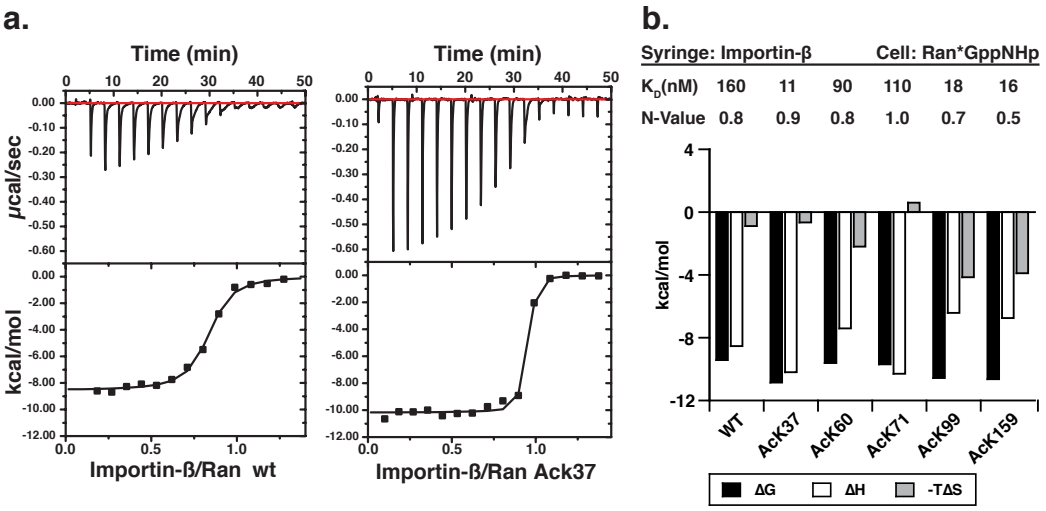

FIGURE 3.12: **Thermodynamic characterization of the Importin-β - Ran interaction.** (a) Representative ITC titrations of Ran∗GppNHp (40 muM) to Importin-β (268 muM) in KP_i at 25 °C. (b) Signature plot showing free energy (ΔG), reaction enthalpy (ΔH) and reaction entropy (-TΔS) of Ran wt and AcKs. Determined K_D-values and stoichiometries are given in the upper panel.

This variance is due to the influence of the used interaction buffer, especially the salt-content. In Tris- and phosphate-buffer containing 150 mM salt the binding affinity of Ran wt to Importin-β is increased to sub-nanomolar levels (data not shown), hence to the detection limit of ITC. To still be able to compare the interaction of Importin-β with Ran wt and the Ran AcKs using ITC, we took advantage of the reduced affinities in the phosphate buffer system (without salt). Ran wt and all Ran AcKs bound to Importin-β in an exothermic reaction with almost identical values for the free energy (ΔG)(Figure 3.12.b). All reactions are enthalpy-driven and exhibit enthalpy-entropy-compensation, which can often be observed for protein-protein- and protein-ligand interactions (Frisch et al., 1997; King et al., 2012). In comparison to Ran wt, Ran AcK99 and AcK159 have a higher reaction entropy contributing to binding, which is compensated by a lower enthalpic contribution. In the case of Ran AcK71 binding to Importin-β a slightly unfavorable reaction entropy was measured, which is counteracted by an increased favorable enthalpy. The K_D-values determined for the acetylated Ran variants are in the low nanomolar range and indicate strong binding. Ran AcK60 and AcK71 bind with comparable, or slightly higher affinity to Importin-β compared to Ran wt. Acetylation on lysines 37, 99 or 159, however, results in a 8 - 14-fold stronger binding to the import receptor.

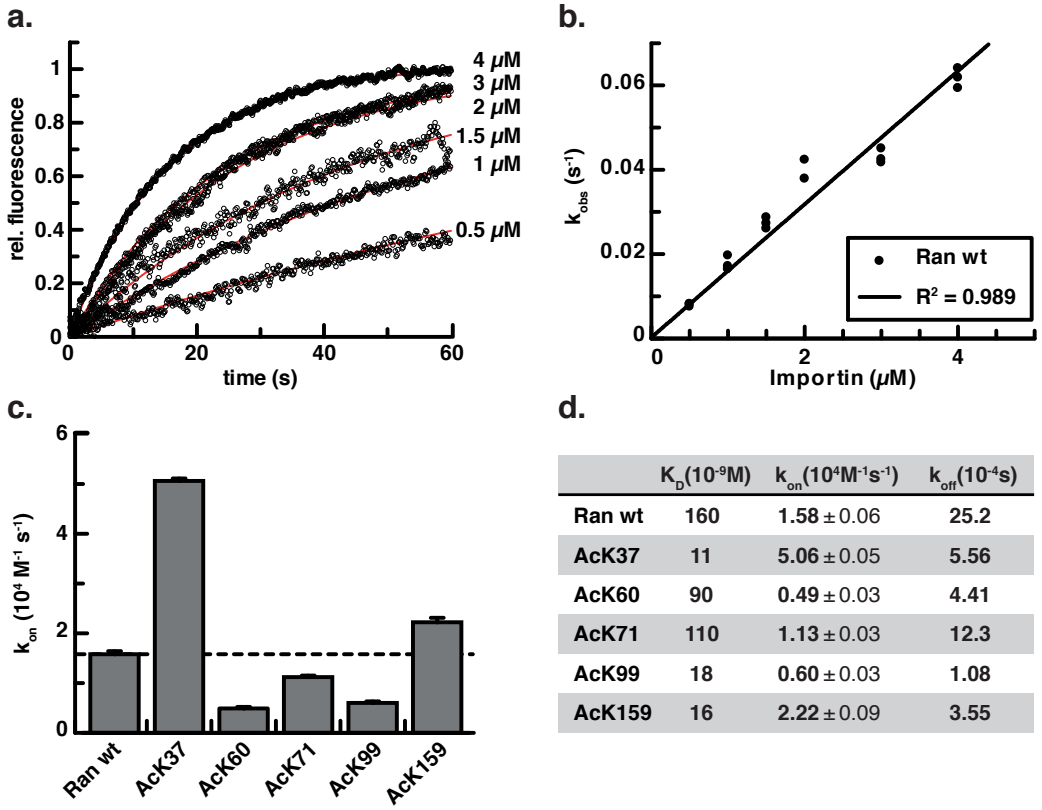

	K_D(10^{-9}M)	k_{on}($10^4 M^{-1}s^{-1}$)	k_{off}(10^{-4}s)
Ran wt	160	1.58 ± 0.06	25.2
AcK37	11	5.06 ± 0.05	5.56
AcK60	90	0.49 ± 0.03	4.41
AcK71	110	1.13 ± 0.03	12.3
AcK99	18	0.60 ± 0.03	1.08
AcK159	16	2.22 ± 0.09	3.55

FIGURE 3.13: **Association of Importin-β and Ran measured by stopped-flow.** Ran∗mantGppNHp (200 nM) was titrated with Importin-β (1 - 8 μM) in K_{Pi} at 25 °C. The increase in fluorescence of the mant-fluorophor (λ_{ex}: 320 nm, λ_{em}: 450 nm) was monitored. (a) Original traces and single-exponential fits for Ran wt. (b) Plot of k_{obs} over the Importin-β concentration and linear fit to determine k_{on} for Ran wt. (c) Determined k_{on} rates for Ran wt and all AcKs. (d) Affinity constants (ITC), k_{on} rates (stopped-flow) and resulting k_{off} rates (calculated).

The association kinetics of the interaction were analyzed by stopped-flow (Figure 3.13). To this end, 200 nM mantGppNHp-labeled Ran was mixed with 1 - 8 μM Importin-β in potassium phosphate buffer at 25 °C. The increase in fluorescence of the mant-fluorophor (λ_{ex}: 320 nm, λ_{em}: 450 nm) was monitored over time and fitted to a single-exponential function to give the observed rates (k_{obs}). The plot of the k_{obs}-values over the Importin-β concentration resulted in a linear curve with the slope k_{on} (see Appendix A.8 and A.9 for original traces and linear fits). The association rate for Ran wt and Importin-β was determined as $1.5{\cdot}10^{-4}\,M^{-1}s^{-1}$, which is in accordance with the published value of $1.3{\cdot}10^{-4}\,M^{-1}s^{-1}$ in HEPES buffer at 20 °C (Villa Braslavsky et al., 2000).

The majority of acetylated Ran variants (namely AcK 60, 71, 99 and 159) only

marginally affects the association rate. In contrast, acetylation of lysine 37 results in a 3-fold increase of the association rate to Importin-β. Since all experiments (ITC, stopped-flow) were conducted under the same conditions (25 °C, KP_i) the Ran∗mGppNHp-Importin-β dissociation rate (k_{off}) can be determined from the measured equilibrium dissociation constant (K_D) and the association rate (k_{on}). The calculated dissociation rate (k_{off}) for all Ran AcKs is slower than for Ran wt, ranging from a 2-fold decrease for Ran AcK71 to a 24-fold reduction for Ran AcK99. Taken together, the interaction studies revealed that acetylation of Ran at different lysine residues may increase the binding affinity by altering the association and dissociation rates likewise.

3.3 Regulation of Ran acetylation

3.3.1 Ran acetylation *in vivo*

Several mass-spectrometry based screens in different species and under different conditions identified up to eleven acetylation sites in Ran. However, the stoichiometry of these acetylation events was neither the major focus of these studies, nor were/are the techniques for stoichiometry determination in these large-scale bottom-up screens advanced enough. Therefore, it is unclear whether lysine acetylation of Ran ranks among a low-stoichiometry background or exists with relevant abundance. I wanted to address this question with a top-down approach, detecting the acetylation on the full-length protein level by immunoblotting of isolated endogenous Ran.

The first technique was based on an anti-acetyl-lysine-antibody coupled to agarose-beads (ImmuneChem). These beads were also used by Choudhary *et al.* to enrich acetylated peptides prior to mass-spectrometrical analysis (Choudhary et al., 2009). Immunodetection of Ran after affinity-pull-down combined with detection of acetyl-lysine with a different antibody would have been a reliable readout for Ran-acetylation. However, this approach proved unsuitable. Tests with recombinant Ran (wt and acetylated) showed that Ran binds unspecifically to the agarose beads. Furthermore, it could not be ruled out, that Ran is pulled-out indirectly due to binding to histone-associated RCC1 or other acetylated proteins.

As an alternative endogenous Ran was isolated from cell lysate with GST-RCC1, the GEF of Ran. Owing to the extensive characterization of the interaction between RCC1 and the Ran AcKs (see section 3.2.2) it can be excluded, that single-acetylation at either of the studied sites prevents RCC1-binding. The determined affinities of 30 nM to 1.4 μM should allow efficient pull-down of all Ran AcKs. In fact, the pull-down with RCC1 worked quantitatively. Lysates of several cell lines (HeLa, MV4-11, NB4) under different growth- and stress-conditions (interphase, mitosis, osmotic stress) were used for the pull-down (Table 3.3). Immunoblotting of the eluates for Ran and AcK demonstrated successful isolation of Ran but no acetylation was detected (data not shown). Thus, a low stoichiometry of Ran-acetylation has to be assumed for the conditions tested.

TABLE 3.3: Cell lines and conditions (all ± Inhibitors) used for the pull-down with RCC1

Cell line	Interphase	Mitosis	Osmotic Stress	24 h Inhibitors
HeLaB	x	x	x	x
NB4	x	-	-	-
MV4-11	x	-	-	-
LoVo	x	-	-	-
HEK293	x	-	-	-

3.3.2 Regulation by specific deacetylases

The availability of natively-folded, site-specifically acetylated Ran provided the opportunity to test all human deacetylases for activity against each of the examined acetylation-sites. To this end all human KDACs (HDAC1-11 and Sirtuins 1-7) were purchased as recombinantly purified, active proteins (see Table 2.6). All enzymes were tested regarding their deacetylase-activity by using commercially available Fluor-de-Lys substrates in a fluorescence-based deacetylation-assay. In this assay all KDACs were applied according to the specific activity given by the manufacturer. Thus, identical levels of deacetylation were expected under identical assay conditions. However, as shown in Figure 3.14 strong variations were observed. Since all reactions were performed in parallel (HDACs and Sirtuins separately) the different deacetylation levels are probably due to deviating enzyme activities under the used assay conditions. In the case of Sirt6 the low activity

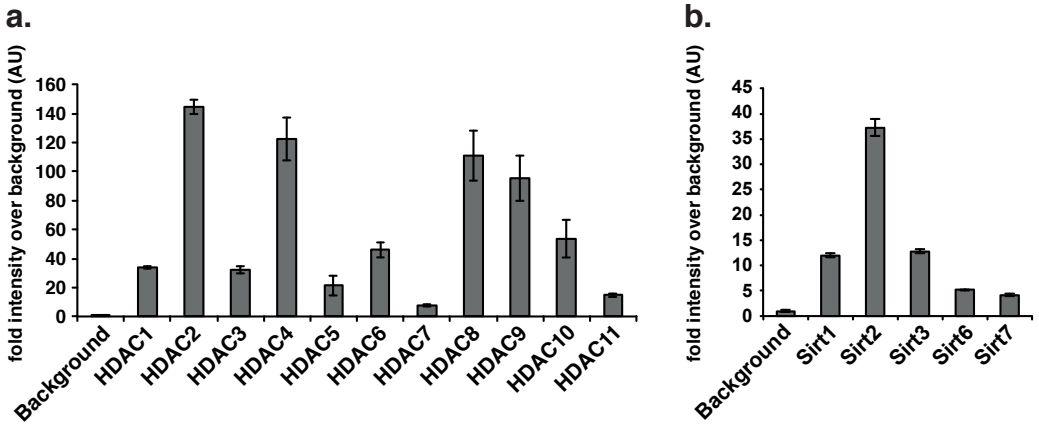

FIGURE 3.14: **Verification of enzymatic activity for all KDACs.**Fluor-de-Lys substrate was incubated with recombinant KDACs according to the enzymatic activity given by the manufacturer. After cleavage with trypsin, fluorescence intensities were determined (λ_{exc} 350 nm, λ_{em} 450 nm). (a) 1000 pmol HDAC substrates 2a or 3 were used. (b) 250 pmol Sirt2 substrate was used.

can be explained by its preference to remove long-chain fatty acyl-chains, such as myristoyl, from lysine residues (Jiang et al., 2013). For Sirt7 no deacetylase activity could be shown for peptides, apart from H3K18, *in vitro* so far, suggesting a high specificity. To provide comparable conditions in the subsequent KDAC screen, the amount of enzyme was normalized to correspond to a 40 % increase of intensity over the background in the initial activity assay. Hence more enzyme was used in the case of HDAC 1, 3, 5, 7 and 11 and less for HDAC 2, 4, 6, 8, 9 and 10. For the sirtuin assay all enzyme amount were increased except for Sirt2.

The KDAC-screen was set up as a dot-blot of triplicates for every acetylation-site with and without the respective enzyme after incubation for 3 h at 25 °C. The sequential detection of acetyl-lysine and Ran (loading control) was done by imunoblotting. The histogram in figure 3.15 shows the mean relative fluorescence

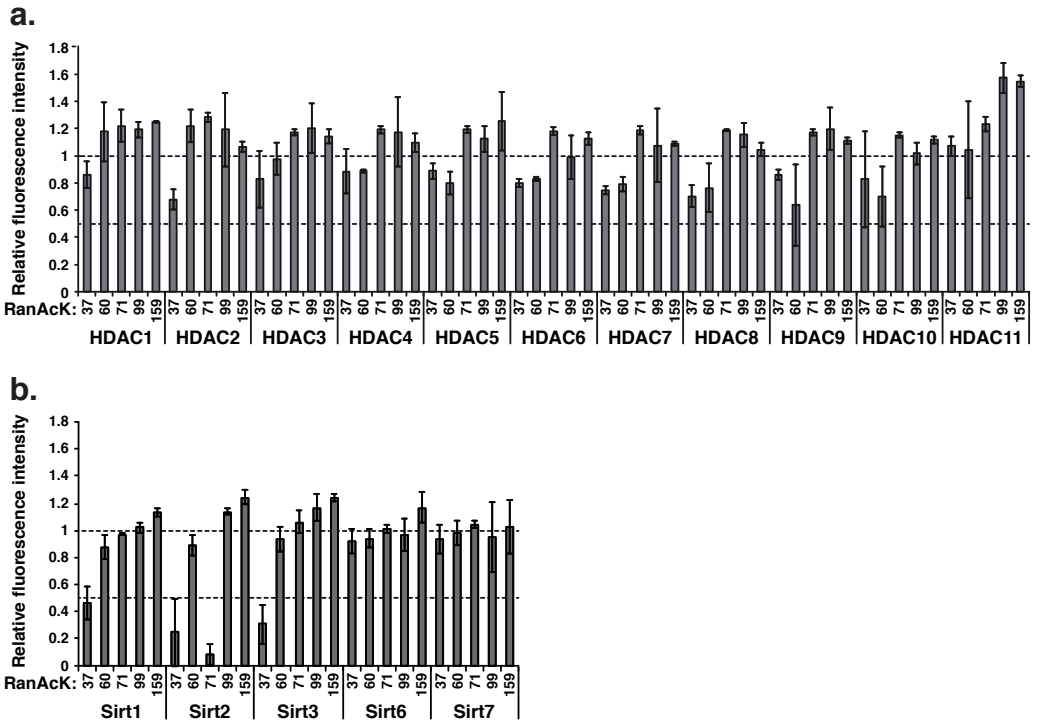

FIGURE 3.15: **Deacetylation of recombinant Ran AcKs by classical KDACs and Sirtuins.**Recombinant Ran AcKs (100 pmol) were incubated in triplicates with/without deacetylases. Amounts of enzymes were adjusted to correspond to 40 % fold intensity in the initial activity assay (Fig. 3.14). Acetylation was detected by dot-blot and subsequent immunoblotting with the anti-AcK antibody and anti-Ran for loading control. AcK-signals were normalized to Ran-loading. The mean ± s.d. of triplicates is shown. (a) All classical HDACs and (b) human sirtuins 1, 2, 3, 6 and 7 were tested for activity against the five Ran acetylation sites.

intensity with standard deviation for every combination tested. For none of the tested human HDACs a substantial deacetylation activity against the tested Ran AcKs was observable under the assay conditions. However, three sirtuins (Sirt1 -3) exhibited activity against Ran AcKs, resulting in a more than 50 % reduction of the AcK-speci c uorescence signal.

In vitro assays followed by immunoblotting veri ed, that sirtuins 1, 2, and 3 deacetylate Ran AcK37, whereas Ran AcK71 is speci cally deacetylated by Sirt2 only (Figure 3.16.a). As expected for sirtuin-catalyzed reactions, deacetylation is NAD^+-dependent and can be inhibited by nicotinamide (NAM).

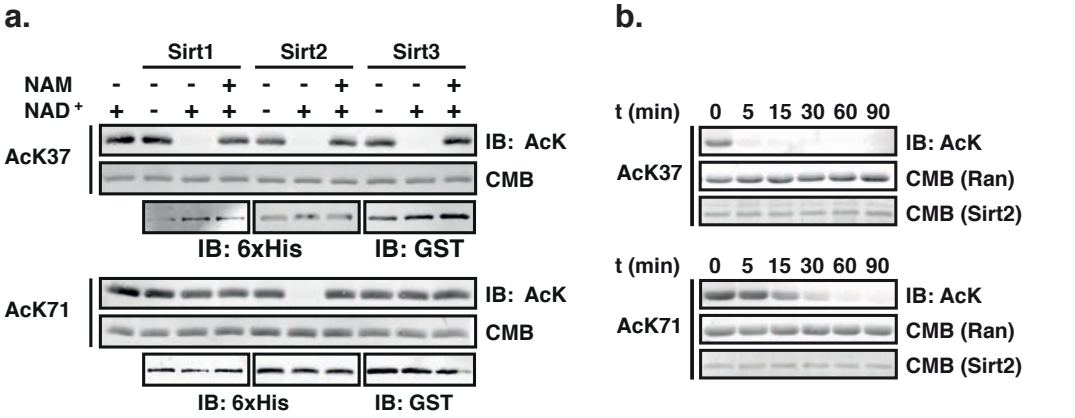

FIGURE 3.16: **Ran is deacetylated by sirtuins 1, 2 and 3.**(a) 3 g recombinant Ran AcK were incubated with sirtuins 1, 2 and 3 (0.6 g, 0.2 g and 0.55 g) for 2 h at room temperature. Shown are immunoblots using the anti-AcK antibody, Coomassie-blue staining (CMB) for Ran-loading and anti-His/anti-GST as input-control for the enzymes used. (b) Time-course experiment with 25 g Ran AcK37 and AcK71 and 1.5 g Sirt2. Signal detection by immunoblotting with anti-AcK antibody, SDS-PAGE as loading control for Ran and Sirt2. Both experiments were conducted by P. Knyphausen.

The time-course experiment with AcK37 and Ran AcK71 in gure 3.16.b reveals that the deacetylation rate of Sirt2 is much higher for AcK37 than for AcK71. Thus, the acetylated lysine 37 of Ran, located in the relatively exible switch I region, seems to be an excellent substrate for Sirt1, Sirt2 and even the mitochondrial Sirt3. In contrast, deacetylation of AcK71, which is also located in a exible region (switch II), is highly speci c for Sirt2, albeit with a slower rate.

Interestingly, both Sirt2-target sites are located in the essential switch regions of Ran. Lysine 37 is located in switch I, whereas lysine 71 is situated in switch II. Both exible loops interact with the bound nucleotide and change conformation dependent on the nucleotide state. This conformational shift is the basis for the

discrimination between active GTP-bound- and inactive GDP-bound-Ran by Ran-effector proteins. As a consequence, the switch regions, and hence lysines 37 and 71, are often/usually part of the binding interface with Ran-binding proteins. To test, whether Sirt2-catalyzed deacetylation is dependent on the nucleotide-state or complex-formation of Ran, time-course experiments were conducted. So far, all deacetylation experiments used Ran∗GDP AcKs as substrates. In this experiment Ran∗GppNHp AcK37 and 71 as well as the Ran∗GDP-NTF2-complex and the, theoretically nucleotide-free, Ran-RCC1-complex of AcK37/71 were used as Sirt2 substrates (Figure 3.17). Ran∗GppNHp was chosen instead of Ran∗GTP to circumvent interference by the intrinsic nucleotide-hydrolysis.

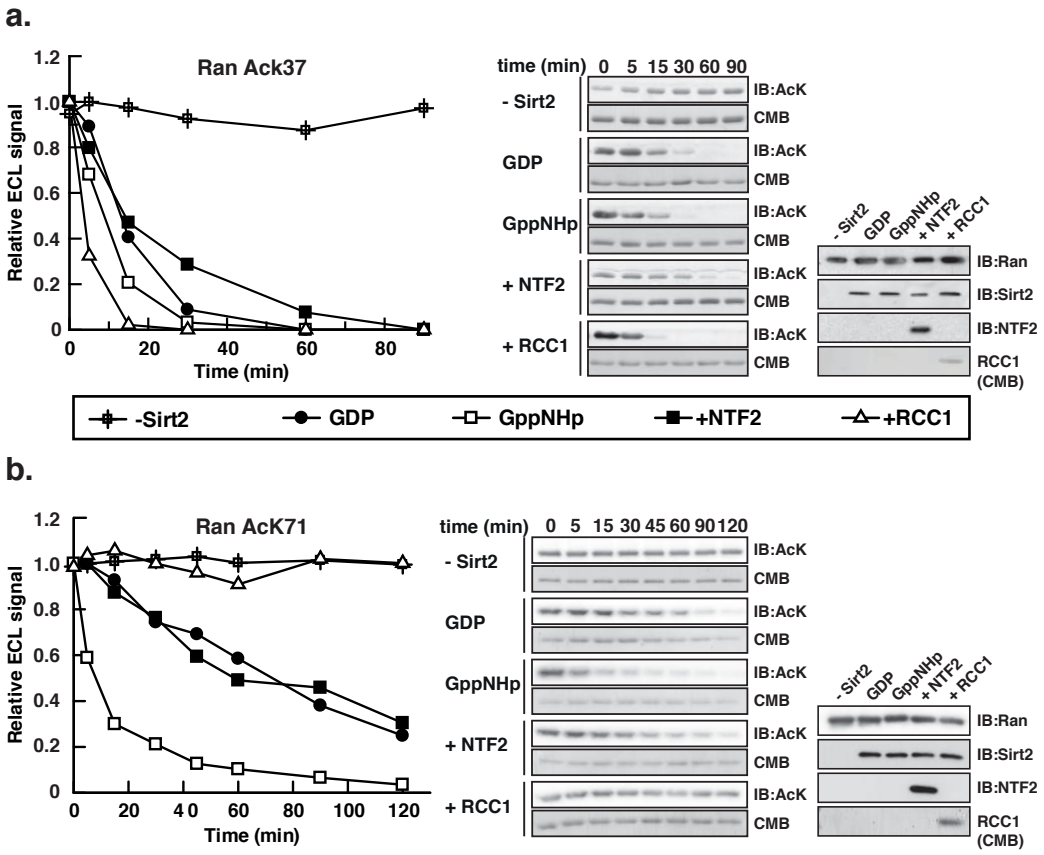

FIGURE 3.17: **Dependence of Sirt2 deacetylation on complex-formation and nucleotide-state.** 65 μg recombinant Ran were incubated with Sirt2 at 25 °C and samples taken after the indicated time points. Immunodetection with anti-AcK antibody and corresponding quantification with ImageJ is shown. Coomassie-blue staining (CMB) serves as Ran-loading control. Input was detected with anti-Ran, anti-Sirt2, anti-NTF2 and CMB for RCC1 (far-right panel). (a) 1 μg Sirt2 was used for Ran AcK37. (b) 3.7 μg Sirt2 were used for Ran AcK71.

In the case of Ran AcK37 no substantial difference between the two nucleotide states was observed. However, NTF2-binding to Ran decreased the deacetylation rate, whereas RCC1-interaction led to a faster deacetylation. In contrast to lysine 71, which forms two salt bridges with NTF2, lysine 37 is not directly involved in NTF2-binding and steric hindrance is not apparent from the crystal structure. The accelerating effect of RCC1 on the deacetylation rate of AcK37 is not surprising, since lysine 37 adopts a more solvent-exposed conformation in the RCC1-complex crystal structure compared to Ran∗GDP (Figure 3.11.b).The analogous experiment was conducted with Ran AcK71, however, to compensate for the slower deacetylation rate of Sirt2 four times more enzyme was used. The deacetylation rate of Ran∗GDP AcK71 is unaffected by NTF2. This result is in agreement with the inability of complex-formation between Ran AcK71 and NTF2, shown in section 3.2.1. RCC1, on the other hand, prevents deacetylation of AcK71. This effect is most likely due to the inaccessibility of lysine 71 in the Ran-RCC1-complex, which is completely burried in the binding interface. Unexpectedly, Sirt2-catalyzed deacetylation of Ran AcK71 is strongly nucleotide dependent. Ran∗GppNHp AcK71 is deacetylated considerably faster than Ran∗GDP AcK71. Lysine 71 is located in the switch II loop, which adopts a rigid conformation in the GppNHp-bound state but exhibits a high degree if flexibility in Ran∗GDP. In other words, the deacetylation of AcK71 by Sirt2 is faster when switch II has a fixed conformation. This effect could indicate that, apart from a consensus sequence, additional structural features are required for substrate recognition and efficient deacetylation at lysine 71 by Sirt2.

In the literature, Sirt2 is widely regarded as a deacetylase preferentially acting in unstructured regions with a rather low specificity (Khan and Lewis, 2005; Martínez-Redondo and Vaquero, 2013). We took advantage of the availability/presence of another lysine residue adjacent to lysine 37 to test this assumption. The recombinant Ran AcK38 served as a control for the specificity of Sirt2. Contradictory to the prevailing opinion Sirt2 clearly discriminates between lysine 37 and 38. Despite the almost identical structural context, AcK38 is deacetylated with a drastically reduced rate (Figure 3.18).

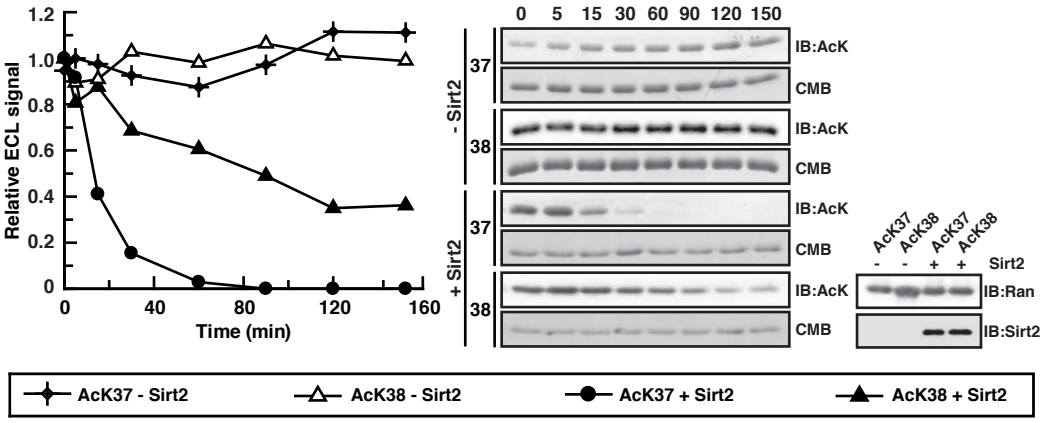

FIGURE 3.18: **Sirt2 distinguishes between Ran AcK37 and AcK38.**The deacetylation of Ran AcK38 is considerably slower than the deacetylation of the adjacent position AcK37. 65 μg recombinant Ran were incubated with Sirt2 at 25 °C and samples taken after the indicated time points. Immunodetection with anti-AcK antibody and corresponding quantification with ImageJ is shown. Coomassie-blue staining (CMB) serves as Ran-loading control. Input was detected with anti-Ran, anti-Sirt2, anti-NTF2 and CMB for RCC1 (far-right panel).

3.3.3 Regulation by acetyl-transferases

In vitro KAT assays analyzed by immunoblotting

Commercially available acetyl-transferases were used to acetylate recombinant Ran wt *in vitro*. The two closely related KATs p300 and CBP represent the p300/CBP-family of KATs. They are the most prominent KATs in the literature. Furthermore Gcn5 and pCAF were chosen as representatives of the Gcn5/pCAF family and Tip60 as a member of the MYST-family. The enzymatic activity of the KATs was verified by *in vitro* acetylation of known histone-substrates. For p300, CBP and Gcn5 the histone H3 was used, whereas H4 was chosen for pCAF and Tip60. The histones were recombinantly expressed and purified from *E.coli* and, thus, unacetylated. Incubation with the respective KATs in KAT-buffer containing acetyl-CoA yielded acetylated histones, as verified by immunoblotting against acetyl-lysine (Figure 3.19.a). Gcn5 exhibited a noticeably weaker acetylation activity than the other KATs. For pCAF and Tip60 more H4 substrate had to be used to obtain a decent acetylation signal, probably due to weaker recognition of the H4-acetylation sites by the used AcK-antibody.

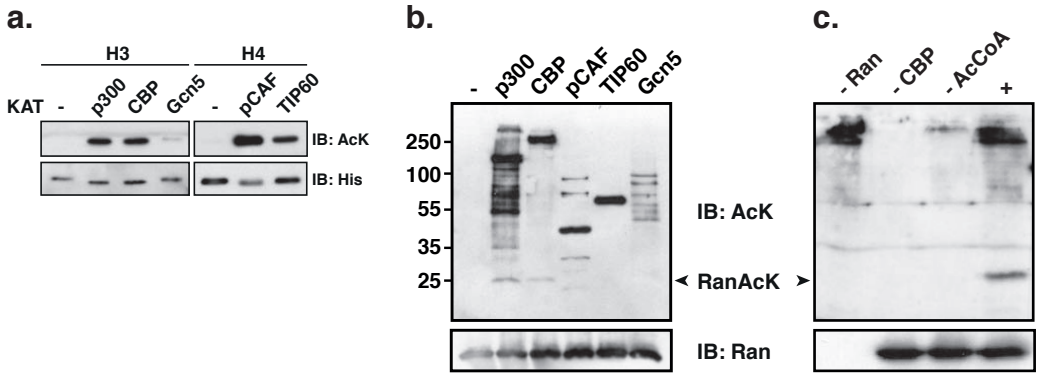

FIGURE 3.19: **Acetylation of Ran by CBP *in vitro*.**(a) KAT activities were tested with histone substrates. 0.75 μg H3 and 7.5 μg H4 were incubated with 1 μl commercially available lysine-acetyltransferase in KAT-buffer. Immunodetection with anti-AcK and anti-His (loading) is shown. (b) *In vitro* transferase assay with Ran wt as substrate. Immunoblotting for AcK reveals acetylation of Ran by p300 and CBP. Immunoblotting for Ran serves as loading control. (c) Specificity of Ran-acetylation by CBP. Negative controls (without Ran, CBP or Acetyl-CoA)

For the *in vitro* KAT assay, recombinant Ran wt was incubated with the KATs in KAT-buffer containing 100 μM acetyl-CoA. A sample with Ran wt and acetyl-CoA without transferase served as negative control. After 4 h at 25 °C samples were processed by SDS-PAGE and subsequent immunoblotting for acetyl-lysine. Due to autoacetylation all KATs are visible on the blot. Since autoacetylation is beneficial for all KATs tested here, the appearance of the autoacetylation-signals is also a good indication for enzymatic activity under the assay conditions used. The negative control shows no acetylation signal. After incubation with p300 and CBP, however, a weak acetylation signal could be observed which corresponds to the molecular weigth of Ran (Figure 3.19.b). Several controls confirmed the specificity of the Ran-acetylation, as shown in Figure 3.19.c. Again, incubation of Ran with CBP and acetyl-CoA (+) resulted in a decent acetylation-signal. In contrast, no acetylation was detectable at this height when Ran was absent. In the sample without CBP (still containing Ran and acetyl-CoA) neither Ran-acetylation nor the autoacetylation of CBP was detectable. This control also excludes an unspecific, chemical acetylation of Ran under these specific assay conditions with a pH of 7.3. This intentionally chosen pH reflects the cytosolic/nuclear pH-conditions (Llopis et al., 1998). A more basic pH would increase the reactivity of the lysine side chains and thereby facilitate chemical acetylation. This effect is postulated for the mitochondrial matrix showing a slightly more basic pH (pH $\approx$ 8). The last

control in Figure 3.19.c, without acetyl-CoA, confirmed the dependence of the CBP-catalyzed reaction on the cofactor acetyl-CoA. The weak autoacetylation signal, even in the absence of acetyl-CoA, suggests that CBP is already partially acetylated after purification of the enzyme.

Taken together, the *in vitro* KAT assays with Ran wt and five representative KATs indicate that Ran is acetylated by p300 and CBP in an acetyl-CoA-dependent manner/reaction. Furthermore, no unspecific, chemical acetylation was observed under cytosolic/nuclear pH-conditions *in vitro*.

In vitro KAT assays analyzed by mass-spectrometry

To verify the results from the in vitro KAT assays by a more sensitive method and to determine the exact acetyl-acceptor-lysines, mass-spectrometry was used as a second, independent detection method. To this end, 10 μg Ran wt was incubated with 1 μl KATs in the presence of acetyl-CoA for 4 h at 25 °C. The samples were digested with trypsin and finally peptides were analyzed by mass-spectrometry (for a detailed description refer to Chapter 2). The raw data was processed with MaxQuant using the implemented Andromeda search engine. To enable comparability all determined peptide intensities were normalized to correspond to a total

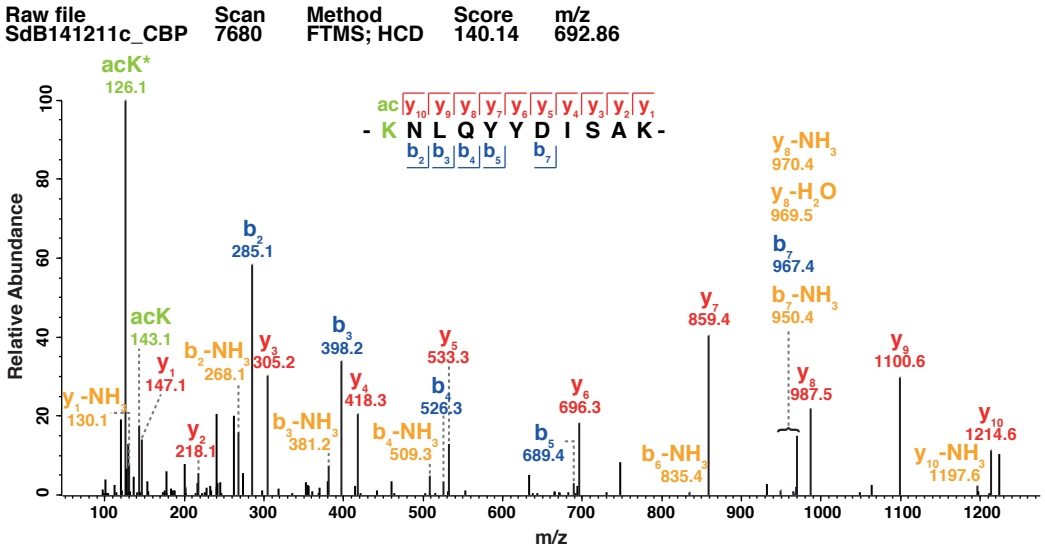

FIGURE 3.20: **MS/MS spectrum of the AcK142-peptide.** Annotated MS/MS spectrum of the modified peptide corresponding to AcK-site 142 in Ran. Fragments are assigned and color-coded and detected masses are given for every fragment. The immonium-ions at m/z 126 and 143 are marker ions for peptides containing ϵ-N-acetyl-lysine. Corresponding spectra for AcK37 and AcK134 are shown in Appendix A.10

protein intensity of $1{\cdot}10^{11}$. A representative MS/MS spectrum is shown in Figure 3.20. In this case the two marker immonium ions with m/z 126 and 143 were fragmented (Trelle and Jensen, 2008).

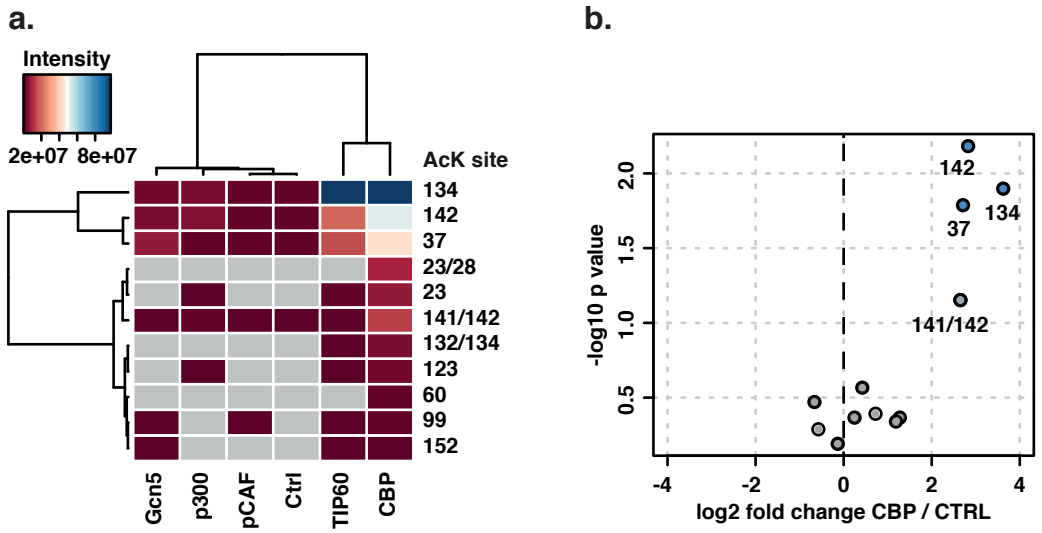

FIGURE 3.21: **Mass-spectrometrical analysis of Ran-acetylation *in vitro*.**(a) Heat-map with hierarchical clustering of identified acetylation-sites. The mean intensities of two independent *in vitro* KAT-assays are shown with missing values in grey (b) Volcano-plot of three independent *in vitro* KAT-assays with Ran and CBP. The Ran lysines 37, 134 and 142 were identified as the most significant acetylation sites (p-value < 0.05).

Two independent experiments were averaged for the heat-map in Figure 3.21.a. The mean normalized intensities of the identified acetylated Ran peptides (n=2) are shown for the control (Ctrl, no KAT) and the five KATs. Missing values (peptide not detected) are shown in grey. In the control experiment four out of eleven acetylated peptides were detected. Compared to the control, the samples with pCAF, p300 and Gcn5 exhibited only marginal upregulation of acetylation. Few additional acetylated peptides were detected and, in the case of Gcn5 and p300, the peptides AcK 134, 142 and 37 had slightly higher intensities. However, for Tip60 and CBP a strong upregulation of Ran acetylation was determined. In agreement with the immunodetection, the CBP-treated samples had the maximum number of acetylated peptides (11) and the highest intensities. The peptide acetylated at lysine 134 was detected with the highest intensity, followed by AcK 142 and AcK37. A similar pattern was observed for Tip60, but only nine out of eleven peptides were detected. Three independent KAT assays with Ran wt and CBP were analyzed by mass-spectrometry and data presented in a volcano-plot

(Figure 3.21.c). Every data point corresponds to one specific acetylated peptide. The majority of acetylated peptides are characterized by a low statistical significance (low -$\log_{10}$ p-value) and a small $\log_2$-fold change of the intensity compared to the control without transferase. Four peptides stand apart from this cluster of low significance/low magnitude fold change, of which AcKs 37, 134 and 142 are characterized by a p-value below 0.05 and a decent intensity change compared to the control.

The interpretation of both experiments/approaches/analysis indicates that CBP and Tip60 are Ran-specific acetyl-transferases, *in vitro*. The mass-spectrometrical approach furthermore identified the lysines 37, 134 and 142 as the major acetyl-acceptors.

***In vivo* KAT assays analyzed by mass-spectrometry**

In the cell, KATs are tightly regulated and often exert their activity as part of large multimeric complexes. The *in vitro* assays are incapable/unsuitable to take necessary, yet unknown, cofactors and regulators of the KATs into account. To provide a more physiological background for the KAT reaction, a human cell line was transiently transfected with the respective acetyl-transferases. This experiment was conducted by Philipp Knyphausen.

His_6-Ran was co-expressed with Myc-tagged KATs (His_6-Tip60) in HEK293T cells. Cells were lysed, Ran was pulled-down with Ni-NTA-beads and subsequently processed for mass-spectrometrical analysis. Immunoblotting of the input of the pull-down confirms the overexpression of the transfected KATs. In addition to the five KATs used in the *in vitro* assay, the α-tubulin-specific acetyl-transferase α-TAT was included in this assay. In contrast to the *in vitro* data, were raw unnormalized peptide intensities were used for analysis, I used the intensities of the label-free quantification (LFQ) for the *in vivo* data. Hence, the peptide intensities were normalized to the protein background present after the pull-down procedure. Intensities of acetylated peptides were normalized to a total protein intensity of $1{\cdot}10^{11}$, averaged over two independent experiments and presented/depicted in the heat-map in Figure 3.22.b.

In contrast to the *in vitro* KAT assay with eleven acetylated peptides, only three acetylated peptides were identified in the *in vivo* assay. The control sample without overexpression of KAT already contained the peptides corresponding to AcK 134 and 142. The strongest intensity increase was observed for AcK134 in the

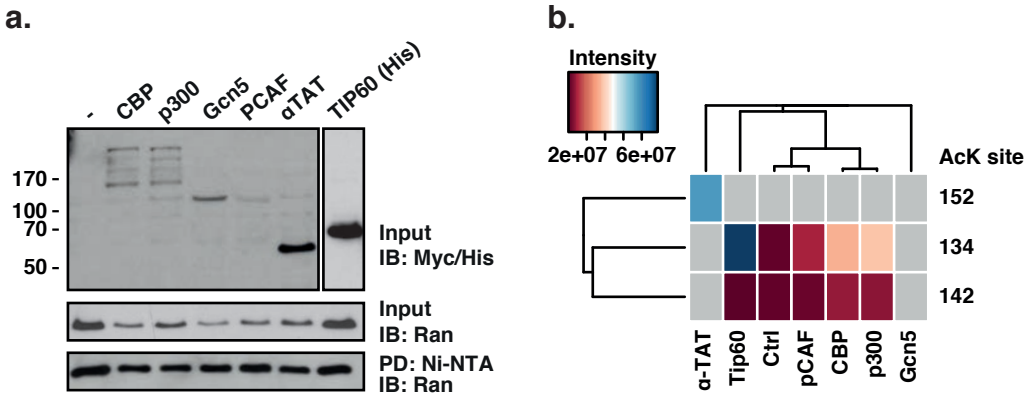

FIGURE 3.22: **Ran-acetylation by KAT-overexpression *in vivo*.**(a) Co-transfection of His_6-Ran and Myc-tagged KATs (His_6-Tip60) in HEK293T cells and subsequent Ni-pulldown of Ran. Successful transfection of KATs was verified by immunoblotting against Myc-tag (His_6-tag for Tip60). Experiment conducted by P. Knyphausen.(b) Heat-map with hierarchical clustering of identified acetylation-sites after *in vivo* acetylation. The mean intensities of two independent pulldowns are shown with missing values in grey

Tip60-sample, followed by CBP and p300 which led to an approximately 2-fold increase in intensity for this peptide. The acetylation of lysine 134 by Tip60 and CBP is in agreement with the *in vitro* assay (Figure 3.21.b), whereas almost no upregulation of AcK142 was detected here. The detected acetylation activity of p300 on Ran supports our initial observation by immunoblotting (Figure 3.19.b). Interestingly, α-TAT seems to acetylate Ran exclusively at lysine 152, which would indicate a high degree of specificity. However this observation is so far not verified by another independent assay. In the sample with Gcn5 overexpressed no acetylated peptide was detected, although the presence of transferase was confirmed by immunoblotting and mass-spectrometry.

Chapter 4

Discussion

4.1 Summary of results

Effects on Ran-function and Ran-interactions

Five Ran acetylation sites were identified in an acetylome screen of human cell lysates by the group of Choudhary *et al.*, which were confirmed - and complemented by additional sites- by subsequent screens in different organisms.(Choudhary et al., 2009). In the course of this study, site-specifically acetylated Ran was produced by recombinant expression from *E.coli*. To introduce the amino acid acetyllysine into the protein, the genetic-code expansion concept was used, which is based on an evolved acetyl-lysyl-tRNA synthethase/$tRNA_{CUA}$ -pair from *Methanosarcina barkeri*(Neumann et al., 2008). The incorporation as well as the subsequent purification was highly efficient, yielding pure protein in quantities suitable for biophysical characterization. Furthermore, Ran-binding proteins, namely NTF2, RCC1 and Importin-β, were successfully purified from *E.coli*. The interactions of the binding-proteins with Ran wt were in agreement with published data and confirmed the activity of the recombinant proteins. The produced acetylated Ran variants exhibited no noticeable difference in intrinsic properties compared to each other or Ran wt. Ran wt and all AcKs were highly stable in the used buffer system and the nucleotide binding ability was unaffected by acetylation, as judged by nucleotide exchange reactions and fluorescence assays (data not shown). The observed identical elution behavior from size exclusion chromatography also indicated similar protein conformations and oligomerization states.

Regarding the interaction with Ran-binding proteins, several Ran AcKs show distinct deviations from the Ran wt behavior. Acetylation at lysine 71 of Ran completely abolishes binding to NTF2, whereas acetylation of the other four lysines do not affect this interaction *in vitro*. Ran AcK71, furthermore, drastically increases the RCC1-binding affinity 6- to 20-fold, depending on the nucleotide state, and decelerates the RCC1-catalyzed nucleotide exchange observed by stopped-flow measurements. Acetylation of lysine 99 results in an even stronger impairment of the RCC1-catalyzed nucleotide exchange, reducing the nucleotide dissociation rate by a factor of ten. This effect is accompanied by an altered binding mechanism, which becomes apparent by different binding thermodynamics of the interaction of RCC1 and Ran AcK99 compared to Ran wt. Regarding the interaction with the import receptor Importin-β, Ran acetylation impacts on the binding affinities and the interaction kinetics. Three Ran AcKs exhibit higher binding affinities for Importin-β (AcK37, AcK99 and AcK159). In the case of Ran AcK37 the tighter binding is due to a 4-fold accelerated association rate in combination with a reduced dissociation rate. For Ran AcK99 and AcK159 a reduction of the dissociation rate appears to be the main reason for the higher affinity constants.

Abundance and regulation of Ran-acetylation

The pull-down of endogenous Ran from cell lysates combined with the specific detection of acetylated lysines by immunoblotting was a major goal of this thesis. Different techniques for the isolation of Ran were tested. A pull-down with GST-RCC1 was chosen, since it proved quantitative and is not interfering with the subsequent specific detection of acetyl-lysine. Different cell lines and growth-/stress-conditions were tested for Ran acetylation. Nevertheless, no acetylated Ran was detected by immunoblotting.

In the absence of direct evidence for the physiological relevance of Ran-acetylation, the identification of enzymes regulating the acetylation of Ran provides indirect evidence. An extensive screening procedure with all human deacetylases (classical HDACs and sirtuins) identified Sirt1, -2 and -3 as deacetylating enzymes for lysine 37 in Ran. Furthermore, Sirt2 specifically removes the acetyl-group from lysine 71. Both lysines (37 and 71) are located in the flexible switch regions of Ran, which adopt different nucleotide-dependent conformations. Interestingly, the Sirt2-catalyzed deacetylation is accelerated in the GppNHp-bound state (compared to the GDP-state) for both positions, but more pronounced for Ran AcK71∗GppNHp.

The enzymatic acetylation of Ran was shown by immunoblotting. Incubation of Ran wt with the human lysine-acetyltransferases p300 and CBP results in a Ran-specific acetylation signal. The acetylation is dependent on the KAT co-factor acetyl-CoA and chemical acetylation (without transferase) could be excluded by several control experiments. No acetylation signal was detected for the transferases Tip60, pCAF and Gcn5. Mass-spectrometrical analysis of all *in vitro* KAT-assays (-KAT, p300, CBP, Tip60, pCAF and Gcn5) detected eleven acetylated peptides, predominantly in the samples treated with CBP and Tip60. Three independent experiments with CBP identified the lysines 37, 134 and 142 as the major acetyl-acceptors with considerable upregulation and statistical significance (p-value < 0.05) over all three measurements. *In vivo* acetylation of Ran by overexpression of the respective transferases supports this result. Again, Tip60 as well as CBP and p300 lead to an increase in acetylation, primarily at lysine 134. Notably, in contrast to the *in vitro* KAT-assays, only three acetylated peptides were detected. The *in vivo* KAT assay, furthermore, indicates acetyltransferase activity of α-TAT at lysine 152 of Ran.

4.2 Implications for the biological relevance of Ran acetylation

This study demonstrates the broad regulatory spectrum of lysine acetylation as a post-translational modification. For the small GTPase Ran the effects of acetylation range from catalytic inactivity or loss-of function due to disruption of protein-protein interactions to fine-regulation by slightly altered binding kinetics.

Acetylation of lysine 71 in switch II

Acetylation at lysine 71 of Ran completely abolishes binding to NTF2, the protein responsible for Ran-relocation to the nuclear compartment. The loss of this interaction restricts Ran relocation to diffusion, which, for Ran-sized proteins, is slowed down more than 500-fold by the permeability barrier of the NPC (Ribbeck and Görlich, 2001). This ultimately results in a cytosolic accumulation of Ran∗GDP AcK71. The disruption of NTF2-binding is not surprising for acetylation of this specific lysine, since it abolishes the formation of two essential salt-bridges. In addition to the NTF2-mediated effect, a dominant negative effect of AcK71 on

RCC1 was observed, resulting from a much slower RCC1-catalyzed nucleotide exchange process and a stronger binding affinity. The same effect is observed for the T24N mutation in Ran (Dasso1994). If acetylation of lysine 71 accumulates to quantitative levels, both effects ultimately disrupt the Ran∗GDP/GTP-gradient crucial for nucleocytoplasmic transport in interphase cells. The high affinity for RCC1 in combination with the decelerated nucleotide exchange results in a prolonged residence time of Ran AcK71 in the nucleus and, consequently, in much slower Ran-cycling and less cargo-transport. The cytosolic accumulation due to diffusion-restricted reentry into the nucleus would almost completely arrest nucleocytoplasmic transport. The role of NTF2 during mitosis is unknown, thus the effect of prevention of NTF2-binding by AcK71 under mitotic conditions needs further investigation.Assuming that only a minor proportion of Ran is acetylated at lysine 71, this modification could modify the Ran-gradient or the Ran-localization in a regulated manner. In response to a certain stimulus (e.g. radicals, osmotic stress, hormone) Ran acetylation at lysine 71 could be up-regulated (refer to subsection 4.2) to either slow-down the transport machinery or to make more Ran∗GDP available for a, yet unknown, cytosolic function. The specific deacetylation by the cytosolic Sirt2 would terminate this temporary state and restore the original Ran-gradient.

Acetylation of lysine 99 (loss-of-function)

The loss-of-function acetylation of lysine 99 would result in a different phenotypical scenario. Ran acetylated in that position binds RCC1 with affinities comparable to Ran wt, but the catalyzed nucleotide exchange reaction is drastically slower. As a consequence, the overall production of Ran∗GTP in the nucleus is inhibited by the blockage of RCC1 by Ran AcK99. Dependent on the proportion of AcK99 the phenotype could range from a slightly reduced transport rate to a drastic reduction of Ran-cycling/transport due to nuclear accumulation of Ran∗GDP AcK99. However, this tremendous regulatory spectrum requires regulatory tools, in this case specific acetyltransferases and deacetylases. Enzymatic acetylation of lysine 99 by acetyltransferases was detected in this study (CBP, Tip60, pCAF and Gcn5), however the data do not allow for an explicit conclusion regarding the KAT-regulation of that position. In fact, almost all acetylome screens published to date prove the existence of Ran AcK99 (Figure 4.1) , either due to chemical or enzymatic acetylation (Beli et al., 2012; Choudhary et al., 2009; Henriksen et al., 2012; Lundby et al., 2012; Mertins et al., 2013; Sol et al., 2012; Weinert et al., 2011). Either way, accumulation of Ran AcK99 would severely impact on

all essential Ran-functions and has to be tightly regulated or the accumulation has to be strictly prevented. Yet, in contrast to AcK71 we did not identify the deacetylase specific for Ran AcK99 with our *in vitro* KDAC-screen, not ruling out the regulation *in vivo*. Acetylation of other lysines Apart from the radical effects

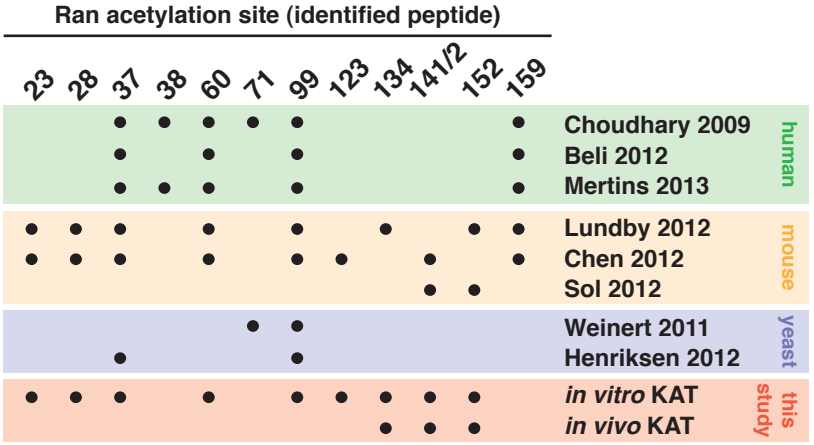

FIGURE 4.1: **Ran acetylation sites detected in different MS-based studies.**Summary of all Ran acetylation sites identified in MS-based acetylome screens in different species and by *in vitro*/*in vivo* KAT assays in the course of this study.

of AcK71 and AcK99, Ran acetylation also has the potential for fine-regulation of interaction processes, as observed for the Ran-Importinβ-interaction. Several Ran AcKs impact on the binding kinetics and the equilibrium dissociation constant. In the physiological context, such small changes could represent regulatory screws to adjust Ran-Importin-β interactions and, consequently, transport-rates. Please note, that the *in vitro* characterization of the effect of Ran-acetylation on Importin-β-binding presented here does not satisfy the complexity of the physiological interaction. Neither the presence of Importin-α nor a cargo protein was taken into account in this study.

The strong regulation of the acetylation on lysine 37 by Sirt1, -2 and -3 and the acetyltransferases Tip60 and CBP/p300 suggests an important function of that specific acetylation site. From the data presented here, a direct effect of AcK37 on RCC1- or NTF2-interaction can be excluded. Furthermore, the interaction with Crm1, Snurportin-1, RanGAP and RanBP1 , as well as the RanGAP-catalyzed nucleotide-hydrolysis reaction are unaffected by acetylation of lysine 37 (P.Knyphausen, unpublished). However, Ran AcK37 has a clear effect on

Importin-β-interaction, drastically increasing the association-rate and the binding affinity. How this impacts on the assembled import-complex (Importinβ-Importinα-cargo) is unclear.

Apart from the five acetylation sites identified in the original screen, several more sites have been reported over the last six years (Figure 4.1). According to our *in vivo* and *in vitro* acetylation data three of these sites, namely K134, K142 and K152, are dominant acetyl-acceptor lysines for some of the KATs tested and, thus, of potential physiological relevance. Lysine 134 (K136 in yeast) is reported to be essential for the interaction of Ran and the nucleotide release factor Mog1 in yeast (Baker et al., 2001; Steggerda and Paschal, 2000). Initial interaction studies with Ran AcK134 and Mog1 indeed suggest that K134-acetylation blocks Mog1-binding (P.Knyphausen, unpublished). Since the function of Mog1 in the Ran-system itself is unknown, a prediction of the physiological consequences of the prevention of Ran-interaction by acetylation of lysine 134 is not possible at that time. Lysine 152 is part of the SAK-motif (G5, Table 1.2) and, hence, involved in nucleotide binding by contacting the guanine base. Thus, lysine acetylation in that position might affect nucleotide binding. Based on available structural data one could, furthermore, speculate about consequences of acetylation of K134/142/152 for nuclear import/export and the formation of RanBP1-complexes. The intramolecular interaction of K152 with the acidic C-terminus (DEDDDL) in RanBP1-containing complexes (Ran∗RanGAP∗RanBP1, PDB: 1K5D/G; Ran∗Crm1∗RanBP1, PDB: 4HB2), for example, might be disturbed. In the case of K152 and K134, electrostatic interactions with Crm1 would be lost upon acetylation (PDB: 3GJX, 4HB2) and also K142 is involved in Crm1- and Importin-β-binding (PDB: 3GJX, 1IBR). However, the actual effects of each of these acetylations on the mentioned interactions would have to be investigated in detail before statements regarding the physiological relevance are feasible.

Crosstalk of PTMs

The possibility of acetylation of more than one lysine *in vivo* impedes the prediction of physiological consequences. Taking all eleven identified acetylation sites in Ran into consideration, the number of possible combinations of lysine acetylation is enormous. And even for the five sites studied here a prediction of the effect of multi-acetylation is not possible, since the assumption of a simple additive effect is not valid. However, in the case of AcK71 and AcK99 such an additive effect regarding the RCC1-interaction and -catalysis is not unlikely. Both lysines are

located in the binding interface and single-acetylation of either of them affects the RCC1 binding affinity and results in the reduction of the nucleotide-dissociation rate from the complex. The actual phenotype of this potential double-acetylation (AcK71/99) needs further investigation.

The crosstalk of Ran acetylation with other post-translational modifications of Ran is another topic, which was not adressed so far, yet might be of physiological relevance. In contrast to many other small GTPases Ran was not found to be regulated by PTMs such as prenylation, phosphorylation or glycosylation. However, proteomic screens identified several of the eighteen lysine residues as potential ubiquitylation sites (Wagner et al., 2011, 2012). In fact all lysines found to be acetylated, were also found to be ubiquitylated. Since this information is exclusively based on mass-spectrometrical analysis, the actual extend as well as the nature of the ubiquitin-modification (mono- or poly-ubiquitylation, sort of chain) is unknown. Furthermore, insights into the functional relevance and the regulation of Ran-ubiquitylation are missing. Even though little is known so far about Ran acetylation and ubiquitylation, a crosstalk between both modifications is very likely and demands further investigations.

This comprehensive study suggests the enormous regulatory potential of site-specific acetylation of Ran. By targeting different lysines, Ran function can be adjusted on different levels. We, furthermore, present strong evidence for the existence of specific regulating enzymes for some of the acetylation sites studied. The attempts of detection and quantification of endogenous, acetylated Ran on protein-level was not successful. Although endogenous Ran was isolated in high quantities from different cell lines and under different growth-/stress-conditions, no acetylated Ran was detected by immunoblotting in either of these samples. To prevent rapid deacetylation upon cell lysis, all isolation steps were carried out at 4 °C and in the presence of deacetylase inhibitors. Enzymatic deacetylation under non-denaturing conditions could be one explanation for the absence of an acetylation signal, however, isolation of acetylated Ran under denaturing conditions (urea) also failed (personal communication with P. Knyphausen). These results suggest a low stoichiometry of Ran acetylation under the conditions tested in the different cell lines. Very low acetylation levels are difficult to detect by immunoblotting, especially in the case of the sites with a low epitope recognition by the AcK-antibody. This holds true for the AcKs 37, 99 and 159, but is unknown for all additional acetylation sites not studied here.

The postulated low abundance of Ran-acetylation in the samples tested questions a possible physiological relevance of this post-translational modification of Ran. The modified peptides detected by mass-spectrometry could represent a low stoichiometry background of acetylation, originating from non-enzymatic, chemical acetylation or unspecific acetylation by transferases. This would be in line with recent publications showing a low stoichiometry background for the majority of proteins in yeast (Weinert et al., 2014). In the mitochondrial matrix, chemical acetylation is an abundant modification event, due to a more basic pH and a high acetyl-CoA-concentration (up to mM) in this cellular compartment. In this context lysine deacetylases might act as detoxifying instead of regulating enzymes, hence a lower substrate specificity is effectual and often observed for these enzymes. In the cytosolic and nuclear compartment chemical acetylation is less likely, since the side-chain reactivity of lysines is reduced at the lower pH (7.3 instead of 8 in mitochondria) and reactive acetyl-donors (acetyl-CoA) are less abundant. Immunoblotting detected no chemical acetylation of Ran in the *in vitro* assay system mimicking cytosolic pH conditions (7.3) even at high concentrations of acetyl-CoA. On the other hand, expression in *E.coli* results in unspecific acetylation of random lysines. The level of these undesired modifications is very low, therefore neither detectable by immunoblotting nor influencing the determination of the correct molecular mass (ESI-MS). Acetylated peptides are only detected by high sensitivity MS-MS measurements following tryptic digest.

Abundance and regulation of Ran-acetylation

[h] And in fact, in a scenario where only a minor proportion of the extensive Ran pool is acetylated, only a gain-of-function modification or a cascade of acetylation events would be of physiological relevance. A cascade, where several acetylations result in the amplification of the final outcome, could be indicated by the fact that several Ran-interacting proteins were also found to be acetylated (e.g. Importin-β, RanGAP and RanBP1). In another scenario, Ran-acetylation is tightly regulated by specific acetylating and deacetylating enzymes. The identification of the Ran-specific acetyltransferases p300/CBP, Tip60 and, potentially, α-TAT as well as the deacetylation of AcK37 and AcK71 by human sirtuins are strong arguments for this scenario. Moreover, the analysis of tissue-specific acetylation patterns in rodents by Lundby *et al.* (Figure 4.2) supports this hypothesis of conditional acetylation of Ran (Lundby et al., 2012). Some tissues exhibit no Ran-acetylation at all, whereas others show a broad spectrum of acetylation sites and -levels.

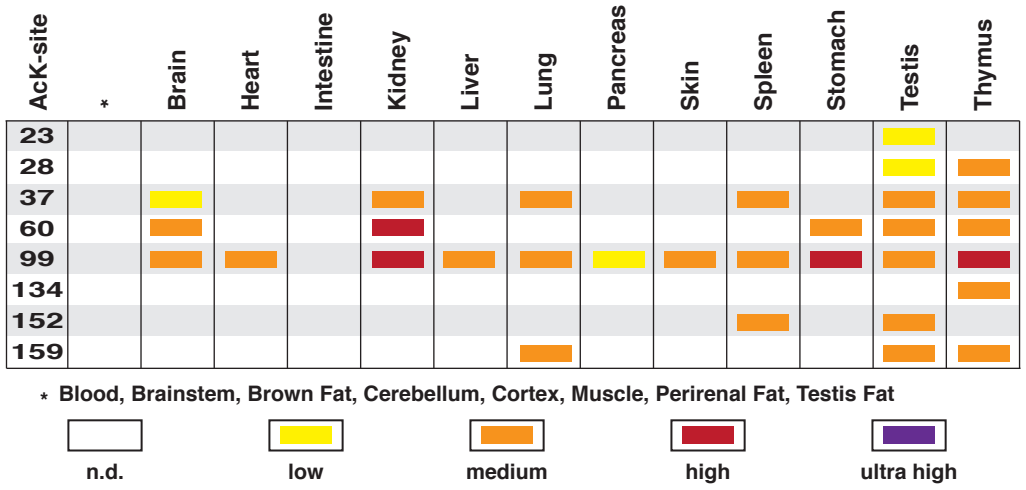

FIGURE 4.2: **The acetylation pattern of Ran is tissue-dependent (in mouse/rat samples).**Relative abundance of acetylated peptides detected by MS in different tissues of rats/mice. Modified after (Lundby et al., 2012)

Acetylation of Ran could increase upon up-regulation of the specific KATs either due to higher expression, increased activity or a change in KAT-localization. These changes could be related to a specific tissue, an external stimulus, a metabolic state as well as growth-/stress- or even disease-specific conditions. In prostate cancer up-regulation of Tip60 as well as oncogenic potential of CBP/p300 was reported (Fu et al., 2000; Halkidou et al., 2003). In hepatocallular carcinoma high expression levels of p300 were identified as a biomarker for poor prognosis (Li et al., 2011). Inversely, the downregulation of the deacetylases of Ran would result in the accumulation of acetylation. This scenario is imaginable for several cancer types. Sirt1-levels, for example, were found to be reduced in prostate and bladder carcinoma, glioblastoma and ovarian cancer (Wang et al., 2008). Moreover, sirtuin-levels (Sirt1, -2, -3, -5, -6 and -7) are decreased in head and neck squamous cell carcinoma (Lai et al., 2013). Furthermore, several publications show interaction and regulation of acetyltransferases with/by lysine-deacetylases and *vice versa*. A functional cooperativity was shown for Tip60 and p300/CBP (Col et al., 2005; Xiao et al., 2014). Deacetylation by Sirt2 inactivates p300, whereas acetylation of Sirt2 by p300 inactivates, creating a feedback loop (Han et al., 2008).

4.3 General implications for the investigation of protein acetylation

Besides the Ran-related gain of knowledge/information described and discussed above, several general conclusions can be drawn from this study. First of all, the strong regulatory potential of lysine-acetylation as a post-translational modification has to be acknowledged. The analysis of only five acetylation sites of Ran revealed a broad regulatory spectrum for this rather small modification even without taking the crosstalk with other PTMs into account. Thus, protein acetylation might approximate the importance of phosphorylation as a regulatory PTM, assuming that the majority of acetylation sites does not turn out as low-stoichiometry background noise. In fact, this major challenge of the current acetylome research also becomes apparent in this study. Despite detection of Ran-acetylation by numerous MS-based acetylome screens, no detectable quantities of acetylated Ran could be isolated from living cells on the protein level. This clearly demonstrates, that the physiological abundance of every acetylation site/ acetylated protein detected by MS-based screens has to be verified by independent and quantifiable methods such as immuno-precipitation (IP) and immunoblotting (IB) (until reliable means of absolute quantification are available for proteomics). If no acetylated protein can be isolated from cells and detected via IP and IB (as in the case of Ran), either the high sensitivity of modern mass-spectrometers detects traces of acetylated peptides or the acetylation is tightly regulated and restricted to distinct conditions.

In contrast to classical approaches we used site-specifically acetylated, recombinant proteins (based on the genetic-code expansion concept) for the *in vitro* characterization of every single acetylation site. The acetylated full-length proteins enable the site-specific verification of acetyl-lysine mimics, the investigation of deacetylase reactions or bromodomain-interactions and even crystallization trials with the latter. The KDAC-screen with the five Ran-acetylation sites identified deacetylase activity for Sirt-1, -2 and -3 against AcK37 and Sirt2-specificity for AcK71. Remarkably, these activities were not detected in an acetylome peptide microarray screening all human sirtuin isoforms for activity against 13-mer-peptides of the acetylation sites identified by Choudhary *et al.*(Choudhary et al., 2009; Rauh et al., 2013). Similar to Ran, also other published sirtuin substrates were not identified in this screen (Figure 4.3). Either the immobilization of the peptide

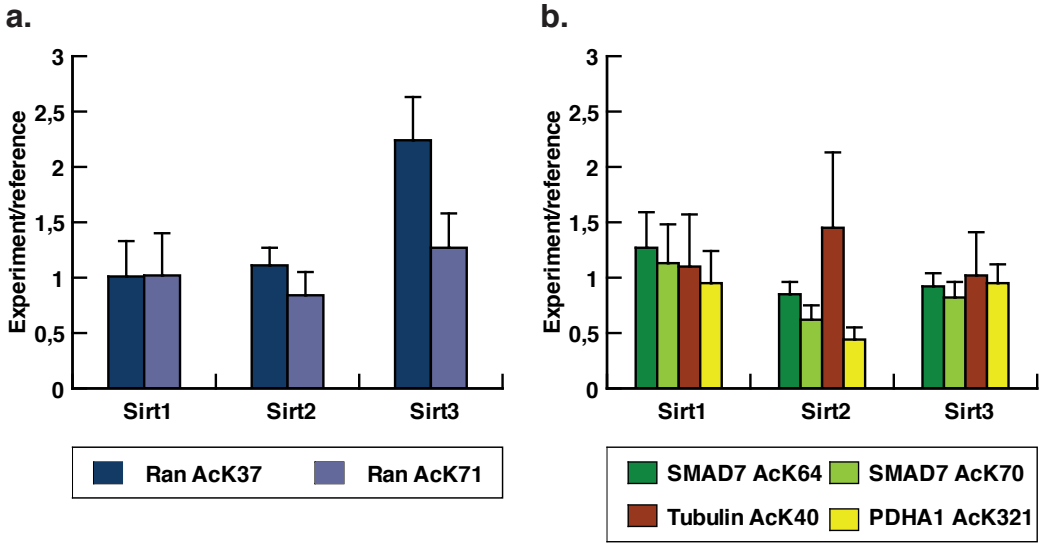

FIGURE 4.3: **Sirtuin activity on published substrates as detected by a microarray screen.** An acetylome peptide microarray screen fails to detect deacetylase activity for Ran AcKs and several published sirtuin substrates. The bar charts show the weighted means of the signal ratios with error bars resulting from three independent experiments (Rauh et al., 2013). (a) Signal ratios for Ran AcK 37 and 71, which were shown to be sirtuin substrates of Sirt1-3 and Sirt2, respectively. (b) Signal ratios for established sirtuin substrates. SMAD7 is deacetylated by Sirt1, Tubulin-α by Sirt2 and PDHA1 is a substrate of Sirt3 (Kume et al., 2007; North et al., 2003; Ozden et al., 2014).

affects the substrate recognition or one or two widely accepted assumptions of the screen are not applicable: 1. 13-meric peptides (six residues N- and C-terminal of the acetylation site) are sufficient for sirtuin substrate recognition, 2. A secondary structure is not needed (or even obstructive) for substrate recognition (Cosgrove et al., 2006; Khan and Lewis, 2005). In fact, there seems to be no defined consensus sequence for sirtuin recognition, neither as a group nor for individual enzymes (Martínez-Redondo and Vaquero, 2013). Blander *et al.* even reported absence of substrate specificity of Sirt1 on peptides *in vitro* and suggest a tertiary fold or protein-protein interactions as determinants of specificity *in vivo* (Blander et al., 2005).

Contradictory to these assumptions and reports regarding sirtuin substrate specificity, we observed a high degree of specificity for Sirt2 indicating dependence of substrate recognition on protein structure and consensus sequence. Strikingly, Sirt2 clearly distinguishes between AcK37 and AcK38 of Ran resulting in a considerably reduced deacetylation rate of AcK38 compared to AcK37. The dependence on structural features becomes apparent trough the fact that the Sirt2-catalyzed

deacetylation rate of AcK71 is nucleotide-dependent. In other words, Sirt2 distinguishes between the (rigid, more structured) GTP-conformation and the (more flexible) GDP-conformation of switch II, notably, in favor of the more structured substrate AcK71∗GppNHp.

Finally, our approach provides the means to evaluate established tools which are crucial to study protein acetylation, such as acetylation mimics and specific anti-acetyl-lysine antibodies. The validity of the acetylation mimics, glutamine and arginine, can be verified prior to cell culture experiments. The knowledge of which is the better mimic (steric or charge) with regard to a specific interaction is crucial for the interpretation of the experimental *in vivo* results. In the case of the Ran∗NTF2 interaction, for example, glutamine was confirmed as a valid AcK71-mimic (abolishes interaction), whereas K71R still binds to NTF2. Localization experiments in cell culture showed the expected nuclear localization of Ran K71Q. However, surprisingly Ran K99R exhibited a phenotype similar to Ran K71Q, although the interaction of Ran AcK99 and NTF2 is unaffected. Either arginine is no suitable mimic, neither for lysine nor for acetyl-lysine, or the observed effect is caused by the manipulation of another, NTF2-independent, process. In this specific case, only the *in vitro* comparison of AcK99 and its Q/R-mimics regarding NTF2-interaction enabled the correct interpretation of the observed result.

The evaluation of a well-established anti-acetyl-lysine antibody disclosed strong variations in the detection specificity of different Ran AcKs, indicating a strong dependence of the AcK-recognition on the residues flanking the acetyl-lysine. This effect could be even more pronounced under native conditions, since structural constraints might also influence the specificity. Consequently, detection limits of recombinant Ran AcKs vary drastically. Since MS-based proteomic screens rely on antibody-dependent affinity-enrichment of acetylated peptides, this site-specific deviation in substrate recognition does directly influence the result of the proteomic screen.

4.4 Conclusion and outlook

In the course of this study five acetylation sites of the small G-protein Ran were characterized regarding their impact on Ran and the Ran system. Ran acetylation has the potential to influence all aspects of Ran-function, namely Ran localization, Ran activation and -inactivation as well as import- and export processes. Several attempts to isolate and detect acetylated full-length Ran from cells failed, though, indicating a low-stoichiometry of Ran-acetylation under the conditions tested. However, the fact that Ran-specific regulatory enzymes were identified (Tip60, CBP/P300 and α-TAT as KATs and Sirt1/2/3 as KDACs) and no chemical acetylation was observed at cytosolic pH-conditions even at high acetyl-CoA concentrations, rather suggests a thight regulation of Ran-acetylation than an unspecific low-level background acetylation. The development of reliable (absolute) quantification methods for high-throughput acetylomics is essential to enable the discrimination of biological relevant from irrelevant sites. An increasing number of (quantified) cell-, tissue- and condition-specific acetylome datasets will provide insight into the role and regulation of protein-acetylation. However, *in vivo* and *in vitro* studies will remain indispensable to unravel the molecular mechanisms underlying the observed effects of single acetylation sites. As shown here, GCEC is a valuable tool for the investigation of the impact of lysine acetylation.

Due to the fact that several KATs and sirtuins also have acylation/ deacylation activity, the comparison of acetylation and other forms of acylation will become more important in the near future (Chen et al., 2007b; Liu et al., 2009). It will be interesting to determine mechanistic differences between the different alkyl-chain lengths and gain insight into the metabolic regulation of the different modification. To judge this, more information about the regulation of KATs and KDACs is needed, though.

Appendix A

Appendix

FIGURE A.1: **tRNA-synthetase/tRNA-pair used for GCEC.**Sequence- and cloning information for the used acetyl-lysyl-tRNA-synthetase (AcKRS3) and the corresponding tRNA (pylT).

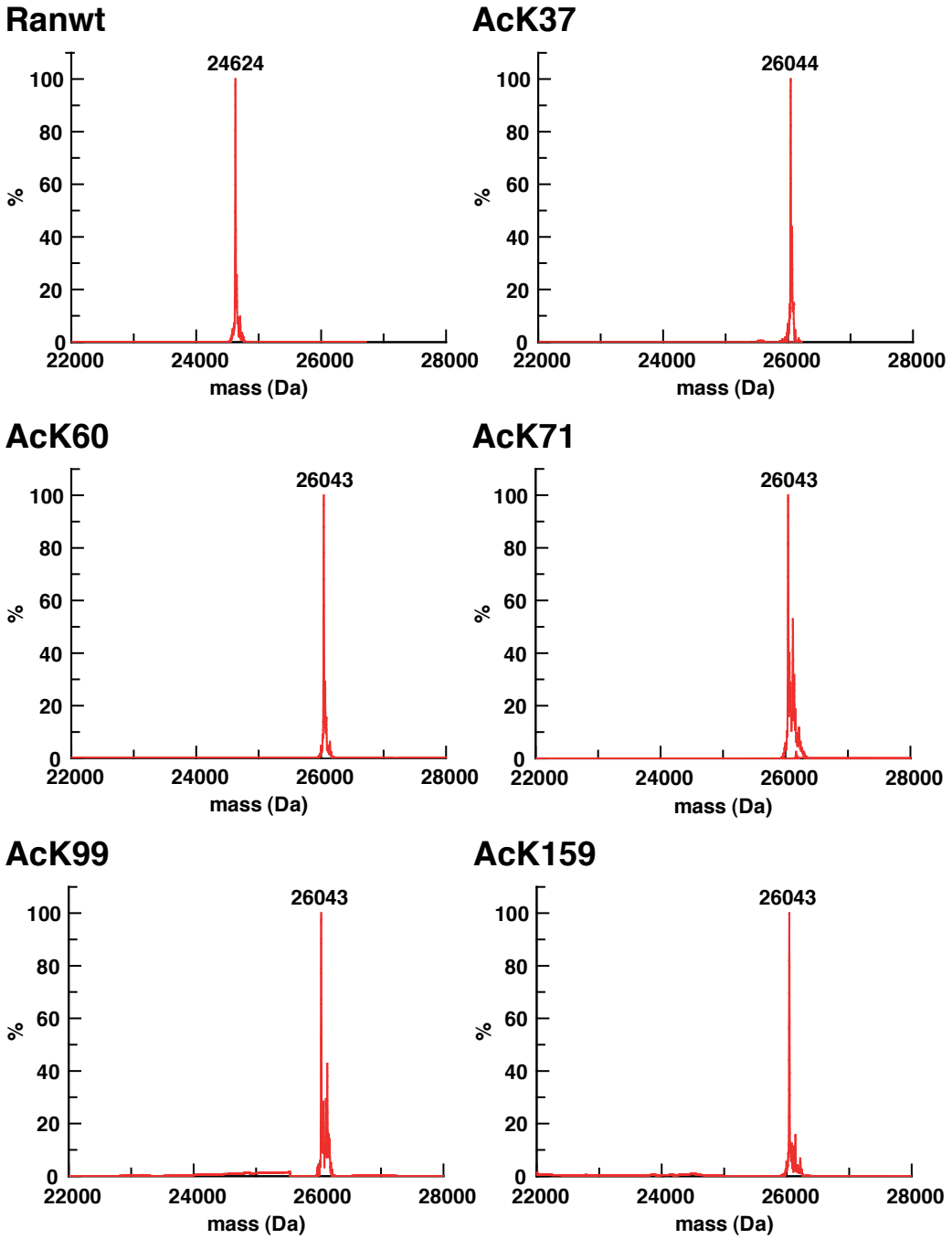

FIGURE A.2: **ESI-MS spectra of Ran wt and all AcKs.** Quantitative incorporation of N-(ϵ)-acetyl-lysine into recombinant His-tagged Ran was verified by ESI-mass spectrometry. The calculated mass for the AcKs is 26043,6 Da. Ran wt does not carry a His-tag and the calculated mass is 24624 Da.

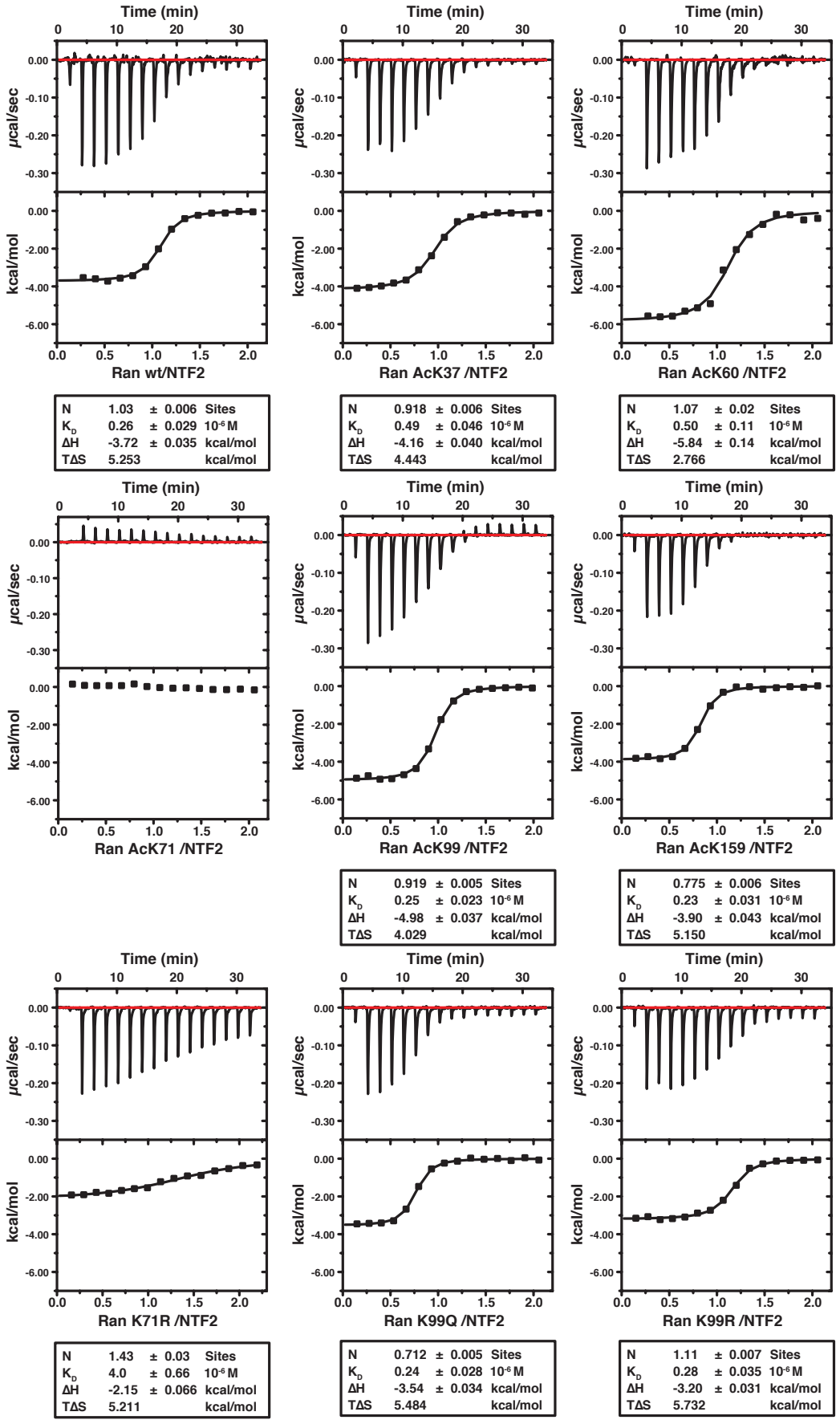

FIGURE A.3: **Interaction of NTF2 and Ran wt/AcKs.** The affinities and thermodynamic interaction parameters of the interaction of NTF2 and Ran wt/AcK/Q/R were determined by ITC.

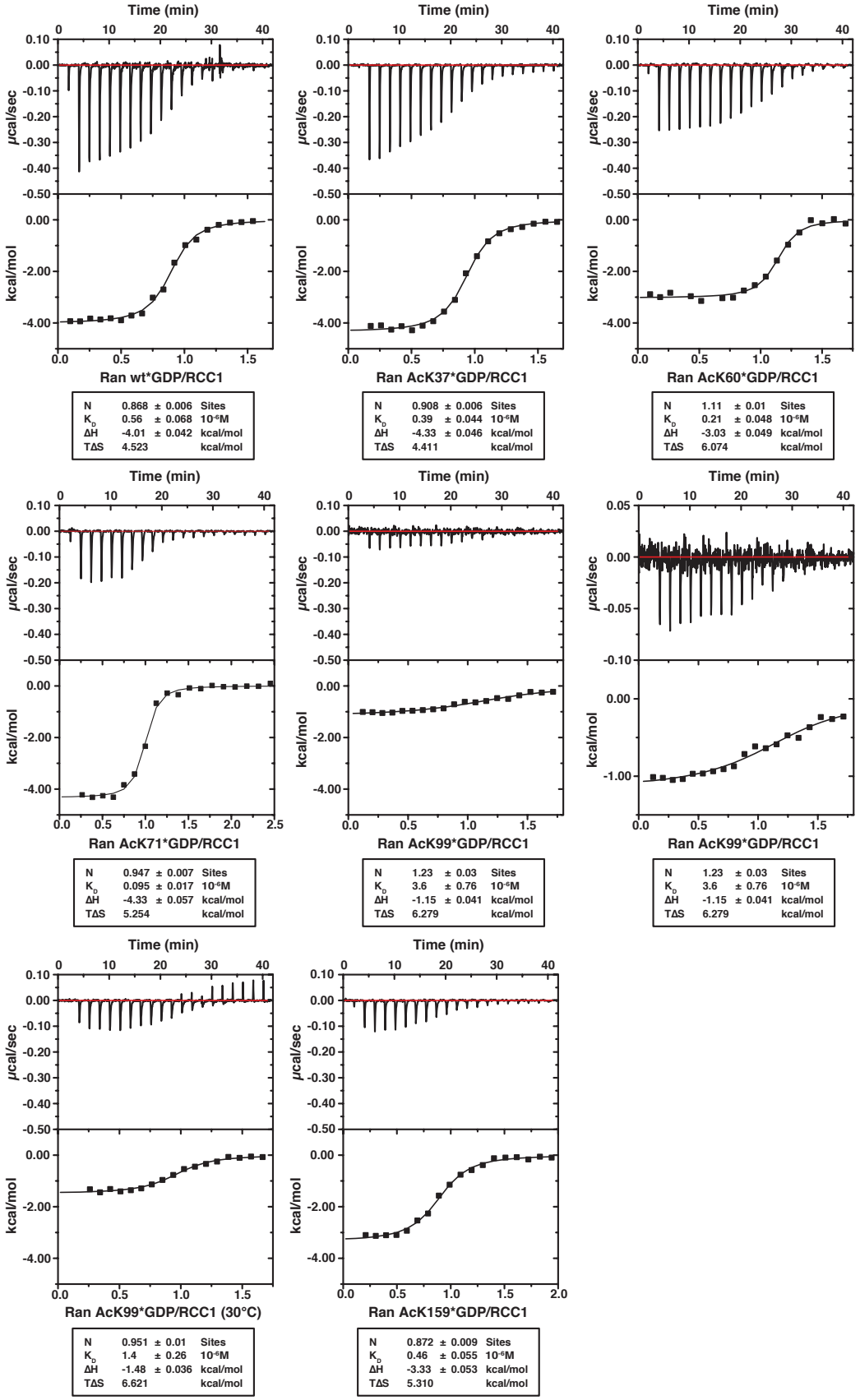

FIGURE A.4: **Interaction of RCC1 and Ran∗GDP wt/AcKs.** The affinities and thermodynamic interaction parameters of the interaction of RCC1 and Ran∗GDP wt/AcKs were determined by ITC.

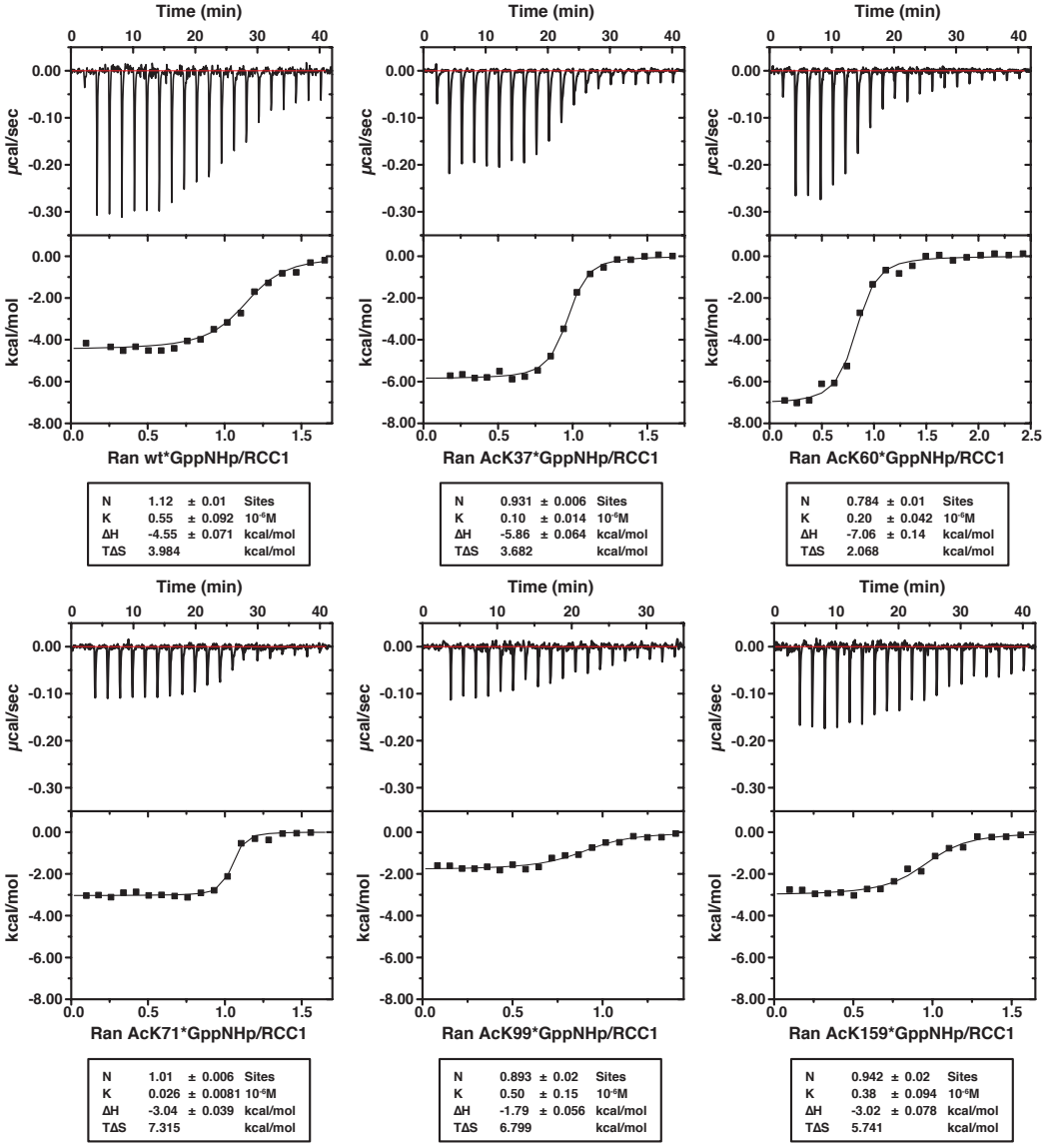

FIGURE A.5: **Interaction of RCC1 and Ran∗GppNHp wt/AcKs.** The affinities and thermodynamic interaction parameters of the interaction of RCC1 and Ran∗GppNHp wt/AcKs were determined by ITC.

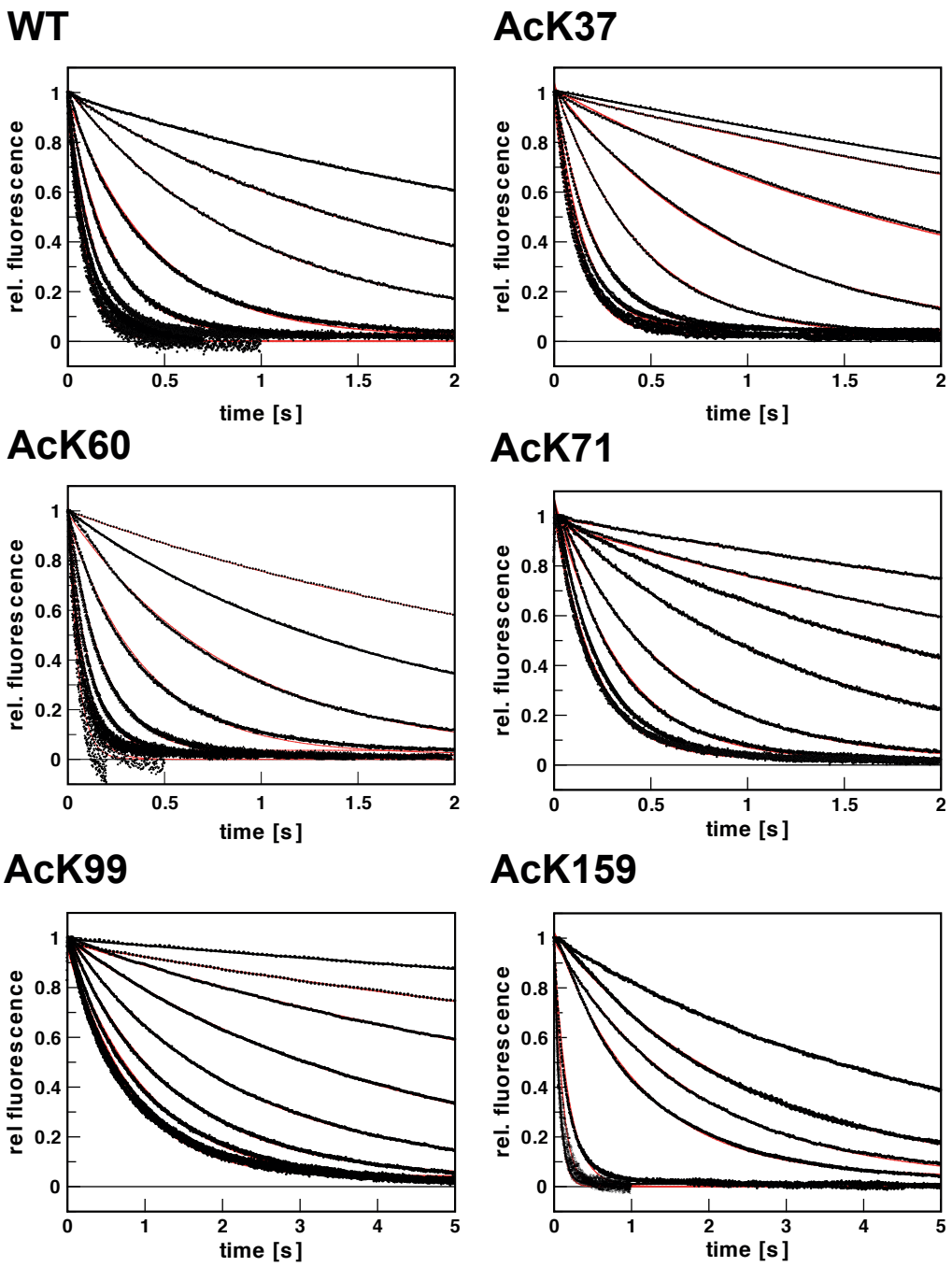

FIGURE A.6: **RCC1-catalyzed nucleotide exchange on Ran.** The RCC1-catalyzed nucleotide exchange on Ran wt/AcKs was determined by stopped-flow measurements. Shown are original traces and fits.

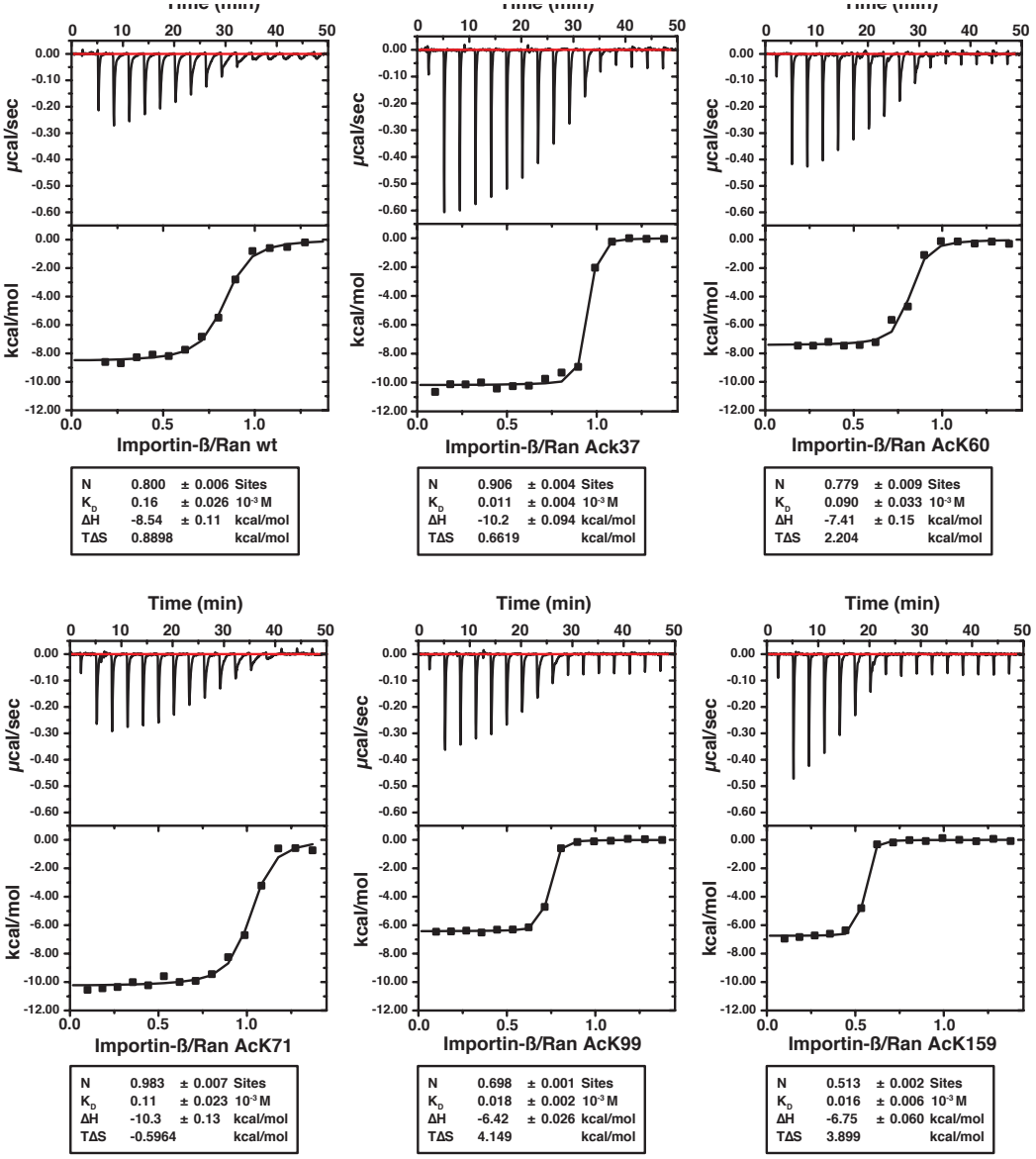

FIGURE A.7: **Interaction of Importin-β and Ran wt/AcKs.** The affinities and thermodynamic interaction parameters of the interaction of Importin-β and Ran wt/AcKs were determined by ITC.

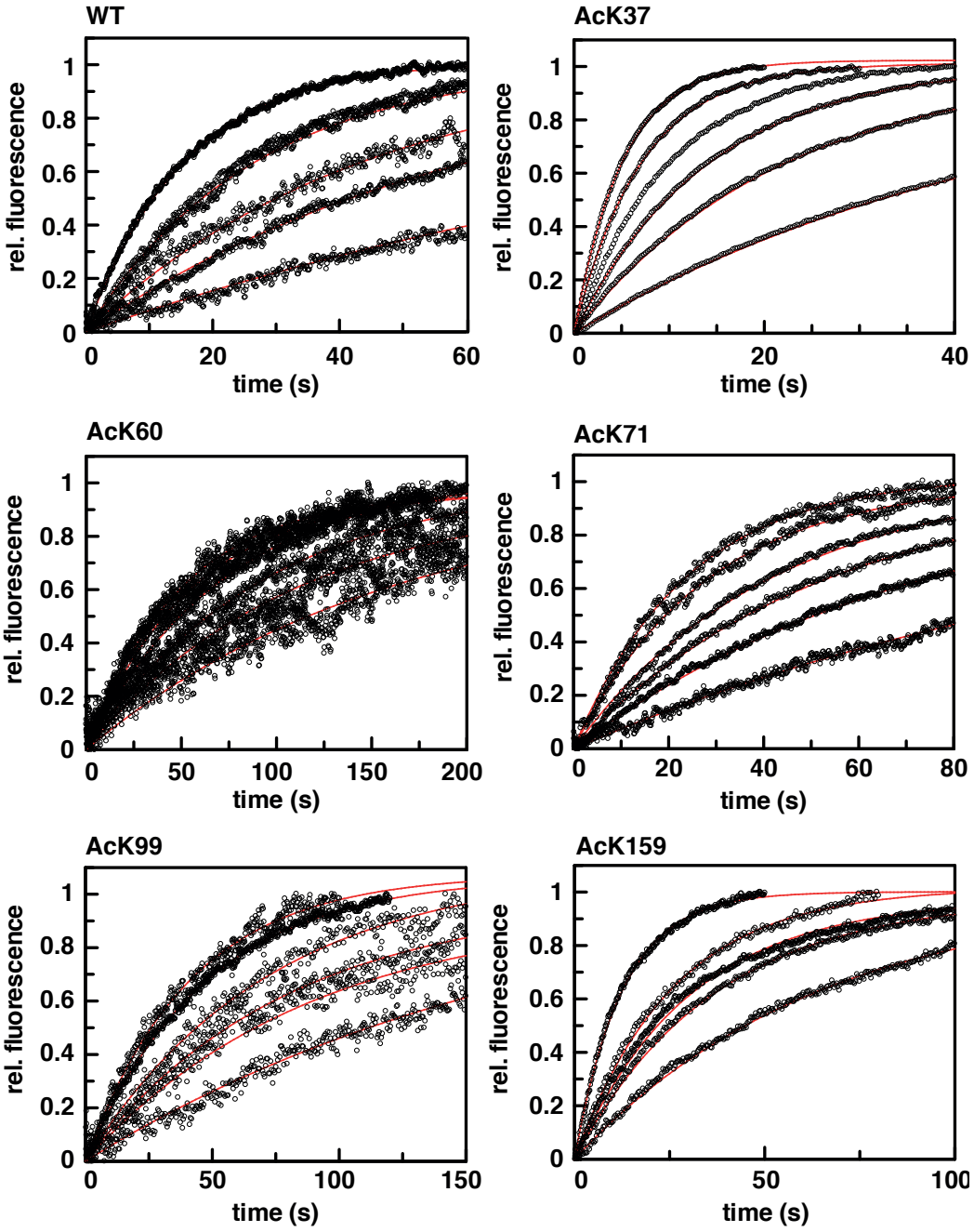

FIGURE A.8: **Association of Importin-β and Ran wt/AcKs.** Original traces and primary fits of the stopped-flow measurements for the determination of the association rate constant of Importin-β and Ran wt/AcKs

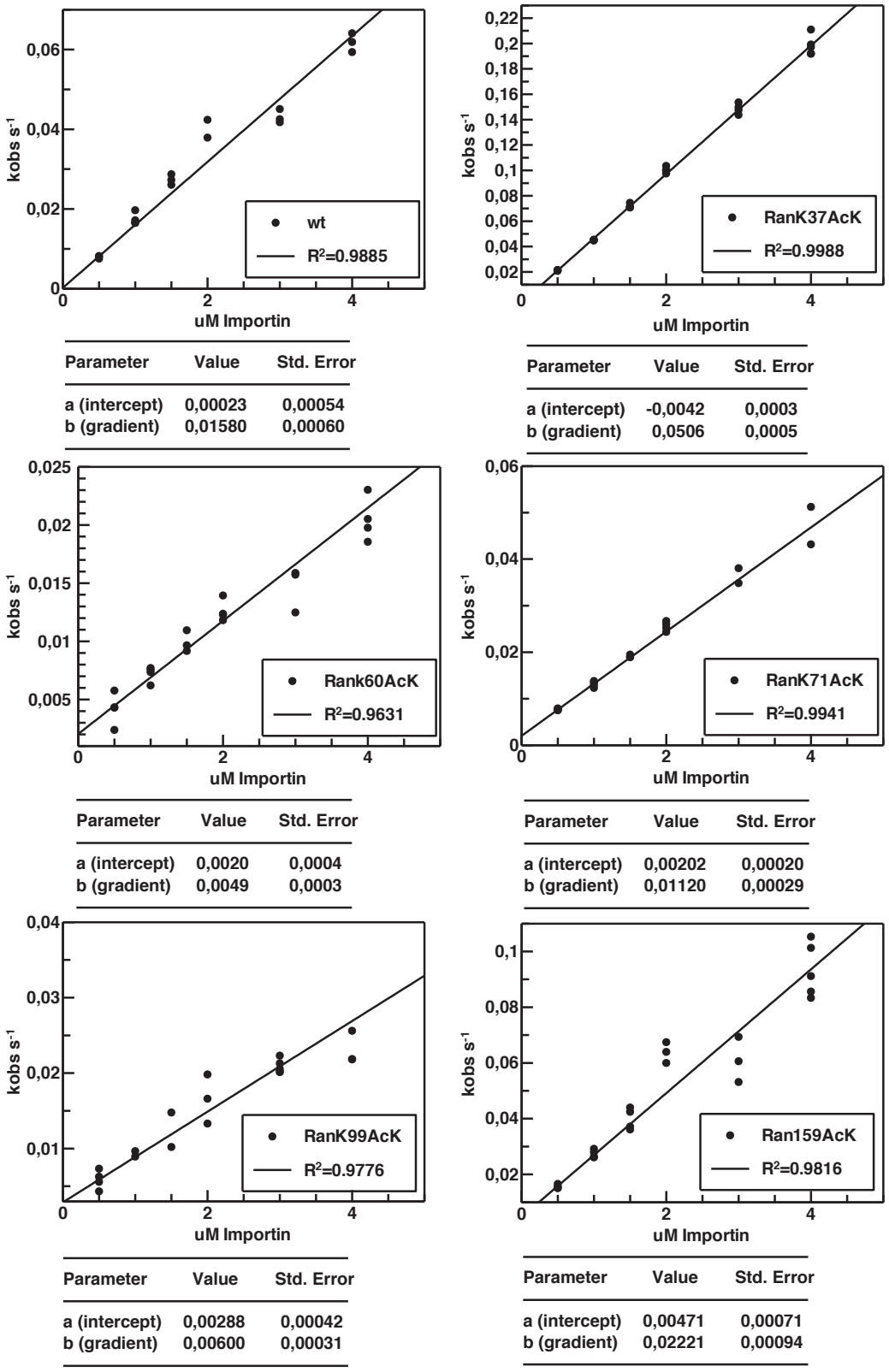

Parameter	Value	Std. Error
a (intercept)	0,00023	0,00054
b (gradient)	0,01580	0,00060

Parameter	Value	Std. Error
a (intercept)	-0,0042	0,0003
b (gradient)	0,0506	0,0005

Parameter	Value	Std. Error
a (intercept)	0,0020	0,0004
b (gradient)	0,0049	0,0003

Parameter	Value	Std. Error
a (intercept)	0,00202	0,00020
b (gradient)	0,01120	0,00029

Parameter	Value	Std. Error
a (intercept)	0,00288	0,00042
b (gradient)	0,00600	0,00031

Parameter	Value	Std. Error
a (intercept)	0,00471	0,00071
b (gradient)	0,02221	0,00094

FIGURE A.9: **Association of Importin-β and Ran wt/AcKs.** Linear fits for the determination of the association rate constant of Importin-β and Ran wt/AcKs

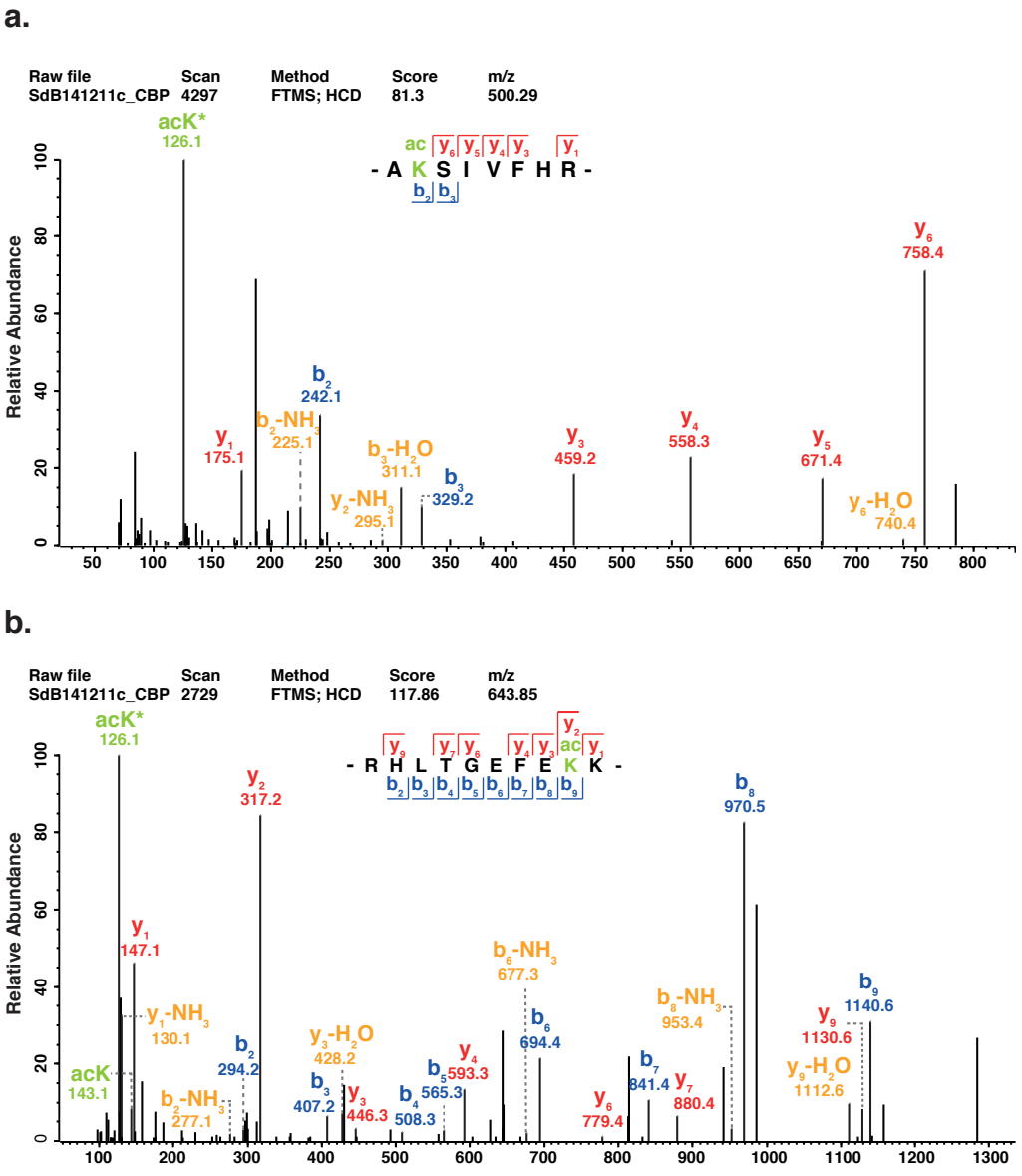

FIGURE A.10: **MS/MS spectra.** MS/MS spectra of the pecific peptide for (a) AcK134 and (b) AcK37.

Abbreviations

AcK	Acetyl-lysine
Amp	Ampicillin
CV	Column volume
CMB	Coomassie Blue
GAP	GTPase-activating protein
GCEC	Genetic-code expansion concept
GDP	Guanosin 5-diphosphat
GEF	Guanine-nucleotide exchange factor
GNBP	Guanine-nucleotide binding protein
GppNHp	5'-Guanylyl imidodiphosphate
GTP	Guanosin 5-triphosphat
IB	Immunoblotting
IPTG	Isopropyl -D-thiogalactosid
ITC	Isothermal titration calorimetry
KAT	Lysine-acetyltransferase
Kan	Kanamycin
KDAC	Lysine-deacetylase
MWCO	Molecular-weight cut-off
MS	Mass spectrometry
Ni-NTA	Nickel-Nitrilotriacetic acid
NPC	Nuclear pore complex
NTF2	Nuclear transport factor
RCC1	Regulator of chromosom condensation (RanGEF)

Bibliography

Ahmadian, M. R., Stege, P., Scheffzek, K., and Wittinghofer, A. (1997). Confirmation of the arginine-finger hypothesis for the gap-stimulated gtp-hydrolysis reaction of ras. *Nature structural biology*, 4(9):686–689.

Albee, A. J., Tao, W., and Wiese, C. (2006). Phosphorylation of maskin by aurora-a is regulated by rangtp and importin β. *Journal of Biological Chemistry*, 281(50):38293–38301.

Allfrey, V., Faulkner, R., and Mirsky, A. (1964). Acetylation and methylation of histones and their possible role in the regulation of rna synthesis. *Proceedings of the National Academy of Sciences of the United States of America*, 51(5):786.

Arnaoutov, A., Azuma, Y., Ribbeck, K., Joseph, J., Boyarchuk, Y., Karpova, T., McNally, J., and Dasso, M. (2005). Crm1 is a mitotic effector of ran-gtp in somatic cells. *Nature cell biology*, 7(6):626–632.

Arnesen, T., Van Damme, P., Polevoda, B., Helsens, K., Evjenth, R., Colaert, N., Varhaug, J. E., Vandekerckhove, J., Lillehaug, J. R., Sherman, F., et al. (2009). Proteomics analyses reveal the evolutionary conservation and divergence of n-terminal acetyltransferases from yeast and humans. *Proceedings of the National Academy of Sciences*, 106(20):8157–8162.

Baeza, J., Dowell, J. A., Smallegan, M. J., Fan, J., Amador-Noguez, D., Khan, Z., and Denu, J. M. (2014). Stoichiometry of site-specific lysine acetylation in an entire proteome. *Journal of Biological Chemistry*, 289(31):21326–21338.

Baker, R. P., Harreman, M. T., Eccleston, J. F., Corbett, A. H., and Stewart, M. (2001). Interaction between ran and mog1 is required for efficient nuclear protein import. *Journal of Biological Chemistry*, 276(44):41255–41262.

Barber, M. F., Michishita-Kioi, E., Xi, Y., Tasselli, L., Kioi, M., Moqtaderi, Z., Tennen, R. I., Paredes, S., Young, N. L., Chen, K., et al. (2012). Sirt7 links h3k18 deacetylation to maintenance of oncogenic transformation. *Nature*, 487(7405):114–118.

Bednenko, J., Cingolani, G., and Gerace, L. (2003). Nucleocytoplasmic transport: navigating the channel. *Traffic*, 4(3):127–135.

Beirowski, B., Gustin, J., Armour, S. M., Yamamoto, H., Viader, A., North, B. J., Michán, S., Baloh, R. H., Golden, J. P., Schmidt, R. E., et al. (2011). Sir-two-homolog 2 (sirt2) modulates peripheral myelination through polarity protein par-3/atypical protein kinase c (apkc) signaling. *Proceedings of the National Academy of Sciences*, 108(43):E952–E961.

Beli, P., Lukashchuk, N., Wagner, S. A., Weinert, B. T., Olsen, J. V., Baskcomb, L., Mann, M., Jackson, S. P., and Choudhary, C. (2012). Proteomic investigations reveal a role for rna processing factor thrap3 in the dna damage response. *Molecular cell*, 46(2):212–225.

Beltrao, P., Albanèse, V., Kenner, L. R., Swaney, D. L., Burlingame, A., Villén, J., Lim, W. A., Fraser, J. S., Frydman, J., and Krogan, N. J. (2012). Systematic functional prioritization of protein posttranslational modifications. *Cell*, 150(2):413–425.

Ben-Efraim, I. and Gerace, L. (2001). Gradient of increasing affinity of importin β for nucleoporins along the pathway of nuclear import. *The Journal of cell biology*, 152(2):411–418.

Bianco, A., Townsley, F. M., Greiss, S., Lang, K., and Chin, J. W. (2012). Expanding the genetic code of drosophila melanogaster. *Nature chemical biology*, 8(9):748–750.

Bischoff, F., Krebber, H., Smirnova, E., Dong, W., and Ponstingl, H. (1995). Co-activation of rangtpase and inhibition of gtp dissociation by ran-gtp binding protein ranbp1. *The EMBO Journal*, 14(4):705.

Bischoff, F. R. and Ponstingl, H. (1991a). Catalysis of guanine nucleotide exchange on ran by the mitotic regulator rcc1.

Bischoff, F. R. and Ponstingl, H. (1991b). Mitotic regulator protein rcc1 is complexed with a nuclear ras-related polypeptide. *Proceedings of the National Academy of Sciences*, 88(23):10830–10834.

Black, J. C., Mosley, A., Kitada, T., Washburn, M., and Carey, M. (2008). The sirt2 deacetylase regulates autoacetylation of p300. *Molecular cell*, 32(3):449–455.

Blander, G., Olejnik, J., Krzymanska-Olejnik, E., McDonagh, T., Haigis, M., Yaffe, M. B., and Guarente, L. (2005). Sirt1 shows no substrate specificity in vitro. *Journal of Biological Chemistry*, 280(11):9780–9785.

Blower, M. D., Nachury, M., Heald, R., and Weis, K. (2005). A rae1-containing ribonucleoprotein complex is required for mitotic spindle assembly. *Cell*, 121(2):223–234.

Bourne, H. R., Sanders, D. A., McCormick, F., et al. (1991). The gtpase superfamily: conserved structure and molecular mechanism. *Nature*, 349(6305):117–127.

Brown, J. L. and Roberts, W. (1976). Evidence that approximately eighty per cent of the soluble proteins from ehrlich ascites cells are nalpha-acetylated. *Journal of Biological Chemistry*, 251(4):1009–1014.

Brucker, S., Gerwert, K., and Kötting, C. (2010). Tyr39 of ran preserves the ran· gtp gradient by inhibiting gtp hydrolysis. *Journal of molecular biology*, 401(1):1–6.

Bullock, T. L., Clarkson, D. W., Kent, H. M., and Stewart, M. (1996). The 1.6 å resolution crystal structure of nuclear transport factor 2 (ntf2). *Journal of molecular biology*, 260(3):422–431.

Carazo-Salas, R. E., Gruss, O. J., Mattaj, I. W., and Karsenti, E. (2001). Ran–gtp coordinates regulation of microtubule nucleation and dynamics during mitotic-spindle assembly. *Nature cell biology*, 3(3):228–234.

Carazo-Salas, R. E., Guarguaglini, G., Gruss, O. J., Segref, A., Karsenti, E., and Mattaj, I. W. (1999). Generation of gtp-bound ran by rcc1 is required for chromatin-induced mitotic spindle formation. *Nature*, 400(6740):178–181.

Cautain, B., Hill, R., Pedro, N., and Link, W. (2014). Components and regulation of nuclear transport processes. *FEBS Journal*.

Chandra, A., Grecco, H. E., Pisupati, V., Perera, D., Cassidy, L., Skoulidis, F., Ismail, S. A., Hedberg, C., Hanzal-Bayer, M., Venkitaraman, A. R., et al. (2012). The gdi-like solubilizing factor pde [delta] sustains the spatial organization and signalling of ras family proteins. *Nature Cell Biology*, 14(2):148–158.

Chen, T., Muratore, T. L., Schaner-Tooley, C. E., Shabanowitz, J., Hunt, D. F., and Macara, I. G. (2007a). N-terminal α-methylation of rcc1 is necessary for stable chromatin association and normal mitosis. *Nature Cell Biology*, 9(5):596–603.

Chen, Y., Sprung, R., Tang, Y., Ball, H., Sangras, B., Kim, S. C., Falck, J. R., Peng, J., Gu, W., and Zhao, Y. (2007b). Lysine propionylation and butyrylation are novel post-translational modifications in histones. *Molecular & Cellular Proteomics*, 6(5):812–819.

Chien, Y.-H., Lai, M., Shih, T. Y., Verma, I. M., Scolnick, E. M., Roy-Burman, P., and Davidson, N. (1979). Heteroduplex analysis of the sequence relationships between the genomes of kirsten and harvey sarcoma viruses, their respective parental murine leukemia viruses, and the rat endogenous 30s rna. *Journal of virology*, 31(3):752–760.

Choudhary, C., Kumar, C., Gnad, F., Nielsen, M. L., Rehman, M., Walther, T. C., Olsen, J. V., and Mann, M. (2009). Lysine acetylation targets protein complexes and co-regulates major cellular functions. *Science*, 325(5942):834–840.

Choudhary, C., Weinert, B. T., Nishida, Y., Verdin, E., and Mann, M. (2014). The growing landscape of lysine acetylation links metabolism and cell signalling. *Nature Reviews Molecular Cell Biology*, 15(8):536–550.

Cingolani, G., Petosa, C., Weis, K., and Müller, C. W. (1999). Structure of importin-β bound to the ibb domain of importin-α. *Nature*, 399(6733):221–229.

Clarke, P. R. and Zhang, C. (2008). Spatial and temporal coordination of mitosis by ran gtpase. *Nature reviews Molecular cell biology*, 9(6):464–477.

Clarkson, W. D., Corbett, A. H., Paschal, B. M., Kent, H. M., McCoy, A. J., Gerace, L., Silver, P. A., and Stewart, M. (1997). Nuclear protein import is decreased by engineered mutants of nuclear transport factor 2 (ntf2) that do not bind gdp-ran. *Journal of molecular biology*, 272(5):716–730.

Col, E., Caron, C., Chable-Bessia, C., Legube, G., Gazzeri, S., Komatsu, Y., Yoshida, M., Benkirane, M., Trouche, D., and Khochbin, S. (2005). Hiv-1 tat targets tip60 to impair the apoptotic cell response to genotoxic stresses. *The EMBO journal*, 24(14):2634–2645.

Conti, E. and Kuriyan, J. (2000). Crystallographic analysis of the specific yet versatile recognition of distinct nuclear localization signals by karyopherin α. *Structure*, 8(3):329–338.

Corbett, A. H. and Silver, P. A. (1996). The ntf2 gene encodes an essential, highly conserved protein that functions in nuclear transport in vivo. *Journal of Biological Chemistry*, 271(31):18477–18484.

Cosgrove, M. S., Bever, K., Avalos, J. L., Muhammad, S., Zhang, X., and Wolberger, C. (2006). The structural basis of sirtuin substrate affinity. *Biochemistry*, 45(24):7511–7521.

Da Silva, I. and Sheppard, K. (2015). Expanding the genetic code with pyroglutamate. *The FASEB Journal*, 29(1 Supplement):892–12.

Dai, Q., Choy, E., Chiu, V., Romano, J., Slivka, S. R., Steitz, S. A., Michaelis, S., and Philips, M. R. (1998). Mammalian prenylcysteine carboxyl methyltransferase is in the endoplasmic reticulum. *Journal of Biological Chemistry*, 273(24):15030–15034.

Daitoku, H., Sakamaki, J.-i., and Fukamizu, A. (2011). Regulation of foxo transcription factors by acetylation and protein–protein interactions. *Biochimica et Biophysica Acta (BBA)-Molecular Cell Research*, 1813(11):1954–1960.

Dorr, A., Kiermer, V., Pedal, A., Rackwitz, H.-R., Henklein, P., Schubert, U., Zhou, M.-M., Verdin, E., and Ott, M. (2002). Transcriptional synergy between tat and pcaf is dependent on the binding of acetylated tat to the pcaf bromodomain. *The EMBO journal*, 21(11):2715–2723.

Drivas, G., Shih, A., Coutavas, E., Rush, M., and D'eustachio, P. (1990). Characterization of four novel ras-like genes expressed in a human teratocarcinoma cell line. *Molecular and Cellular Biology*, 10(4):1793–1798.

Ems-McClung, S. C., Zheng, Y., and Walczak, C. E. (2004). Importin α/β and ran-gtp regulate xctk2 microtubule binding through a bipartite nuclear localization signal. *Molecular biology of the cell*, 15(1):46–57.

Eyers, P. A. and Maller, J. L. (2004). Regulation of xenopus aurora a activation by tpx2. *Journal of Biological Chemistry*, 279(10):9008–9015.

Fan, S., Fogg, V., Wang, Q., Chen, X.-W., Liu, C.-J., and Margolis, B. (2007). A novel crumbs3 isoform regulates cell division and ciliogenesis via importin β interactions. *The Journal of cell biology*, 178(3):387–398.

Farnsworth, C. L. and Feig, L. A. (1991). Dominant inhibitory mutations in the mg (2+)-binding site of rash prevent its activation by gtp. *Molecular and cellular biology*, 11(10):4822–4829.

Feig, L. A. (1999). Tools of the trade: use of dominant-inhibitory mutants of ras-family gtpases. *Nature cell biology*, 1(2):E25–E27.

Filippakopoulos, P., Picaud, S., Mangos, M., Keates, T., Lambert, J.-P., Barsyte-Lovejoy, D., Felletar, I., Volkmer, R., Müller, S., Pawson, T., et al. (2012). Histone recognition and large-scale structural analysis of the human bromodomain family. *Cell*, 149(1):214–231.

Fontes, M. R., Teh, T., and Kobe, B. (2000). Structural basis of recognition of monopartite and bipartite nuclear localization sequences by mammalian importin-α. *Journal of molecular biology*, 297(5):1183–1194.

Frey, S. and Görlich, D. (2009). Fg/fxfg as well as glfg repeats form a selective permeability barrier with self-healing properties. *The EMBO journal*, 28(17):2554–2567.

Frey, S., Richter, R. P., and Görlich, D. (2006). Fg-rich repeats of nuclear pore proteins form a three-dimensional meshwork with hydrogel-like properties. *Science*, 314(5800):815–817.

Fried, H. and Kutay, U. (2003). Nucleocytoplasmic transport: taking an inventory. *Cellular and Molecular Life Sciences CMLS*, 60(8):1659–1688.

Friedmann, D. R. and Marmorstein, R. (2013). Structure and mechanism of non-histone protein acetyltransferase enzymes. *FEBS Journal*, 280(22):5570–5581.

Frisch, C., Schreiber, G., Johnson, C. M., and Fersht, A. R. (1997). Thermodynamics of the interaction of barnase and barstar: changes in free energy versus changes in enthalpy on mutation. *Journal of molecular biology*, 267(3):696–706.

Fu, M., Wang, C., Reutens, A. T., Wang, J., Angeletti, R. H., Siconolfi-Baez, L., Ogryzko, V., Avantaggiati, M.-L., and Pestell, R. G. (2000). p300 and p300/camp-response element-binding protein-associated factor acetylate the androgen receptor at sites governing hormone-dependent transactivation. *Journal of Biological Chemistry*, 275(27):20853–20860.

Garland, P. B., Shepherd, D., and Yates, D. (1965). Steady-state concentrations of coenzyme a, acetyl-coenzyme a and long-chain fatty acyl-coenzyme a in rat-liver mitochondria oxidizing palmitate. *Biochem. J*, 97:587–594.

Gasper, R., Thomas, C., Ahmadian, M. R., and Wittinghofer, A. (2008). The role of the conserved switch ii glutamate in guanine nucleotide exchange factor-mediated nucleotide exchange of gtp-binding proteins. *Journal of molecular biology*, 379(1):51–63.

Gerber, S. A., Rush, J., Stemman, O., Kirschner, M. W., and Gygi, S. P. (2003). Absolute quantification of proteins and phosphoproteins from cell lysates by tandem ms. *Proceedings of the National Academy of Sciences*, 100(12):6940–6945.

Görlich, D., Pante, N., Kutay, U., Aebi, U., and Bischoff, F. (1996). Identification of different roles for rangdp and rangtp in nuclear protein import. *The EMBO journal*, 15(20):5584.

Greiss, S. and Chin, J. W. (2011). Expanding the genetic code of an animal. *Journal of the American Chemical Society*, 133(36):14196–14199.

Groen, A. C., Cameron, L. A., Coughlin, M., Miyamoto, D. T., Mitchison, T. J., and Ohi, R. (2004). Xrhamm functions in ran-dependent microtubule nucleation and pole formation during anastral spindle assembly. *Current biology*, 14(20):1801–1811.

Grönroos, E., Hellman, U., Heldin, C.-H., and Ericsson, J. (2002). Control of smad7 stability by competition between acetylation and ubiquitination. *Molecular cell*, 10(3):483–493.

Grossman, E., Medalia, O., and Zwerger, M. (2012). Functional architecture of the nuclear pore complex. *Annual review of biophysics*, 41:557–584.

Gruss, O. J., Carazo-Salas, R. E., Schatz, C. A., Guarguaglini, G., Kast, J., Wilm, M., Le Bot, N., Vernos, I., Karsenti, E., and Mattaj, I. W. (2001). Ran induces

spindle assembly by reversing the inhibitory effect of importin α on tpx2 activity. *Cell*, 104(1):83–93.

Gu, W. and Roeder, R. G. (1997). Activation of p53 sequence-specific dna binding by acetylation of the p53 c-terminal domain. *Cell*, 90(4):595–606.

Guan, K.-L. and Xiong, Y. (2011). Regulation of intermediary metabolism by protein acetylation. *Trends in biochemical sciences*, 36(2):108–116.

Guarani, V., Deflorian, G., Franco, C. A., Krüger, M., Phng, L.-K., Bentley, K., Toussaint, L., Dequiedt, F., Mostoslavsky, R., Schmidt, M. H., et al. (2011). Acetylation-dependent regulation of endothelial notch signalling by the sirt1 deacetylase. *Nature*, 473(7346):234–238.

Guzik, B. W. and Goldstein, L. S. (2004). Microtubule-dependent transport in neurons: steps towards an understanding of regulation, function and dysfunction. *Current opinion in cell biology*, 16(4):443–450.

Haigis, M. C., Mostoslavsky, R., Haigis, K. M., Fahie, K., Christodoulou, D. C., Murphy, A. J., Valenzuela, D. M., Yancopoulos, G. D., Karow, M., Blander, G., et al. (2006). Sirt4 inhibits glutamate dehydrogenase and opposes the effects of calorie restriction in pancreatic β cells. *Cell*, 126(5):941–954.

Halkidou, K., Gnanapragasam, V. J., Mehta, P. B., Logan, I. R., Brady, M. E., Cook, S., Leung, H. Y., Neal, D. E., and Robson, C. N. (2003). Expression of tip60, an androgen receptor coactivator, and its role in prostate cancer development. *Oncogene*, 22(16):2466–2477.

Han, Y., Jin, Y.-H., Kim, Y.-J., Kang, B.-Y., Choi, H.-J., Kim, D.-W., Yeo, C.-Y., and Lee, K.-Y. (2008). Acetylation of sirt2 by p300 attenuates its deacetylase activity. *Biochemical and biophysical research communications*, 375(4):576–580.

Hancock, J. F., Magee, A. I., Childs, J. E., and Marshall, C. J. (1989). All ras proteins are polyisoprenylated but only some are palmitoylated. *Cell*, 57(7):1167–1177.

Hancock, J. F., Paterson, H., and Marshall, C. J. (1990). A polybasic domain or palmitoylation is required in addition to the caax motif to localize p21ras to the plasma membrane. *Cell*, 63(1):133–139.

Hancock, S. M., Uprety, R., Deiters, A., and Chin, J. W. (2010). Expanding the genetic code of yeast for incorporation of diverse unnatural amino acids via a pyrrolysyl-trna synthetase/trna pair. *Journal of the American Chemical Society*, 132(42):14819–14824.

Hanz, S., Perlson, E., Willis, D., Zheng, J.-Q., Massarwa, R., Huerta, J. J., Koltzenburg, M., Kohler, M., van Minnen, J., Twiss, J. L., et al. (2003). Axoplasmic importins enable retrograde injury signaling in lesioned nerve. *Neuron*, 40(6):1095–1104.

Harel, A., Orjalo, A. V., Vincent, T., Lachish-Zalait, A., Vasu, S., Shah, S., Zimmerman, E., Elbaum, M., and Forbes, D. J. (2003). Removal of a single pore subcomplex results in vertebrate nuclei devoid of nuclear pores. *Molecular cell*, 11(4):853–864.

Hartwell, L. H. (1967). Macromolecule synthesis in temperature-sensitive mutants of yeast. *Journal of bacteriology*, 93(5):1662–1670.

Haynes, S. R., Dollard, C., Winston, F., Beck, S., Trowsdale, J., and Dawid, I. B. (1992). The bromodomain: a conserved sequence found in human, drosophila and yeast proteins. *Nucleic acids research*, 20(10):2603.

He, S., Bauman, D., Davis, J. S., Loyola, A., Nishioka, K., Gronlund, J. L., Reinberg, D., Meng, F., Kelleher, N., and McCafferty, D. G. (2003). Facile synthesis of site-specifically acetylated and methylated histone proteins: reagents for evaluation of the histone code hypothesis. *Proceedings of the National Academy of Sciences*, 100(21):12033–12038.

Henriksen, P., Wagner, S. A., Weinert, B. T., Sharma, S., Bačinskaja, G., Rehman, M., Juffer, A. H., Walther, T. C., Lisby, M., and Choudhary, C. (2012). Proteome-wide analysis of lysine acetylation suggests its broad regulatory scope in saccharomyces cerevisiae. *Molecular & Cellular Proteomics*, 11(11):1510–1522.

Hetzer, M., Bilbao-Cortés, D., Walther, T. C., Gruss, O. J., and Mattaj, I. W. (2000). Gtp hydrolysis by ran is required for nuclear envelope assembly. *Molecular cell*, 5(6):1013–1024.

Hood, F. E. and Clarke, P. R. (2007). Rcc1 isoforms differ in their affinity for chromatin, molecular interactions and regulation by phosphorylation. *Journal of cell science*, 120(19):3436–3445.

Hopper, A. K., Banks, F., and Evangelidis, V. (1978). A yeast mutant which accumulates precursor trnas. *Cell*, 14(2):211–219.

Houtkooper, R. H., Pirinen, E., and Auwerx, J. (2012). Sirtuins as regulators of metabolism and healthspan. *Nature reviews Molecular cell biology*, 13(4):225–238.

Huang, R., Holbert, M. A., Tarrant, M. K., Curtet, S., Colquhoun, D. R., Dancy, B. M., Dancy, B. C., Hwang, Y., Tang, Y., Meeth, K., et al. (2010). Site-specific introduction of an acetyl-lysine mimic into peptides and proteins by cysteine alkylation. *Journal of the American Chemical Society*, 132(29):9986–9987.

Hutchins, J. R., Moore, W. J., Hood, F. E., Wilson, J. S., Andrews, P. D., Swedlow, J. R., and Clarke, P. R. (2004). Phosphorylation regulates the dynamic interaction of rcc1 with chromosomes during mitosis. *Current biology*, 14(12):1099–1104.

Hwang, C.-S., Shemorry, A., and Varshavsky, A. (2010). N-terminal acetylation of cellular proteins creates specific degradation signals. *Science*, 327(5968):973–977.

Imai, S.-I., Armstrong, C. M., Kaeberlein, M., and Guarente, L. (2000). Transcriptional silencing and longevity protein sir2 is an nad-dependent histone deacetylase. *Nature*, 403(6771):795–800.

Isgro, T. A. and Schulten, K. (2007). Association of nuclear pore fg-repeat domains to ntf2 import and export complexes. *Journal of molecular biology*, 366(1):330–345.

Ismail, S. A., Chen, Y.-X., Rusinova, A., Chandra, A., Bierbaum, M., Gremer, L., Triola, G., Waldmann, H., Bastiaens, P. I., and Wittinghofer, A. (2011). Arl2-gtp and arl3-gtp regulate a gdi-like transport system for farnesylated cargo. *Nature chemical biology*, 7(12):942–949.

Ivanov, G. S., Ivanova, T., Kurash, J., Ivanov, A., Chuikov, S., Gizatullin, F., Herrera-Medina, E. M., Rauscher, F., Reinberg, D., and Barlev, N. A. (2007). Methylation-acetylation interplay activates p53 in response to dna damage. *Molecular and cellular biology*, 27(19):6756–6769.

Jäkel, S., Mingot, J.-M., Schwarzmaier, P., Hartmann, E., and Görlich, D. (2002). Importins fulfil a dual function as nuclear import receptors and cytoplasmic chaperones for exposed basic domains. *The EMBO journal*, 21(3):377–386.

Jeanmougin, F., Wurtz, J.-M., Le Douarin, B., Chambon, P., and Losson, R. (1997). The bromodomain revisited. *Trends in biochemical sciences*, 22(5):151–153.

Jiang, H., Khan, S., Wang, Y., Charron, G., He, B., Sebastian, C., Du, J., Kim, R., Ge, E., Mostoslavsky, R., et al. (2013). Sirt6 regulates tnf-[agr] secretion through hydrolysis of long-chain fatty acyl lysine. *Nature*, 496(7443):110–113.

Jiang, W., Wang, S., Xiao, M., Lin, Y., Zhou, L., Lei, Q., Xiong, Y., Guan, K.-L., and Zhao, S. (2011). Acetylation regulates gluconeogenesis by promoting pepck1 degradation via recruiting the ubr5 ubiquitin ligase. *Molecular cell*, 43(1):33–44.

John, J., Rensland, H., Schlichting, I., Vetter, I., Borasio, G. D., Goody, R. S., and Wittinghofer, A. (1993). Kinetic and structural analysis of the mg (2+)-binding site of the guanine nucleotide-binding protein p21h-ras. *Journal of Biological Chemistry*, 268(2):923–929.

John, J., Sohmen, R., Feuerstein, J., Linke, R., Wittinghofer, A., and Goody, R. S. (1990). Kinetics of interaction of nucleotides with nucleotide-free h-ras p21. *Biochemistry*, 29(25):6058–6065.

Joukov, V., Groen, A. C., Prokhorova, T., Gerson, R., White, E., Rodriguez, A., Walter, J. C., and Livingston, D. M. (2006). The brca1/bard1 heterodimer modulates ran-dependent mitotic spindle assembly. *Cell*, 127(3):539–552.

Kaláb, P., Pralle, A., Isacoff, E. Y., Heald, R., and Weis, K. (2006). Analysis of a rangtp-regulated gradient in mitotic somatic cells. *Nature*, 440(7084):697–701.

Kalab, P., Pu, R. T., and Dasso, M. (1999). The ran gtpase regulates mitotic spindle assembly. *Current Biology*, 9(9):481–484.

Kang, J.-Y., Kawaguchi, D., Coin, I., Xiang, Z., OLeary, D. D., Slesinger, P. A., and Wang, L. (2013). In vivo expression of a light-activatable potassium channel using unnatural amino acids. *Neuron*, 80(2):358–370.

Kauppinen, A., Suuronen, T., Ojala, J., Kaarniranta, K., and Salminen, A. (2013). Antagonistic crosstalk between nf-κb and sirt1 in the regulation of inflammation and metabolic disorders. *Cellular signalling*, 25(10):1939–1948.

Kent, H. M., Moore, M. S., Quimby, B. B., Baker, A. M., McCoy, A. J., Murphy, G. A., Corbett, A. H., and Stewart, M. (1999). Engineered mutants in the switch ii loop of ran define the contribution made by key residues to the interaction with nuclear transport factor 2 (ntf2) and the role of this interaction in nuclear protein import. *Journal of molecular biology*, 289(3):565–577.

Khan, A. N. and Lewis, P. N. (2005). Unstructured conformations are a substrate requirement for the sir2 family of nad-dependent protein deacetylases. *Journal of Biological Chemistry*, 280(43):36073–36078.

Khan, S. N. and Khan, A. U. (2010). Role of histone acetylation in cell physiology and diseases: An update. *Clinica Chimica Acta*, 411(19):1401–1411.

Kim, G.-W. and Yang, X.-J. (2011). Comprehensive lysine acetylomes emerging from bacteria to humans. *Trends in biochemical sciences*, 36(4):211–220.

Kim, S. C., Sprung, R., Chen, Y., Xu, Y., Ball, H., Pei, J., Cheng, T., Kho, Y., Xiao, H., Xiao, L., et al. (2006). Substrate and functional diversity of lysine acetylation revealed by a proteomics survey. *Molecular cell*, 23(4):607–618.

King, N. M., Prabu-Jeyabalan, M., Bandaranayake, R. M., Nalam, M. N., Nalivaika, E. A., O zen, A. e. l., Halilog lu, T. r., Yılmaz, N. e. K., and Schiffer, C. A. (2012). Extreme entropy–enthalpy compensation in a drug-resistant variant of hiv-1 protease. *ACS chemical biology*, 7(9):1536–1546.

Klebe, C., Bischoff, F. R., Ponstingl, H., and Wittinghofer, A. (1995a). Interaction of the nuclear gtp-binding protein ran with its regulatory proteins rcc1 and rangap1. *Biochemistry*, 34(2):639–647.

Klebe, C., Prinz, H., Wittinghofer, A., and Goody, R. S. (1995b). The kinetic mechanism of ran-nucleotide exchange catalyzed by rcc1. *Biochemistry*, 34(39):12543–12552.

Knauer, S. K., Bier, C., Habtemichael, N., and Stauber, R. H. (2006). The survivin–crm1 interaction is essential for chromosomal passenger complex localization and function. *EMBO reports*, 7(12):1259–1265.

Koffa, M. D., Casanova, C. M., Santarella, R., Köcher, T., Wilm, M., and Mattaj, I. W. (2006). Hurp is part of a ran-dependent complex involved in spindle formation. *Current biology*, 16(8):743–754.

Köhler, A. and Hurt, E. (2007). Exporting rna from the nucleus to the cytoplasm. *Nature reviews Molecular cell biology*, 8(10):761–773.

Kouzarides, T. (2000). Acetylation: a regulatory modification to rival phosphorylation? *The EMBO journal*, 19(6):1176–1179.

Kume, S., Haneda, M., Kanasaki, K., Sugimoto, T., Araki, S.-i., Isshiki, K., Isono, M., Uzu, T., Guarente, L., Kashiwagi, A., et al. (2007). Sirt1 inhibits transforming growth factor β-induced apoptosis in glomerular mesangial cells via smad7 deacetylation. *Journal of Biological Chemistry*, 282(1):151–158.

Kutay, U., Izaurralde, E., Bischoff, F. R., Mattaj, I. W., and Görlich, D. (1997). Dominant-negative mutants of importin-β block multiple pathways of import and export through the nuclear pore complex. *The EMBO journal*, 16(6):1153–1163.

Lai, C.-C., Lin, P.-M., Lin, S.-F., Hsu, C.-H., Lin, H.-C., Hu, M.-L., Hsu, C.-M., and Yang, M.-Y. (2013). Altered expression of sirt gene family in head and neck squamous cell carcinoma. *Tumor Biology*, 34(3):1847–1854.

Lammers, M., Neumann, H., Chin, J. W., and James, L. C. (2010). Acetylation regulates cyclophilin a catalysis, immunosuppression and hiv isomerization. *Nature chemical biology*, 6(5):331–337.

Langbeheim, H., Shih, T. Y., and Scolnick, E. M. (1980). Identification of a normal vertebrate cell protein related to the p21 src of harvey murine sarcoma virus. *Virology*, 106(2):292–300.

Lee, J. T. and Gu, W. (2013). Sirt1 regulator of p53 deacetylation. *Genes & cancer*, 4(3-4):112–117.

Lee, K. K. and Workman, J. L. (2007). Histone acetyltransferase complexes: one size doesn't fit all. *Nature reviews Molecular cell biology*, 8(4):284–295.

Leipe, D. D., Wolf, Y. I., Koonin, E. V., and Aravind, L. (2002). Classification and evolution of p-loop gtpases and related atpases. *Journal of molecular biology*, 317(1):41–72.

Lenzen, C., Cool, R. H., Prinz, H., Kuhlmann, J., and Wittinghofer, A. (1998). Kinetic analysis by fluorescence of the interaction between ras and the catalytic domain of the guanine nucleotide exchange factor cdc25mm. *Biochemistry*, 37(20):7420–7430.

L'Hernault, S. W. and Rosenbaum, J. L. (1983). Chlamydomonas alpha-tubulin is posttranslationally modified in the flagella during flagellar assembly. *The Journal of cell biology*, 97(1):258–263.

Li, H.-Y. and Zheng, Y. (2004). Phosphorylation of rcc1 in mitosis is essential for producing a high rangtp concentration on chromosomes and for spindle assembly in mammalian cells. *Genes & development*, 18(5):512–527.

Li, M., Luo, R.-Z., Chen, J.-W., Cao, Y., Lu, J.-B., He, J.-H., Wu, Q.-L., and Cai, M.-Y. (2011). High expression of transcriptional coactivator p300 correlates with aggressive features and poor prognosis of hepatocellular carcinoma. *Journal of translational medicine*, 9(1):5.

Lima, B. P., Antelmann, H., Gronau, K., Chi, B. K., Becher, D., Brinsmade, S. R., and Wolfe, A. J. (2011). Involvement of protein acetylation in glucose-induced transcription of a stress-responsive promoter. *Molecular microbiology*, 81(5):1190–1204.

Liu, B., Lin, Y., Darwanto, A., Song, X., Xu, G., and Zhang, K. (2009). Identification and characterization of propionylation at histone h3 lysine 23 in mammalian cells. *Journal of Biological Chemistry*, 284(47):32288–32295.

Llopis, J., McCaffery, J. M., Miyawaki, A., Farquhar, M. G., and Tsien, R. Y. (1998). Measurement of cytosolic, mitochondrial, and golgi ph in single living cells with green fluorescent proteins. *Proceedings of the National Academy of Sciences*, 95(12):6803–6808.

Lombard, D. B., Alt, F. W., Cheng, H.-L., Bunkenborg, J., Streeper, R. S., Mostoslavsky, R., Kim, J., Yancopoulos, G., Valenzuela, D., Murphy, A., et al. (2007). Mammalian sir2 homolog sirt3 regulates global mitochondrial lysine acetylation. *Molecular and cellular biology*, 27(24):8807–8814.

Lowy, D. R. and Willumsen, B. M. (1989). Protein modification: new clue to ras liquid glue. *Nature*, 341(6241):384–385.

Lundby, A., Lage, K., Weinert, B. T., Bekker-Jensen, D. B., Secher, A., Skovgaard, T., Kelstrup, C. D., Dmytriyev, A., Choudhary, C., Lundby, C., et al. (2012). Proteomic analysis of lysine acetylation sites in rat tissues reveals organ specificity and subcellular patterns. *Cell reports*, 2(2):419–431.

Mahajan, R., Delphin, C., Guan, T., Gerace, L., and Melchior, F. (1997). A small ubiquitin-related polypeptide involved in targeting rangap1 to nuclear pore complex protein ranbp2. *Cell*, 88(1):97–107.

Martínez-Redondo, P. and Vaquero, A. (2013). The diversity of histone versus nonhistone sirtuin substrates. *Genes & cancer*, page 1947601913483767.

Matunis, M. J., Coutavas, E., and Blobel, G. (1996). A novel ubiquitin-like modification modulates the partitioning of the ran-gtpase-activating protein rangap1 between the cytosol and the nuclear pore complex. *The Journal of cell biology*, 135(6):1457–1470.

Matunis, M. J., Wu, J., and Blobel, G. (1998). Sumo-1 modification and its role in targeting the ran gtpase-activating protein, rangap1, to the nuclear pore complex. *The Journal of cell biology*, 140(3):499–509.

Mertins, P., Qiao, J. W., Patel, J., Udeshi, N. D., Clauser, K. R., Mani, D., Burgess, M. W., Gillette, M. A., Jaffe, J. D., and Carr, S. A. (2013). Integrated proteomic analysis of post-translational modifications by serial enrichment. *Nature methods*, 10(7):634–637.

Moore, W. J., Zhang, C., and Clarke, P. R. (2002). Targeting of rcc1 to chromosomes is required for proper mitotic spindle assembly in human cells. *Current biology*, 12(16):1442–1447.

Mujtaba, S., He, Y., Zeng, L., Farooq, A., Carlson, J. E., Ott, M., Verdin, E., and Zhou, M.-M. (2002). Structural basis of lysine-acetylated hiv-1 tat recognition by pcaf bromodomain. *Molecular cell*, 9(3):575–586.

Mujtaba, S., Zeng, L., and Zhou, M. (2007). Structure and acetyl-lysine recognition of the bromodomain. *Oncogene*, 26(37):5521–5527.

Nachury, M. V., Maresca, T. J., Salmon, W. C., Waterman-Storer, C. M., Heald, R., and Weis, K. (2001). Importin β is a mitotic target of the small gtpase ran in spindle assembly. *Cell*, 104(1):95–106.

Nehrbass, U. and Blobel, G. (1996). Role of the nuclear transport factor p10 in nuclear import. *Science*, 272(5258):120–122.

Neumann, H., Hancock, S. M., Buning, R., Routh, A., Chapman, L., Somers, J., Owen-Hughes, T., van Noort, J., Rhodes, D., and Chin, J. W. (2009). A method for genetically installing site-specific acetylation in recombinant histones defines the effects of h3 k56 acetylation. *Molecular cell*, 36(1):153–163.

Neumann, H., Peak-Chew, S. Y., and Chin, J. W. (2008). Genetically encoding nε-acetyllysine in recombinant proteins. *Nature chemical biology*, 4(4):232–234.

Newman, J. C., He, W., and Verdin, E. (2012). Mitochondrial protein acylation and intermediary metabolism: regulation by sirtuins and implications for metabolic disease. *Journal of Biological Chemistry*, 287(51):42436–42443.

Nishimoto, T., Eilen, E., and Basilico, C. (1978). Premature chromosome condensation in a ts dna-mutant of bhk cells. *Cell*, 15(2):475–483.

North, B. J., Marshall, B. L., Borra, M. T., Denu, J. M., and Verdin, E. (2003). The human sir2 ortholog, sirt2, is an nad+-dependent tubulin deacetylase. *Molecular cell*, 11(2):437–444.

Ohba, T., Nakamura, M., Nishitani, H., and Nishimoto, T. (1999). Self-organization of microtubule asters induced in xenopus egg extracts by gtp-bound ran. *Science*, 284(5418):1356–1358.

Ohtsubo, M., Okazaki, H., and Nishimoto, T. (1989). The rcc1 protein, a regulator for the onset of chromosome condensation locates in the nucleus and binds to dna. *The Journal of Cell Biology*, 109(4):1389–1397.

Ott, M., Schnölzer, M., Garnica, J., Fischle, W., Emiliani, S., Rackwitz, H.-R., and Verdin, E. (1999). Acetylation of the hiv-1 tat protein by p300 is important for its transcriptional activity. *Current Biology*, 9(24):1489–1493.

Ozden, O., Park, S.-H., Wagner, B. A., Song, H. Y., Zhu, Y., Vassilopoulos, A., Jung, B., Buettner, G. R., and Gius, D. (2014). Sirt3 deacetylates and increases pyruvate dehydrogenase activity in cancer cells. *Free Radical Biology and Medicine*, 76:163–172.

Pan, P. W., Feldman, J. L., Devries, M. K., Dong, A., Edwards, A. M., and Denu, J. M. (2011). Structure and biochemical functions of sirt6. *Journal of Biological Chemistry*, 286(16):14575–14587.

Park, J., Chen, Y., Tishkoff, D. X., Peng, C., Tan, M., Dai, L., Xie, Z., Zhang, Y., Zwaans, B. M., Skinner, M. E., et al. (2013). Sirt5-mediated lysine desuccinylation impacts diverse metabolic pathways. *Molecular cell*, 50(6):919–930.

Paschal, B. M., Delphin, C., and Gerace, L. (1996). Nucleotide-specific interaction of ran/tc4 with nuclear transport factors ntf2 and p97. *Proceedings of the National Academy of Sciences*, 93(15):7679–7683.

Ponugoti, B., Kim, D.-H., Xiao, Z., Smith, Z., Miao, J., Zang, M., Wu, S.-Y., Chiang, C.-M., Veenstra, T. D., and Kemper, J. K. (2010). Sirt1 deacetylates and inhibits srebp-1c activity in regulation of hepatic lipid metabolism. *Journal of Biological Chemistry*, 285(44):33959–33970.

Prinz, H. and Striessnig, J. (1993). Ligand-induced accelerated dissociation of (+)-cis-diltiazem from l-type ca2+ channels is simply explained by competition for individual attachment points. *Journal of Biological Chemistry*, 268(25):18580–18585.

Prior, I. A., Lewis, P. D., and Mattos, C. (2012). A comprehensive survey of ras mutations in cancer. *Cancer research*, 72(10):2457–2467.

Pyhtila, B. and Rexach, M. (2003). A gradient of affinity for the karyopherin kap95p along the yeast nuclear pore complex. *Journal of Biological Chemistry*, 278(43):42699–42709.

Qiu, X., Brown, K., Hirschey, M. D., Verdin, E., and Chen, D. (2010). Calorie restriction reduces oxidative stress by sirt3-mediated sod2 activation. *Cell metabolism*, 12(6):662–667.

Rauh, D., Fischer, F., Gertz, M., Lakshminarasimhan, M., Bergbrede, T., Aladini, F., Kambach, C., Becker, C. F., Zerweck, J., Schutkowski, M., et al. (2013). An acetylome peptide microarray reveals specificities and deacetylation substrates for all human sirtuin isoforms. *Nature communications*, 4.

Rehmann, H. and Bos, J. L. (2004). Signal transduction: thumbs up for inactivation. *Nature*, 429(6988):138–139.

Reichelt, R., Holzenburg, A., Buhle, E., Jarnik, M., Engel, A., and Aebi, U. (1990). Correlation between structure and mass distribution of the nuclear pore complex and of distinct pore complex components. *The Journal of Cell Biology*, 110(4):883–894.

Ren, M., Coutavas, E., D'Eustachio, P., and Rush, M. G. (1994). Effects of mutant ran/tc4 proteins on cell cycle progression. *Molecular and cellular biology*, 14(6):4216–4224.

Ren, M., Drivas, G., D'Eustachio, P., and Rush, M. G. (1993). Ran/tc4: a small nuclear gtp-binding protein that regulates dna synthesis. *The Journal of cell biology*, 120(2):313–323.

Renault, L., Kuhlmann, J., Henkel, A., and Wittinghofer, A. (2001). Structural basis for guanine nucleotide exchange on ran by the regulator of chromosome condensation (rcc1). *Cell*, 105(2):245–255.

Renault, L., Nassar, N., Vetter, I., Becker, J., Klebe, C., Roth, M., and Wittinghofer, A. (1998). The 1.7 å crystal structure of the regulator of chromosome condensation (rcc1) reveals a seven-bladed propeller. *Nature*, 392(6671):97–101.

Rensland, H., John, J., Linke, R., Simon, I., Schlichting, I., Wittinghofer, A., and Goody, R. S. (1995). Substrate and product structural requirements for binding of nucleotides to h-ras p21: the mechanism of discrimination between guanosine and adenosine nucleotides. *Biochemistry*, 34(2):593–599.

Resat, H., Straatsma, T., Dixon, D. A., and Miller, J. H. (2001). The arginine finger of rasgap helps gln-61 align the nucleophilic water in gap-stimulated hydrolysis of gtp. *Proceedings of the National Academy of Sciences*, 98(11):6033–6038.

Ribbeck, K. and Görlich, D. (2001). Kinetic analysis of translocation through nuclear pore complexes. *The EMBO journal*, 20(6):1320–1330.

Ribbeck, K., Groen, A. C., Santarella, R., Bohnsack, M. T., Raemaekers, T., Köcher, T., Gentzel, M., Görlich, D., Wilm, M., Carmeliet, G., et al. (2006). Nusap, a mitotic rangtp target that stabilizes and cross-links microtubules. *Molecular biology of the cell*, 17(6):2646–2660.

Ribbeck, K., Lipowsky, G., Kent, H. M., Stewart, M., and Görlich, D. (1998). Ntf2 mediates nuclear import of ran. *The EMBO Journal*, 17(22):6587–6598.

Richards, S. A., Lounsbury, K. M., and Macara, I. G. (1995). The c terminus of the nuclear ran/tc4 gtpase stabilizes the gdp-bound state and mediates interactions with

rcc1, ran-gap, and htf9a/ranbp1. *Journal of Biological Chemistry*, 270(24):14405–14411.

Rocks, O., Peyker, A., Kahms, M., Verveer, P. J., Koerner, C., Lumbierres, M., Kuhlmann, J., Waldmann, H., Wittinghofer, A., and Bastiaens, P. I. (2005). An acylation cycle regulates localization and activity of palmitoylated ras isoforms. *Science*, 307(5716):1746–1752.

Rojas, A. M., Fuentes, G., Rausell, A., and Valencia, A. (2012). The ras protein superfamily: evolutionary tree and role of conserved amino acids. *The Journal of cell biology*, 196(2):189–201.

Roth, S. Y., Denu, J. M., and Allis, C. D. (2001). Histone acetyltransferases. *Annual review of biochemistry*, 70(1):81–120.

Rout, M. and Aitchison, J. (2000). Pore relations: nuclear pore complexes and nucleocytoplasmic exchange. *Essays Biochem*, 36:79–88.

Ryan, K. J., McCaffery, J. M., and Wente, S. R. (2003). The ran gtpase cycle is required for yeast nuclear pore complex assembly. *The Journal of cell biology*, 160(7):1041–1053.

Saraste, M., Sibbald, P. R., and Wittinghofer, A. (1990). The p-loopa common motif in atp-and gtp-binding proteins. *Trends in biochemical sciences*, 15(11):430–434.

Sato, M. and Toda, T. (2007). Alp7/tacc is a crucial target in ran-gtpase-dependent spindle formation in fission yeast. *Nature*, 447(7142):334–337.

Sazer, S. and Nurse, P. (1994). A fission yeast rcc1-related protein is required for the mitosis to interphase transition. *The EMBO journal*, 13(3):606.

Scheffzek, K., Ahmadian, M. R., Kabsch, W., Wiesmüller, L., Lautwein, A., Schmitz, F., and Wittinghofer, A. (1997). The ras-rasgap complex: structural basis for gtpase activation and its loss in oncogenic ras mutants. *Science*, 277(5324):333–339.

Scheffzek, K., Klebe, C., Fritz-Wolf, K., Kabsch, W., and Wittinghofer, A. (1995). Crystal structure of the nuclear ras-related protein ran in its gdp-bound form.

Schmidt, G., Lenzen, C., Simon, I., Deuter, R., Cool, R. H., Goody, R. S., and Wittinghofer, A. (1996). Biochemical and biological consequences of changing the specificity of p21ras from guanosine to xanthosine nucleotides. *Oncogene*, 12(1):87–96.

Schmidt, W. K., Tam, A., Fujimura-Kamada, K., and Michaelis, S. (1998). Endoplasmic reticulum membrane localization of rce1p and ste24p, yeast proteases involved in carboxyl-terminal caax protein processing and amino-terminal a-factor cleavage. *Proceedings of the National Academy of Sciences*, 95(19):11175–11180.

Scott, D. C., Monda, J. K., Bennett, E. J., Harper, J. W., and Schulman, B. A. (2011). N-terminal acetylation acts as an avidity enhancer within an interconnected multiprotein complex. *Science*, 334(6056):674–678.

Scrima, A., Thomas, C., Deaconescu, D., and Wittinghofer, A. (2008). The rap–rapgap complex: Gtp hydrolysis without catalytic glutamine and arginine residues. *The EMBO Journal*, 27(7):1145–1153.

Seewald, M. J., Körner, C., Wittinghofer, A., and Vetter, I. R. (2002). Rangap mediates gtp hydrolysis without an arginine finger. *Nature*, 415(6872):662–666.

Shahbazian, M. D. and Grunstein, M. (2007). Functions of site-specific histone acetylation and deacetylation. *Annu. Rev. Biochem.*, 76:75–100.

Shaw, P. G., Chaerkady, R., Zhang, Z., Davidson, N. E., and Pandey, A. (2011). Monoclonal antibody cocktail as an enrichment tool for acetylome analysis. *Analytical chemistry*, 83(10):3623–3626.

Shih, T. Y., Weeks, M. O., Young, H. A., and Scolnick, E. M. (1979). Identification of a sarcoma virus-coded phosphoprotein in nonproducer cells transformed by kirsten or harvey murine sarcoma virus. *Virology*, 96(1):64–79.

Shore, D., Squire, M., and Nasmyth, K. A. (1984). Characterization of two genes required for the position-effect control of yeast mating-type genes. *The EMBO journal*, 3(12):2817.

Silljé, H. H., Nagel, S., Körner, R., and Nigg, E. A. (2006). Hurp is a ran-importin β-regulated protein that stabilizes kinetochore microtubules in the vicinity of chromosomes. *Current biology*, 16(8):731–742.

Simonsson, M., Heldin, C.-H., Ericsson, J., and Grönroos, E. (2005). The balance between acetylation and deacetylation controls smad7 stability. *Journal of Biological Chemistry*, 280(23):21797–21803.

Smith, A., Brownawell, A., and Macara, I. G. (1998). Nuclear import of ran is mediated by the transport factor ntf2. *Current biology*, 8(25):1403–S1.

Sol, E. M., Wagner, S. A., Weinert, B. T., Kumar, A., Kim, H.-S., Deng, C.-X., and Choudhary, C. (2012). Proteomic investigations of lysine acetylation identify diverse substrates of mitochondrial deacetylase sirt3. *PloS one*, 7(12):e50545.

Someya, S., Yu, W., Hallows, W. C., Xu, J., Vann, J. M., Leeuwenburgh, C., Tanokura, M., Denu, J. M., and Prolla, T. A. (2010). Sirt3 mediates reduction of oxidative damage and prevention of age-related hearing loss under caloric restriction. *Cell*, 143(5):802–812.

Song, L. and Rape, M. (2010). Regulated degradation of spindle assembly factors by the anaphase-promoting complex. *Molecular cell*, 38(3):369–382.

Soufi, B., Soares, N. C., Ravikumar, V., and Macek, B. (2012). Proteomics reveals evidence of cross-talk between protein modifications in bacteria: focus on acetylation and phosphorylation. *Current opinion in microbiology*, 15(3):357–363.

Spoerner, M., Herrmann, C., Vetter, I. R., Kalbitzer, H. R., and Wittinghofer, A. (2001). Dynamic properties of the ras switch i region and its importance for binding to effectors. *Proceedings of the National Academy of Sciences*, 98(9):4944–4949.

Starai, V. J. and Escalante-Semerena, J. C. (2004). Identification of the protein acetyltransferase (pat) enzyme that acetylates acetyl-coa synthetase in salmonella enterica. *Journal of molecular biology*, 340(5):1005–1012.

Steggerda, S. M. and Paschal, B. M. (2000). The mammalian mog1 protein is a guanine nucleotide release factor for ran. *Journal of Biological Chemistry*, 275(30):23175–23180.

Steggerda, S. M. and Paschal, B. M. (2001). Identification of a conserved loop in mog1 that releases gtp from ran. *Traffic*, 2(11):804–811.

Stewart, M. (2003). Nuclear trafficking. *Science*, 302(5650):1513–1514.

Stewart, M., Kent, H. M., and McCoy, A. J. (1998). Structural basis for molecular recognition between nuclear transport factor 2 (ntf2) and the gdp-bound form of the ras-family gtpase ran. *Journal of molecular biology*, 277(3):635–646.

Tahara, K., Takagi, M., Ohsugi, M., Sone, T., Nishiumi, F., Maeshima, K., Horiuchi, Y., Tokai-Nishizumi, N., Imamoto, F., Yamamoto, T., et al. (2008). Importin-β and the small guanosine triphosphatase ran mediate chromosome loading of the human chromokinesin kid. *The Journal of cell biology*, 180(3):493–506.

Tamkun, J. W., Deuring, R., Scott, M. P., Kissinger, M., Pattatucci, A. M., Kaufman, T. C., and Kennison, J. A. (1992). brahma: a regulator of drosophila homeotic genes structurally related to the yeast transcriptional activator snf2swi2. *Cell*, 68(3):561–572.

Thompson, P. R., Wang, D., Wang, L., Fulco, M., Pediconi, N., Zhang, D., An, W., Ge, Q., Roeder, R. G., Wong, J., et al. (2004). Regulation of the p300 hat domain via a novel activation loop. *Nature structural & molecular biology*, 11(4):308–315.

Tran, J. C., Zamdborg, L., Ahlf, D. R., Lee, J. E., Catherman, A. D., Durbin, K. R., Tipton, J. D., Vellaichamy, A., Kellie, J. F., Li, M., et al. (2011). Mapping intact protein isoforms in discovery mode using top-down proteomics. *Nature*, 480(7376):254–258.

Trelle, M. B. and Jensen, O. N. (2008). Utility of immonium ions for assignment of ε-n-acetyllysine-containing peptides by tandem mass spectrometry. *Analytical chemistry*, 80(9):3422–3430.

Trieselmann, N., Armstrong, S., Rauw, J., and Wilde, A. (2003). Ran modulates spindle assembly by regulating a subset of tpx2 and kid activities including aurora a activation. *Journal of cell science*, 116(23):4791–4798.

Tsai, M.-Y., Wang, S., Heidinger, J. M., Shumaker, D. K., Adam, S. A., Goldman, R. D., and Zheng, Y. (2006). A mitotic lamin b matrix induced by rangtp required for spindle assembly. *Science*, 311(5769):1887–1893.

Tsai, M.-Y., Wiese, C., Cao, K., Martin, O., Donovan, P., Ruderman, J., Prigent, C., and Zheng, Y. (2003). A ran signalling pathway mediated by the mitotic kinase aurora a in spindle assembly. *Nature cell biology*, 5(3):242–248.

Tse, C., Sera, T., Wolffe, A. P., and Hansen, J. C. (1998). Disruption of higher-order folding by core histone acetylation dramatically enhances transcription of nucleosomal arrays by rna polymerase iii. *Molecular and cellular biology*, 18(8):4629–4638.

Tucker, J., Sczakiel, G., Feuerstein, J., John, J., Goody, R. S., and Wittinghofer, A. (1986). Expression of p21 proteins in escherichia coli and stereochemistry of the nucleotide-binding site. *The EMBO Journal*, 5(6):1351.

Uchida, S., Sekiguchi, T., Nishitani, H., Miyauchi, K., Ohtsubo, M., and Nishimoto, T. (1990). Premature chromosome condensation is induced by a point mutation in the hamster rcc1 gene. *Molecular and cellular biology*, 10(2):577–584.

van Noort, V., Seebacher, J., Bader, S., Mohammed, S., Vonkova, I., Betts, M. J., Kühner, S., Kumar, R., Maier, T., O'Flaherty, M., et al. (2012). Cross-talk between phosphorylation and lysine acetylation in a genome-reduced bacterium. *Molecular systems biology*, 8(1).

Vetter, I. R., Arndt, A., Kutay, U., Görlich, D., and Wittinghofer, A. (1999). Structural view of the ran–importin β interaction at 2.3 å resolution. *Cell*, 97(5):635–646.

Vetter, I. R. and Wittinghofer, A. (2001). The guanine nucleotide-binding switch in three dimensions. *Science*, 294(5545):1299–1304.

Via, A., Ferrè, F., Brannetti, B., Valencia, A., and Helmer-Citterich, M. (2000). Three-dimensional view of the surface motif associated with the p-loop structure: cis and trans cases of convergent evolution. *Journal of molecular biology*, 303(4):455–465.

Villa Braslavsky, C. I., Nowak, C., Görlich, D., Wittinghofer, A., and Kuhlmann, J. (2000). Different structural and kinetic requirements for the interaction of ran with the ran-binding domains from ranbp2 and importin-β. *Biochemistry*, 39(38):11629–11639.

Wagner, G. R. and Hirschey, M. D. (2014). Nonenzymatic protein acylation as a carbon stress regulated by sirtuin deacylases. *Molecular cell*, 54(1):5–16.

Wagner, G. R. and Payne, R. M. (2013). Widespread and enzyme-independent n -acetylation and n -succinylation of proteins in the chemical conditions of the mitochondrial matrix. *Journal of Biological Chemistry*, 288(40):29036–29045.

Wagner, S. A., Beli, P., Weinert, B. T., Nielsen, M. L., Cox, J., Mann, M., and Choudhary, C. (2011). A proteome-wide, quantitative survey of in vivo ubiquitylation sites reveals widespread regulatory roles. *Molecular & Cellular Proteomics*, 10(10):M111–013284.

Wagner, S. A., Beli, P., Weinert, B. T., Schölz, C., Kelstrup, C. D., Young, C., Nielsen, M. L., Olsen, J. V., Brakebusch, C., and Choudhary, C. (2012). Proteomic analyses reveal divergent ubiquitylation site patterns in murine tissues. *Molecular & Cellular Proteomics*, 11(12):1578–1585.

Walther, T. C., Askjaer, P., Gentzel, M., Habermann, A., Griffiths, G., Wilm, M., Mattaj, I. W., and Hetzer, M. (2003). Rangtp mediates nuclear pore complex assembly. *Nature*, 424(6949):689–694.

Wang, R.-H., Sengupta, K., Li, C., Kim, H.-S., Cao, L., Xiao, C., Kim, S., Xu, X., Zheng, Y., Chilton, B., et al. (2008). Impaired dna damage response, genome instability, and tumorigenesis in sirt1 mutant mice. *Cancer cell*, 14(4):312–323.

Wang, W., Takimoto, J. K., Louie, G. V., Baiga, T. J., Noel, J. P., Lee, K.-F., Slesinger, P. A., and Wang, L. (2007). Genetically encoding unnatural amino acids for cellular and neuronal studies. *Nature neuroscience*, 10(8):1063–1072.

Weinert, B. T., Iesmantavicius, V., Moustafa, T., Schölz, C., Wagner, S. A., Magnes, C., Zechner, R., and Choudhary, C. (2014). Acetylation dynamics and stoichiometry in saccharomyces cerevisiae. *Molecular systems biology*, 10(1).

Weinert, B. T., Iesmantavicius, V., Wagner, S. A., Schölz, C., Gummesson, B., Beli, P., Nyström, T., and Choudhary, C. (2013). Acetyl-phosphate is a critical determinant of lysine acetylation in e. coli. *Molecular cell*, 51(2):265–272.

Weinert, B. T., Wagner, S. A., Horn, H., Henriksen, P., Liu, W. R., Olsen, J. V., Jensen, L. J., and Choudhary, C. (2011). Proteome-wide mapping of the drosophila acetylome demonstrates a high degree of conservation of lysine acetylation. *Science signaling*, 4(183):ra48–ra48.

Weis, K. (2002). Nucleocytoplasmic transport: cargo trafficking across the border. *Current opinion in cell biology*, 14(3):328–335.

Werner, A., Flotho, A., and Melchior, F. (2012). The ranbp2/rangap1* sumo1/ubc9 complex is a multisubunit sumo e3 ligase. *Molecular cell*, 46(3):287–298.

Wiese, C., Wilde, A., Moore, M. S., Adam, S. A., Merdes, A., and Zheng, Y. (2001). Role of importin-β in coupling ran to downstream targets in microtubule assembly. *Science*, 291(5504):653–656.

Wilde, A., Lizarraga, S. B., Zhang, L., Wiese, C., Gliksman, N. R., Walczak, C. E., and Zheng, Y. (2001). Ran stimulates spindle assembly by altering microtubule dynamics and the balance of motor activities. *Nature cell biology*, 3(3):221–227.

Wiseman, T., Williston, S., Brandts, J. F., and Lin, L.-N. (1989). Rapid measurement of binding constants and heats of binding using a new titration calorimeter. *Analytical biochemistry*, 179(1):131–137.

Wisniewski, J. R., Zougman, A., and Mann, M. (2009). Combination of fasp and stagetip-based fractionation allows in-depth analysis of the hippocampal membrane proteome. *Journal of proteome research*, 8(12):5674–5678.

Wittinghofer, A. and Pal, E. F. (1991). The structure of ras protein: a model for a universal molecular switch. *Trends in biochemical sciences*, 16:382–387.

Wittinghofer, A. and Waldmann, H. (2000). Rasa molecular switch involved in tumor formation. *Angewandte Chemie International Edition*, 39(23):4192–4214.

Wittmann, T., Wilm, M., Karsenti, E., and Vernos, I. (2000). Tpx2, a novel xenopus map involved in spindle pole organization. *The Journal of cell biology*, 149(7):1405–1418.

Xiao, Y., Nagai, Y., Deng, G., Ohtani, T., Zhu, Z., Zhou, Z., Zhang, H., Ji, M. Q., Lough, J. W., Samanta, A., et al. (2014). Dynamic interactions between tip60 and p300 regulate foxp3 function through a structural switch defined by a single lysine on tip60. *Cell reports*, 7(5):1471–1480.

Yang, W., Gelles, J., and Musser, S. M. (2004). Imaging of single-molecule translocation through nuclear pore complexes. *Proceedings of the National Academy of Sciences of the United States of America*, 101(35):12887–12892.

Yokoyama, H., Gruss, O. J., Rybina, S., Caudron, M., Schelder, M., Wilm, M., Mattaj, I. W., and Karsenti, E. (2008). Cdk11 is a rangtp-dependent microtubule stabilization factor that regulates spindle assembly rate. *The Journal of cell biology*, 180(5):867–875.

Yuan, H. and Marmorstein, R. (2013). Histone acetyltransferases: Rising ancient counterparts to protein kinases. *Biopolymers*, 99(2):98–111.

Zhang, C. and Clarke, P. R. (2000). Chromatin-independent nuclear envelope assembly induced by ran gtpase in xenopus egg extracts. *Science*, 288(5470):1429–1432.

Zhang, C., Hughes, M., and Clarke, P. R. (1999). Ran-gtp stabilises microtubule asters and inhibits nuclear assembly in xenopus egg extracts. *Journal of cell science*, 112(14):2453–2461.

Zhang, J., Sprung, R., Pei, J., Tan, X., Kim, S., Zhu, H., Liu, C.-F., Grishin, N. V., and Zhao, Y. (2009). Lysine acetylation is a highly abundant and evolutionarily conserved modification in escherichia coli. *Molecular & Cellular Proteomics*, 8(2):215–225.

Zhao, S., Xu, W., Jiang, W., Yu, W., Lin, Y., Zhang, T., Yao, J., Zhou, L., Zeng, Y., Li, H., et al. (2010). Regulation of cellular metabolism by protein lysine acetylation. *Science*, 327(5968):1000–1004.

Acknowledgements

An dieser Stelle möchte ich den Menschen danken, die mich in den letzten vier Jahren begleitet und unterstützt haben.

Meinem Betreuer, Dr. Michael Lammers, danke ich für das Projekt, die ausgezeichneten Arbeitsbedingungen und viele Freiräume. Ich bin die meiste Zeit sehr gern zur Arbeit gegangen!

Prof. Dr. Hofmann und Prof. Dr. Baumann danke ich für ihr Mitwirken im letzten Abschnitt dieser Arbeit.

Den anderen Mitgliedern der Arbeitsgruppe danke ich für das gute Arbeitsklima und die Unterstützung, falls ich mal wieder überstürzt aufbrechen musste. Den Mädels (Sarah, Nora, Linda) bin ich dankbar für die kurzen Pausen vom Arbeitsalltag, sei es beim Mittagessen oder abends beim Sushi.

Ein besonderer Dank geht an Philipp, mit dem eine produktive und bereichernde Teamarbeit möglich war. Am Anfang war ich etwas skeptisch, doch letzten Endes bin ich sehr froh die letzten zwei Jahre nicht allein geforscht zu haben.

Den Facility-Mitarbeitern danke ich für die Hilfsbereitschaft und Geduld, mit der sie mir immer begegnet sind. Gerade in den letzten Monaten haben Rene und Astrid viel zu dieser Arbeit beigetragen. An dieder Stelle möchte ich auch Hendrik danken, der aus unzähligen Exel-Daten tatsächlich verwertbare Ergebnisse gezaubert hat.

Johannes, danke für die Kritik, den Ansporn und die Unterstützung in den letzten Jahren. Und am Ende hast du sogar das stille Zuhören gelernt!

Eidesstattliche Erklärung

Ich versichere, dass ich die von mir vorgelegte Dissertation selbständig angefertigt, die benutzten Quellen und Hilfsmittel vollständig angegeben und die Stellen der Arbeit −
einschließlich Tabellen, Karten und Abbildungen −, die anderen Werken im Wortlaut oder dem Sinn nach entnommen sind, in jedem Einzelfall als Entlehnung kenntlich gemacht habe; dass diese Dissertation noch keiner anderen Fakultät oder Universität zur Prüfung vorgelegen hat; dass sie − abgesehen von unten angegebenen Teilpublikationen − noch nicht veröffentlicht worden ist sowie, dass ich eine solche Veröffentlichung vor Abschluss des Promotionsverfahrens nicht vornehmen werde. Die Bestimmungen der Promotionsordnung sind mir bekannt. Die von mir vorgelegte Dissertation ist von Dr. Michael Lammers betreut worden.

_____

Susanne de Boor (geb. Haase)